FACULDADE DE CIÊNCIAS E TECNOLOGIA DA UNIVERSIDADE DE COIMBRA

DEPARTAMENTO DE ENGENHARIA MECÂNICA

DYNAMIC MODEL FOR FIRE BEHAVIOUR PREDICTION

Carlos Gonçalves Rossa

COIMBRA

2009

FACULDADE DE CIÊNCIAS E TECNOLOGIA DA UNIVERSIDADE DE COIMBRA

DEPARTAMENTO DE ENGENHARIA MECÂNICA

DYNAMIC MODEL FOR FIRE BEHAVIOUR PREDICTION

by

Carlos Gonçalves Rossa

Thesis for the degree of

Doctor of Philosophy in

Mechanical Engineering

(Natural and Technological Hazards)

COIMBRA

2009

To my Father

Acknowledgements

Being that all great journeys start with one step, it is also true that ending them requires motivation, perseverance, power of will and a lot of sacrifice. But regardless of the merit that one might have for having done an individual work, we can hardly attribute a great deed to the work of only one person. I cannot not express my gratitude and acknowledgement to those that in the last five years I consider to have contributed in a significant manner, either by direct collaboration in my work or by support that I have been given, for having accomplished with success this challenge. Taking the risk of forgetting someone, it would be of great injustice not to mention these people to whom I write these words of thankfulness.

Firstly to my Father Ulisses Rossa, to whom I dedicate this Thesis, and to whom I owe great part, if not all, of what I have achieved. To my brother Pedro Rossa for the support that he has been giving me, most times without need to ask. To my girlfriend Raquel Roliz, my companion for almost ten years now, and that has been a great part of my support in times of discouragement.

To my friend Marco Caetano, colleague in my academic path since High School and, more than any other has accompanied me during my best and worst moments. To António Pires, my friend for over twenty years and that during this period has always supported me whenever I needed.

To Prof. Xavier Viegas for having accepted to supervise this research program and for having allowed me to be able to benefit from the experience of the group he created, the *Centro de Estudos sobre Incêndios Florestais* (*CEIF*), that works in this area for over twenty years with acknowledged merit at National and International level. To the *CEIF* team members for the help I have been given, in particular in the performance of many laboratory experiments. A special acknowledgment to Pedro Palheiro, that it is not part of the present team but to whom I owe a lot of the understanding I have today of fire behaviour and for which contributed the many hours we spent monitoring forest fires in 2005 and doing prescribed fire in 2006 and 2007, and to Luís Mário for the cooperation in some of my research works.

To Yolanda Perez, Alba Àgueda, Elsa Pastor and Eulàlia Planas from *Centre d'Estudis del Risc Tecnològic* (*CERTEC*), from Polytechnic University of Catalonia, Barcelona, for all the cooperation and support that I have been given during the period I spent there doing research between May and August 2007.

Abstract

The present work aims to develop a calculus algorithm for simulating the fire perimeter evolution of a point ignition fire spreading upslope or under constant wind. A study of the dynamic effects of favourable and contrary wind or slope on surface fires spreading in fine fuels was made. Based on experimental evidence it was shown that in the general situation forest fires exhibit a dynamic behaviour, *i.e.* the spread properties change with time even for constant boundary conditions, and in particular the fire rate of spread does not remain constant from one point of the fire line to another. For this reason, the use of a single rate of spread is not sufficient for a correct description of the fire perimeter evolution. The concepts of the fire line elements extension and rotation were introduced as a complement to describe their movement and shown to be associated to the reduction of the fire line curvature. Using semi-empirical and empirical formulations a mathematical model for predicting the fire line evolution of a point ignition fire under constant wind or slope was proposed.

In an experimental program using four test rigs a total of 155 laboratory experiments have been conducted, analysing the following situations: fire spread on horizontal ground with no wind or slope (41 exp., $4 < m_f < 19\%$), under the effect of favourable wind (56 exp., $0 - 4.5$ m/s), favourable slope (16 exp., $0 - 40°$), contrary wind (12 exp., $-4.5 - 0$ m/s), and contrary slope (30 exp., $-55 - 0°$). Tests with *Pinus pinaster* dead needles and dry straw fuel beds have been conducted but in some cases also *Eucalyptus globulus* slash fuel beds were used. For all fuel beds a fuel load of 0.6 kg/m^2 has been used and in some cases also 0.8 and 1.0 kg/m^2 were tested.

Parameters were determined for four empirical model functions, one for the dependence of the rate of spread on fuel moisture content, for fire spreading with no wind or slope, other two for the dependence of the rate of spread on wind velocity or slope angle, and one for determining an equivalent wind velocity that produces the same rate of spread value on a horizontal ground than on a given slope angle. It was shown that fire spreading with contrary wind or slope attains velocities slightly lower than spreading under no wind on level ground and that the rate of spread successively decreases and increases as we increase the absolute value of the wind velocity or slope angle.

Analysing the fire line evolution by infrared imaging, the fire line elements extension and rotation were assessed and the parameters necessary to the extension and rotation prediction model were determined. It was shown that, for wind or slope point ignition fires, there is a

tendency for the flank fire line to become parallel to the reference wind or slope direction and for the back fire line to become perpendicular to that direction. The model was compared positively with experimental laboratory results from two dedicated tests for a 30º slope, on pine needles and straw fuel beds. The extension to the simulation of real forest fires was analysed and further work was proposed.

iv

Resumo

O objectivo deste trabalho é o desenvolvimento de um algoritmo de cálculo para a simulação da evolução do perímetro de um fogo, originado por um foco pontual, em propagação sob o efeito do declive ou vento constante. Fez-se um estudo dos efeitos dinâmicos do vento e declive favoráveis e contrários em fogos de superfície em combustíveis finos. Mostrou-se, com base em resultados experimentais, que em geral os incêndios florestais exibem um comportamento dinâmico, *i.e.* as propriedades de propagação alteram-se ao longo do tempo mesmo para condições de fronteira constantes, e em particular a velocidade de propagação não se mantém constante de um ponto da linha de fogo para outro. Por este motivo, o uso de uma velocidade de propagação única não é suficiente para descrever correctamente a evolução do perímetro de fogo. Introduziram-se os conceitos de extensão e de rotação dos elementos da linha de fogo como complemento para descrever o seu movimento, mostrando que estão associados à redução da curvatura da mesma. Usando formulações semi-empíricas e empíricas propôs-se um modelo matemático para prever a evolução da linha de fogo de um foco pontual sob o efeito de vento ou declive constantes.

Num programa experimental realizado usando quatro mesas de teste fez-se um total de 155 ensaios laboratoriais, analisando as seguintes situações: propagação em leito horizontal sem vento e sem declive (41 ensaios, $4 < m_f < 19\,\%$), sob o efeito de vento favorável (56 ensaios, $0 - 4.5$ m/s), declive favorável (16 ensaios, $0 - 40°$), vento contrário (12 ensaios, $-4.5 - 0$ m/s), e declive contrário (30 ensaios, $-55 - 0°$). Fizeram-se ensaios com leitos de agulhas mortas de *Pinus pinaster* e palha seca mas em alguns casos também foram usados resíduos de corte de *Eucalyptus globulus*. Para todos os leitos foi usada uma carga de $0.6\,\text{kg/m}^2$ e em alguns casos também 0.8 e $1.0\,\text{kg/m}^2$.

Determinaram-se parâmetros para quatro funções empíricas, uma para a velocidade de propagação como função do teor de humidade dos combustíveis, para propagação sem vento e sem declive, outras duas para a velocidade de propagação como função da velocidade do vento ou ângulo de inclinação, e uma para a determinação de uma velocidade de vento equivalente que produz a mesma velocidade de propagação em leito horizontal que um dado declive. Mostrou-se que a propagação do fogo contra o vento ou o declive atinge velocidades ligeiramente mais baixas que sem vento e sem declive e que a velocidade de propagação diminui e aumenta sucessivamente à medida que aumenta o valor absoluto da velocidade do vento ou do declive.

Analisando a evolução da linha de fogo através de imagens de infravermelhos, avaliaram-se a extensão e rotação dos elementos da linha de fogo e determinaram-se os parâmetros necessários ao modelo de previsão da extensão e da rotação. Mostrou-se que, para fogos sob o efeito do vento ou declive originados por um foco pontual, existe uma tendência para a linha de flanco se tornar paralela à direcção do vento de referência ou do declive e para a linha da cauda se tornar perpendicular a essa direcção. O modelo foi comparado positivamente com resultados experimentais de dois ensaios realizados para este propósito com um declive de 30º, com leitos de agulhas de pinheiro e palha. Analisou-se a extensão à simulação de incêndios reais e propôs-se trabalho futuro.

Palavras-chave: modelação do comportamento do fogo, fogo de superfície, efeitos do vento ou declive favoráveis e contrários, comportamento dinâmico do fogo, efeitos convectivos, extensão e rotação da linha de fogo, ensaios laboratoriais.

Index

Nomenclature

Symbol	Units	Description
a	m	Length of fire line element at time instant t
a'	m	Length of fire line element at time instant $t'=t+dt$
a_0	-	Coefficient in Eq. (2.1)
a_3	-	Coefficient in Eq. (2.17)
a_α	-	Coefficient in Eq. (2.7)
$a_{1,u}$	-	Coefficient in Eq. (2.2)
$a_{1,\alpha}$	-	Coefficient in Eq. (2.3)
b_0	-	Coefficient in Eq. (2.1)
b_3	-	Coefficient in Eq. (2.17)
b_α	-	Coefficient in Eq. (2.7)
b_β	-	Coefficient in Eq. (2.26)
b_ε	-	Coefficient in Eq. (4.1)
$b_{1,u}$	-	Coefficient in Eq. (2.2)
$b_{1,\alpha}$	-	Coefficient in Eq. (2.3)
c_0	-	Coefficient in Eq. (2.1)
d	-	Variation of a given parameter during time step dt
d_0	-	Coefficient in Eq. (2.1)
dt	s	Time step
f_1	-	Empirical function given by Eq. (2.2) and (2.3)
f_3	-	Empirical function given by Eq. (2.17)
m_f	%	Fuel moisture content on a dry basis
m_r	-	Coefficient in Eq. (2.27)
m_β	-	Coefficient in Eq. (2.26)
m_ε	-	Coefficient in Eq. (4.1)
n	-	Number of points in the fire perimeter at time instant t
p	-	Number of fire perimeter contours
s	m	Position of a point at time instant t
s'	m	Position of a point at time instant $t'=t+dt$
t	s	Time elapsed since fire origin
t_0	s	Initial time instant
t'	s	Next instant of time
u	m/s	Local flow velocity parallel to the fuel bed
u'	m/s	Approximate value of local flow velocity given by Eq. (4.2)
u_0	m/s	General flow velocity (due to general wind or equivalent to slope)
u_i	m/s	Local flow velocity induced by the fire

u_x	m/s	Local flow velocity OX component
u_y	m/s	Local flow velocity OY component
u_{eq}	m/s	General flow velocity in a slope fire equivalent to a wind induced fire
x_i	m	Local coordinate tangent to the fire line at point P_i
x_0	m	Basic coordinate perpendicular to u_0
y_i	m	Local coordinate perpendicular to the fire line at point P_i
y_0	m	Basic coordinate parallel to u_0
P_i	-	Generic point at the fire line at time instant t
P'_i	-	Generic point at the fire line at time instant $t'=t+dt$
R	m/s	Local rate of spread (ROS)
R_i	m/s	Local rate of spread at a generic point
R_0	m/s	Basic rate of spread (ROS under no wind or slope effects)
R_b	m/s	Local rate of spread at the most advanced point in the back fire
R_f	m/s	Local rate of spread at the most advanced point in the flank fire
R_h	m/s	Local rate of spread at the most advanced point in the head fire
R_n	m/s	Rate of spread component perpendicular to the fire line element
R_{ij}	m/s	Average rate of spread at the midpoint of a fire line element
R'	-	Non dimensional rate of spread
S_i	-	Generic fire line element at time instant t
S'_i	-	Generic fire line element at time instant $t'=t+dt$
α	º	Slope angle of the fuel bed in relation to the horizontal
β	º	Angle between the local rate of spread and O_0Y_0 axis
β_{ini}	º	Angle of the fire line element at time instant t_0
β_{int}	º	Angle of the back fire line corresponding to a null ω
β'	º	Angle at time instant $t'=t+dt$
$\beta*$	º	Value of β corresponding to the maximum of ω
ε_{av}	1/s	Rate of average relative extension
θ	º	Angle between the local flow velocity and O_0Y_0 axis
$\theta*$	º	Value of θ corresponding to the maximum of ω
ω	º/s	Rotational velocity of a generic fire line element
ω_b	º/s	Rotational velocity of a back fire line element
ω_f	º/s	Rotational velocity of a flank fire line element
ω_{max}	º/s	Maximum rotational velocity

x

1. Introduction

1.1. The forest fires problem

Forest fires: a Nature destructor or just a natural phenomenon?

It is not consensual if forest fires are something undesirable that cause nothing but the destruction of natural habitats and man-made structures, and something that we should avoid and suppress at any cost, or if they are a natural phenomenon that makes part of a healthy natural environment. Most people think of fire as something negative and it is true that, as Man shapes nature in order to satisfy his needs fire often threatens his way of live. In this section, a brief discussion will be made on the negative and positive effects of forest fires, giving a worldwide perspective on the subject, in particular in Portugal.

Despite the negative connotation that most people have towards forest fire, this phenomenon is part of the ecosystems and it contributed to its' shaping for millennia (Beck *et al.*, 2005). In fact Man itself has been using fire for many purposes such as fuel management, reducing pest populations, clearing sites, and hunting. Since the earliest recorded use of fire by hominids 1.5 million years ago (Brain and Sillen, 1988) and with mankind spreading all over the planet, forest fires have been increasingly Man caused, whether intentionally or by negligence, and this became the most common source of wildland fire (Gill, 1981). But forest fires do occur naturally, for example caused by lightning (Pyne, 2001). Many ecosystems, like for example the Mediterranean one, are used to recover from fire and need fire for maintaining healthy conditions (Cramer, 2001). Policies of fire management that try to simply eliminate fire from the ecosystems have recently been questioned and considered to deteriorate the forests health (Kimmerer and Lake, 2001) and, together with climate changes (Viegas, 2007a), are considered as one of the causes of the so called mega-fires, *i.e.* fires of huge proportions, that recently have been occurring all over the world (USA, Australia, Portugal, Greece, etc.).

The forest fire problem worldwide

The problems commonly associated to forest fires are not an exclusive of a given country or region but global problems that affect communities all over the world. Every year we hear about incidents caused by forest fires all over the world, such as the recent examples of the forest fires in California (USA) in 2008, Greece in 2007, and Australia in 2009 where near 200 people were

killed in several forest fires related accidents. But we also verify that neither we get the same amount of information from everywhere in the world, being the most developed countries those who supply bigger amounts of information regarding those issues, nor the forest fires affect all the countries and regions in the same manner. In FAO (2007) a worldwide assessment on Fire Management is made and not only the negative aspects of forest fires are discussed but also the positive ones, recognising that fire is essential to maintain some ecosystem dynamics, biodiversity and productivity. Despite the diversity of situations we can find all over the world, regarding the fires that cause a negative economic and ecological impact, there are common denominators associated to the problem: increasing land use pressure, economic interests and lack of an effective fire management policy either by lack of resources or as in many causes due to an absence of focus in the correct approach to the problem. Although in some regions of the World naturally caused fires can have a significant contribution to the total number of ignitions, in the majority of situations the main causes of forest fires are human related, either by negligence or with intent. In most situations, given the great amount of unknown causes, it is difficult to quantify accurately the human caused fires by arson.

The places where Man interacts or depends upon forests or other landscapes prone to be affected by forest fires are those where fire is most likely to be considered as a serious issue and where a forest management policy is most required. A particular case is the Wildland Urban Interface (WUI), *i.e.* the frontier between forest fuel areas and Manmade structures. Ribeiro (2008) introduces the concept of the Wildland Human Interface (WHI). An example of WHI is a camping park in the forest: although we don't actually have a case of WUI, because a camping park is not necessarily an urban structure, we still have the problem of protecting human lives if a fire comes in that direction. In fact, the priorities of defence against forest fires are the Wildland Human Interfaces.

In order to address the problems commonly associated with forest fires, institutions dedicated to fire fighting and fire management were created. Historically, countries like the USA, Canada, and Australia, are known for having active fire management policies, including fire research. For example in Canada there are fire prevention laws which are over 125 years old and the organized suppression of wildfires began in 1905 (Beck *et al.*, 2005). In the USA the *U.S. Forest Service*, created in 1905, formalized the national approach to wildland protection. In Victoria, Australia, in 1907 the *State Forests Department* was established beginning the formal

management of Victoria's forests, and great awareness of the need for fire protection followed the 1939 fires that caused the death of 71 people, the destruction of entire townships and the razing of millions of hectares of forest and agricultural land.

In South America, that is divided in 13 countries, over fifty percent of the surface area (in a total of 17.450.478 km^2) is covered by forests, but although forest fires represent a serious problem due to the destruction of natural renewable resources, and economic, social and environmental impact, there have not been any effective changes in national policies or in the attitude of the local populations in response to these problems (Julio, 2008).

Africa is the most fire-prone continent in the world and in 2000 eight percent of the continent burned, corresponding in global terms to 64 % of the world's burned area and 54 % of the number of fires (FAO, 2008). It is estimated that forest fires in Africa are responsible for 42 % of the biomass burned globally each year, with major consequences in terms of deforestation and CO_2 emissions. As these fires often spread over large areas, as a result of high plant productivity, relatively low rural population densities and rugged landscapes that are not fragmented by settlements, agricultural lands or roads, a regional assessment of fires in Sub Saharan Africa concluded that the key to effective fire management is to involve agriculture practitioners in using fires in a controlled way.

The Asian continent covers a large area of the world and presents a great diversity in terms of fuels, causes and impacts of forest fires. Nevertheless, in the last decades the number and size of wildfires have increased all over the continent, causing considerable economical and ecological damage (FAO, 2008). Although in some areas some fires are ignited by lightning, the great majority is human caused, either deliberately or by negligence. Considering the importance of the Eurasia/Central Asia's Boreal forest in the functioning of the Earth's climate it is urgent to implement or improve Fire Management policies in those regions.

In Europe, the Mediterranean region is the most affected by forest fires. Nevertheless, the impacts of fire in the Northern and Central European countries should not be overlooked because, in some situations, fires of moderate or low intensity and small extent and that apparently do not have very negative effects, can seriously disrupt the fragile balance of some ecosystems. In the countries of the Mediterranean basin, forest fires cause enormous economic and ecological damage as well as the loss of human lives. The problem is in great part related to the climate, characterized by prolonged dry and hot summers (Durão and Real, 2006). Naturally

caused fires represent a fraction of the total number of ignitions and again people are responsible for most fires. Social issues are behind the problem, such as burning for promoting vegetation growth for grazing purposes, making room for agricultural purposes, attempting to change land-use classification, private vengeance, or generating employment in fire prevention and suppression activities.

The forest fires problem in Portugal

Portugal, being a country of the Mediterranean region, has major problems regarding forest fires and follows the worldwide trend of increasing burned area and number of ignitions in the last decades (Figure 1.1). Although there is a tendency for a moderate increase in terms of burned area since 1980, with two peaks in 2003 and 2005, the raise in the number of ignitions in the same period is overwhelming. Several reasons could have contributed for this tendency, such as demographic expansion, leading to more areas of WUI, and technological development, leading to the existence of more activities prone to originate fires (ex. railroads, agricultural machinery). Nevertheless, beyond the fact that forest fires causes are mostly human, arson seems to have a preponderant role. However, due to the lack of adequate information that results in around 30% of ignitions with undetermined causes every year (Damasceno and Silva, 2007), it is very difficult to quantify the real amount of purposely set fires, in particular those which aim to obtain any type of benefit.
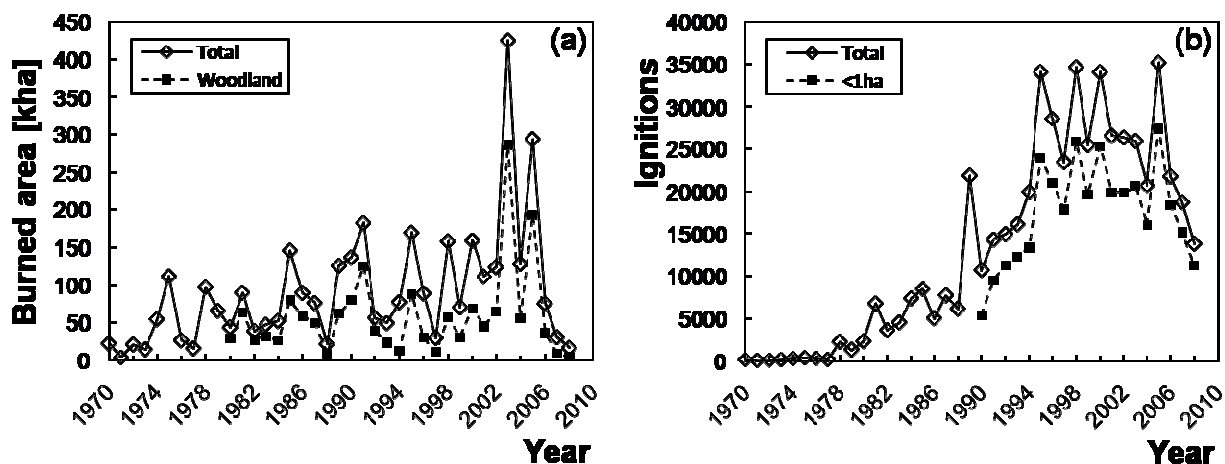

Figure 1.1 – Statistical data related with forest fires in Portugal between 1970 and 2008 (source: *DGRF*): (a) Burned area. (b) Number of ignitions.

4

There are three measures that would be of paramount importance towards minimizing the negative impacts caused by forest fires in Portugal. Firstly, it is essential that fire managers understand that fire is part of the Mediterranean ecosystems and cannot and should not be eliminated. People from rural areas should not be prohibited from burning nor obliged to go through difficult or expensive bureaucratic processes to obtain a burning permit, since this will only create disrespect with authorities as people will try to burn clandestinely, increasing the risk of negative consequences that sometimes even lead to the loss of human lives. Instead, conditions should be created for them to easily obtain a burning permit and to burn with safety, involving for example volunteer firefighters. Secondly, an effort should be made for increasing people awareness regarding fire: people from rural areas who use fire must understand that basic safety measures must be applied, preventing the loss of lives and the occurrence of uncontrolled forest fires that have many negative short term impacts but also long term ones, such as on climate; people who live outside the rural areas should not think of fire as something purely negative that must be eliminated at all cost and that fire sometimes can be used as a managing tool with many positive effects. Finally, mechanisms should be created to systematically investigate and determine fire causes. Those who are proved to be directly or indirectly responsible for arson with the purpose of obtaining any type of benefit should be severally punished. The population cannot have the feeling that one can commit this type of crime and end unpunished and must understand that forest fires have very negative impacts, not only in the forests and other ecosystems that are burned but also in the amount of greenhouse gases that are released to the atmosphere, that cause great pollution and have a great impact on climate change. Everyone must think in what kind of legacy we want to leave for our children and understand that sustainability is the key for building a world in which we are in equilibrium with Nature.

The importance of studying forest fire behaviour

It is clear that forest fires are associated with many negative impacts that generally are highlighted in relation to positive ones, especially because wildfires can cause massive destruction and unavoidably, as Man has to deal with the problem of fire fighting and since fire is a hazardous phenomenon, often people get injured or killed, either when involved directly in fire suppression activities or sometimes in collateral events (Viegas, 2004c; Viegas *et al.*, 2006a).

Research is of paramount importance to assess a wide variety of issues related with forest fires such as fire effects in the ecosystems, hazards associated with the Wildland-Urban Interface, firefighter's safety, smoke dispersion in the atmosphere, and forest fire behaviour, among many others. A better knowledge of each of these subjects has great importance to minimize wildfires negative impacts. In particular, forest fire behaviour studies can have a major contribution for improving the effectiveness of fire management both in suppression and prevention activities, fire fighters safety, definition of prescribed burning conditions that would minimize negative impacts in the ecosystems, etc. This work aims to contribute to a better understanding of fire behaviour and to improve the global knowledge on the phenomenon.

1.2. The study of forest fire behaviour

Scope of this section

A review will be made on the research on surface forest fire behaviour, in particular fire behaviour modelling. Crown fires, ground fires and spotting will not be considered. It is not intended however to make a detailed approach to the subject but instead to have an overall look at what has been done since the beginning of the twentieth century. Many reviews have been made, like in Catchpole and de Mestre (1986), Weber (1991), Perry (1998), André and Viegas (2001), André and Viegas (2002), Pastor *et al.* (2003) and Sullivan (2009a, 2009b, 2009c), that can be consulted by those who wish to have more information regarding this subject.

Types of forest fire behaviour models and calculation systems

A fire behaviour model is usually a set of equations whose solution gives numerical values corresponding to parameters that characterize fire spread properties, such as the rate of spread (ROS), the flame geometry, and the amount of energy released during the combustion process. In this work, fire spread models shall be classified as physical (or theoretical), semi-physical (or semi-empirical) or empirical. This classification is used by many authors although sometimes the definition of each type of model might vary. The definition of each modelling approach considered here will be described below.

Physical or theoretical models are those based on the laws that govern fluid mechanics, combustion and heat transfer (Pastor *et al.*, 2003). One major advantage of physical models is that they are based on known relationships, which facilitates their scaling (Chandler *et al.*, 1983;

Weber, 1991). However, there are various reasons hindering their widespread use and development: they are very complex, the input parameters are very difficult to obtain, simulations require great computation power and large periods of processing time when using personal computers, and it is difficult to accurately model all the phenomena involved in the complex and dynamic process of combustion through forest fuels. Due to these limitations these models are still far from being built into operational fire management tools.

Semi-empirical models result of a combination of physical and empirical modelling techniques (Perry, 1998) and use some form of physical framework upon which to base the chosen statistical modelling. They do not provide a physical process for the transfer of heat from the combustion zone to the unburnt fuel and use data from field or laboratory experimental fires for determining the parameters necessary to close the problem.

Empirical models are in essence a statistical description of wildland, field or laboratory test fires and make no attempt to incorporate any physical process. As they are developed for a particular set of conditions, their lack of a physical basis means that their use outside of these conditions must be made with caution (Catchpole and de Mestre, 1986).

The ultimate aim of a fire spread model is fire behaviour prediction. A *Fire Behaviour Prediction System* is obtained by using adequate methods for incorporating fire spread models into fire growth simulators and its objective is to enable an end user to carry out useful estimations of fire perimeter evolution (Sullivan, 2009c) that can be used as a *Support Decision System* in fire management, both in suppression and prevention operations. The increasing computation power of personal computers, that in the last three decades became accessible to practically everyone, made possible the implementation of mathematical fire behaviour prediction models that could be used at a broad scale by forest fire managers. There are two types of computer simulation models: i) those which work as independent software; ii) those who operate with a *Geographic Information System* (GIS) as a platform. In the second case it is possible to integrate the simulation output and the landscape data and, using methods like bond percolation or cellular automation simulation techniques (discrete propagation) or elliptical wave propagation (continuous propagation), to estimate fire growth. Examples of a computer simulation model working as independent software or integrated with a GIS are *Behave* (Burgan and Rothermel, 1984; Andrews, 1986; Andrews and Chase, 1989) and *FireStation* (Lopes *et al.*,

1998), respectively, both using the Rothermel (1972) propagation model. Many simulation models integrated with GIS use Rothermel's model.

Previous work on surface forest fire behaviour

The physical and chemical processes involved in forest fire spread are very complex and the understanding of the individual aspects of the phenomenon requires a great knowledge of combustion, heat transfer, fluid mechanics, and chemistry. Also one must have in mind that, as this is a reacting system, changes in the conditions of an individual process will interfere with the remaining, making forest fire behaviour modelling a very difficult task. The development of a fire behaviour prediction model that could accurately compute the spread parameters, such as the ROS and fireline intensity, at a field scale, is still far from the present state of the art on fire behaviour modelling, despite the technological and scientific means that we have nowadays.

In an early work of Show (1919) the flammability of litter is assessed as related with fuel moisture content variation with climate seasonal changes along the year. The author also analyzed the fire perimeter evolution, as a measure of ROS of 33 small field experiments, concluding that the fire perimeter increase varies as the square of wind velocity. After almost two decades Curry and Fons (1938) presented data from around 160 field experiments of surface fires performed in *Pinus ponderosa* litter and proposed an empirical model equation for predicting the perimeter evolution as a function of time, wind velocity, fuel moisture content and slope. Few years later Fons (1946) developed the first theoretical model for the ROS of a forest fire by establishing an energy balance between the fire and the fuel particles, considering heat transfer by convection and radiation, and used laboratory experiments performed in a wind tunnel using ponderosa pine needles and vertical ponderosa twigs for parameter determination and for the model validation.

Several aspects of the combustion of forest fuels are described in some detail in Byram (1959) such as the chemistry of combustion, phases of combustion, heat release, heat transfer, fuel size and arrangement, retardants and inhibitors of combustion, and fire intensity. Byram concluded that the heat energy release by burning forest fuels does not vary widely between different types of fuels, for a complete combustion reaction and referred to the fire triangle (fuel, oxygen and temperature) highlighting that the purpose of all fire suppression efforts is to break or weaken, directly or indirectly, one or more sides of the triangle. He proposed the well known

equation for determining the linear fire line intensity as a function of the fuel heat of combustion, weight of fuel consumed per unit area, and linear ROS ($I = H.w.R$) and also an empirical equation for estimating the flame length as a power law function of the fire line intensity.

Until the 60's, research on forest fires was scarce and lacking of guidelines showing researchers common approaches that would enable focus on particular aspects of fire behaviour allowing an improvement of key knowledge towards common objectives. In this new period of fire research, the first trend was the development of physical modelling with Thomas (1960, 1963), Hottel (1961), Taylor (1961) and Thomas (1964) making theoretical analysis of static fires, the first using wood crib fires and the last three using gas burners. Work on the physical modelling of spreading fires also arose with Fons *et al.* (1963), Thomas and Simms (1964), Thomas and Law (1965), and Thomas (1967) using crib fires for developing their models of fire spread on level ground, with the last two accounting for wind effect. Hottel *et al.* (1965) and Anderson (1969) also proposed physical models for fire spread on level ground in the absence of wind with the first using laboratory experiments in fuel beds of newsprint, rectangular computer-card punchings and computer card squares to evaluate the model and the second using fuel beds of pine needles. Albini (1967) developed a theoretical model for fire spread on level ground in brush fuels with elementary account of the wind effect by adjusting the tilt flame angle.

In parallel with the approach of theoretical studies using small scale laboratory experiments for testing the models, a new line of research using wider sets of laboratory experiments at a larger scale and testing a broad range of parameters started to emerge. Eventually, the results obtained by those means would become the basis of semi-physical and empirical modelling that, especially due to their simplicity, had great acceptance within the scientific community but also among operational professionals. Anderson (1964) performed 32 laboratory experiments of fire spread, on level ground with no wind in fuel beds of pine needles, in a facility where the air temperature and relative humidity could be conditioned, presenting a summary of the test data and main results and analysing the influence of several fuel bed properties on the ROS. Anderson (1968) analysed the radiation emission from a flame and the flame width influence on the ROS, using laboratory experiments in fuel beds of pine needles. Rothermel and Anderson (1966) also performed laboratory experiments in fuel beds of pine needles, with controlled air temperature and relative humidity, on level ground under the influence of wind and presented empirical relationships for predicting the ROS. They concluded

that, in the absence of wind, radiation is the prevalent way of heat transfer but with wind, convection plays an important role heating the fuel ahead of the fire. Van Wagner (1968) presented laboratory and field experiments on red pine plantation surface fuels, performing back and head fires, and analysing wind or slope effects. Field experiments would also come to gain popularity as an alternative for laboratory experiments or, as in many cases, as a complement. McArthur (1966, 1967) presented a very wide set of results from field experiments, in the first work for grassland fires on level ground in the presence of wind, and in the second work for eucalyptus forests fires, assessing several parameters effects on fire spread such as fuel moisture content, fuel load, wind velocity, and slope. He also proposed the well known *Forest Fire Danger Meter*. Woolliscroft (1968, 1969a, 1969b) also presented some results of field experiments on shrub fuels, mostly on level ground, for head and backing fires in a light wind.

In the decade of 70, physical modelling continued to deserve the attention of researchers, with more attention being given to wind effects and sometimes slope. Pagni and Peterson (1973) developed a theoretical model for fire spread on level ground accounting for wind effect and compared the model against laboratory experiments from Rothermel and Anderson (1966). They concluded that with no ambient flow the dominating preheating mechanism is flame radiation but for nonzero wind velocities, although radiation still has a significant role, convection dominates preheating. Cekirge (1978) used the finite difference method for developing a theoretical model considering wind as influencing convective transfers and flame geometry as influencing radiative heat transfers. Telisin (1974), on the other hand, proposed a theoretical model based on flame radiation, within and above the fuel bed, assuming that radiation above the fuel bed preheats only a surface layer of fuel. The model accounts indirectly for wind or slope effects by considering the flame length and tilt angle. These last two authors both compared their models results against field experiments data from Woolliscroft (1968, 1969a, 1969b).

During the 70's, field experiments and especially consistent sets of laboratory experiments assessing the effect of a wide type and range of parameters continued to gain popularity. Packham and Pompe (1971) measured effective radiation temperatures of around $900\,°C$, making one field experiment in which they burned one pile of slash. Beyreis *et al.* (1971) also analysed radiation, determining the emissivity of wood crib flames on level ground, and also estimated the convective heat transfer coefficient. Frandsen (1971) developed a semi-physical model for fire spread on level ground in the absence of wind, that would become the basis of the Rothermel's

(1972) model. This semi-physical model is probably the best known fire spread model and is incorporated in many operational systems of fire behaviour prediction, such as *Behave* (Andrews *et al.*, 2003) and *Farsite* (Finney, 1998). The model's parameters, including those that account for wind and slope effects, are determined using a wide set of laboratory experiments using fuel beds of pine needles, excelsior, wood cribs, and wood sticks. Frandsen (1973a) performed laboratory experiments in wood cribs on level ground with no wind and determined an empirical relation for estimating the effective heating of fuel ahead of a spreading fire, *i.e.* the fractional amount of the bulk density effectively brought to ignition. The same author (Frandsen, 1973b) proposed the use of that effective heating number for solving an inconsistency in the Rothermel's (1972) model that obtains different results inserting a given fuel load as one category or inserting the same fuel load split into two or more categories. Thomas (1970), based on field experiments in shrub fuels mostly on level ground but under the effect of wind, concluded that head fires spread at a rate significantly faster that could be accounted just by considering radiation heat transfer. Thomas (1971) used field and laboratory experiments in wood cribs on level ground for analyzing the influence of wind on the ROS and presented semi-physical derived heat balances. Van Wagner (1977) made a comparison between results from five other references for fire spread on a slope including field fires and Rothermel's (1972) model results, and based on the entire set of data proposed an empirical equation for estimating the slope effect.

Wind is widely recognized as one of the most influencing parameters on fire spread and for this reason many spread models account for favourable wind effect. As most models are developed for spread on level ground, many authors assume that slope enhances fire spread by bringing the flame closer to the fuel bed, just like the wind does, and estimate slope effect by considering an equivalent wind to that slope. However, slope and wind effects are not usually considered to be additive. Given the importance of wind, it is common to find research that aims to provide methods for determining wind velocities that can be inputted in fire behaviour prediction models. In Baughman and Albini (1980), in a similar work to that of Albini and Baughman (1979), methods are presented for determining the mid-flame wind velocity over the vegetation cover and under a forest canopy, and in Albini (1982) semi-physical modelling is used for analysing the response of fires intensity and ROS to non-steady winds.

As researchers continued working on physical modelling we started to see more variety in the approaches used to solve the problem and also focus on other parameters other than simply

11

the ROS. Fuji *et al.* (1980) tried to develop a physical non-stationary model formulated as a free boundary problem, called a Stefan problem, for fire spread on level ground in the absence of wind but considering it can be included by changing the coefficient of heat transfer by convection. The model was compared with data from Emmons and Shen (1971). Albini (1981) proposed a physical model to estimate flame geometry comparing it against data from Anderson and Rothermel (1965) and Rothermel and Anderson (1966). In Hwang and Yusheng (1984) the theoretical modelling of Vogel and Williams (1970), for the flame propagation on horizontal matchstick arrays, was extended for estimating the ROS along inclined arrays and laboratory experiments of flame propagation along matchstick arrays on inclined base boards with inclinations of 0º, -20º and 20º, -40º and 40º were used for validating the model. Albini (1985) proposed a physical model, based on radiation heat transfer, for estimating the ROS and the shape of the ignition interface between the flame and the fuel, defined by the ignition temperature isotherm. Flame height and tilt angle were determined using three laboratory experiments on level ground and still air in excelsior, and used as model inputs. In Albini (1986) that model was improved by including fuel cooling by natural convection. De Mestre *et al.* (1989) formulated a physical model based on radiative heat transfer, for fire spread on level ground in the absence of wind and, testing it against a laboratory experiment in a pine needles fuel bed, concluded that if not including convective cooling the ROS would be highly overestimated. Weber (1989) developed a physical model based on radiative heat transfer, for fire spread on level ground in the absence of wind, applying it to a planar fire front and to a curved fire front caused by a point ignition, concluding for the second situation that after an initial acceleration the fire reaches a steady state ROS.

Nelson and Adkins (1988) used data from 59 laboratory and field wind-driven experiments extracted from the literature and from other 6 field fires, in diverse fuel beds such as grass, pine logging slash, and excelsior, and using dimensional analysis derived a semi-physical model for fire ROS as a function of fuel consumption, ambient wind velocity, and flame residence time, concluding that the strong correlation between dimensionless forms of the ROS and wind velocities indicates that all essential variables were included in the analysis. Van Wagner (1988) in a study of fire spread downhill, a subject that at that time did not deserve much attention and still does not, presented an empirical model function for relating the ROS with the slope angle for back fires in the range -45 to 0º, based on 22 laboratory experiments in fuel beds of pine

12

needles, concluding that the ROS decreased from 0º to -20º, increasing again from -20º to -45º where it attained a value equal to level ground. Also using experimental fires, Nelson and Adkins (1986) used video techniques to determine relationships between flame characteristics and fire behaviour from 22 laboratory experiments in a wind tunnel and 8 field experiments, concluding that relationships between flame tilt angle, flame height, and wind velocity, observed in wind tunnel experiments are not in agreement with theories of the structure of buoyant flames.

The ROS is without any doubt the parameter that most fire spread models aim to estimate. However, predicting other variables, such as fireline intensity, could be of great utility in fire management activities, for example when trying to assess the means to use when fighting a fire or when evaluating the impacts of a prescribed or wildfire. Rothermel and Deeming (1980) proposed methods for quantifying the heat per unit area and fireline intensity from observations of flame height and ROS. Alexander (1982) also referred to the importance of the fireline intensity as a means to assess fire effects and to objectively compare different fires and Catchpole *et al.* (1982) made a mathematical determination of the Byram's (1959) fireline intensity along an elliptical fire front perimeter.

There was a significant increase of papers on forest fire behaviour in the decade of 90 that corresponded not only to more volume of publications on already studied subjects, but also to work coming from new approaches, coinciding with the appearance of new researchers or with the growing of the scientific work from already known ones. Physical modelling, for example, continued representing a similar number of papers but in global terms loosing share to semi-physical modelling. Baines (1990) discussed the physical processes that affect the ROS on a surface fuel bed and defined a dimensionless number to quantify if the flame radiation alone is capable of sustaining fire propagation. Carrier *et al.* (1991) developed a physical model for wind-driven fire spread on level ground concluding that convection and diffusion are the dominant mechanisms of preheating of unburned fuel and that the ROS is proportional to the ratio between wind velocity and the mass of burnt fuel, at least for the range of parameters analysed in the laboratory experiments presented in Wolff *et al.* (1991), in arrays of thin woody fuel elements. The authors performed around 50 experiments, testing a wide variety of situations such as different fuel beds, assessment of the addition of non combustible elements, variable load, and variable fuel bed width including tapered fuel beds. Lyons and Weber (1993), using laboratory experiments, concluded that *Eucalyptus globulus* individual leaves can be a good predictor of the

ROS under no-wind and no-slope conditions. In Albini and Reinhardt (1995), Albini *et al.* (1995), and Albini and Reinhardt (1997), a physical model for the time delay to ignition and weight loss of a moist woody cylinder immerged into a fire environment was formulated and calibrated, using data from laboratory experiments and prescribed burns. Beer (1995), following the work of Weber (1990), presented a geometrical theory for fire propagation trough arrays of vertical fuel elements, accounting for the effects of wind, concluding that the model performed well only at low wind velocities, below around 0.5 m/s.

Regarding the use of new approaches in modelling, Lopes *et al.* (1995) developed a theoretical model for the simulation of the wind flow in canyons that is afterwards used in a fire spread simulation system that uses the Rothermel's (1972) spread model, the double ellipse model for estimating fire growth, and Dijkstra's (1959) algorithm for simulating the fire propagation from cell to cell. From numerical simulations they concluded that the highest ROS were observed in the more narrow canyons. The use of atmosphere and fire growth simulation systems, called atmosphere-fire coupling, would gain some popularity in the following years. Porterie *et al.* (1998) used physical modelling, based on the new approach of Grishin (1997), including the plume vertical development for fire spread on a slope on a non-homogeneous fuel bed constituted by several phases. They compared the model against laboratory experiments in fuel beds of pine needles with slope angles of -20, 0, and 20º, concluding that the results give a faithful reproduction of slope effects and also lead to realistic ROS.

As referred above, semi-physical modelling was responsible for many publications in the 90's, with a significant contribution from Australian researchers. Catchpole and Catchpole (1991) proposed a model for the moisture damping process for incorporating in Rothermel's (1972) model, testing it against field experiments from Van Wilgen *et al.* (1985), concluding that the results from the original model were improved. Viegas and Neto (1991) proposed the use of the wall shear-stress as an alternative to the use of the mid-flame height, concluding that it can be related with the wind velocity measurement at a fixed standard height, addressing the problem of the uncertainty of the wind velocity to use in fire spread models derived from the change of the flame geometry. Beer (1993) analysed the ROS dependence on the wind velocity using a model function proposed by Rothermel (1972), but incorporating a non dimensional wind velocity. The author determined the fit parameters from field and laboratory experiments. Cheney *et al.* (1993) used a multiple regression analysis of data from 121 field experiments, in grass fuels on level

ground under the effect of wind for relating fire spread with fuel, weather, and fire shape. It was concluded that fuel load did not have significant influence on the ROS but, on the contrary, the ignition line length was found to have great influence on fire behaviour. Cheney and Gould (1995) proposed an empirical model function for estimating the ROS as a function of the wind velocity and the width of the head fire, based on data from a series of field experiments on level ground in open grasslands and eucalypt woodland with a grassy understorey. Catchpole *et al.* (1998a) developed a semi-physical model for wind-driven fire spread on level ground. They performed 357 experiments, testing fuel beds of regular poplar excelsior, coarse poplar excelsior, pine needles, and pine sticks, and tested their model and three other ones (Rothermel, 1972; Nelson and Adkins, 1988; Carrier *et al.*, 1991), concluding that theirs gives better estimations.

Laboratory experiments continued being used as valuable tools, not only to serve as a base for modelling, but also to assess fire behaviour. Catchpole *et al.* (1993) performed laboratory experiments of fire spread on level ground in a wind tunnel on mixed fuel bed complexes of wood excelsior and wood sticks and concluded that Rothermel's (1972) model needed modification for estimating fire behaviour in those fuel beds. Ventura *et al.* (1998), following the work of Ventura and Rego (1998) where a description of the modelling of temperature-time curves from laboratory and field experimental fires was made, assessed the vertical temperature profile and ROS of fire spread under the joint effect of wind (-3 to 3 m/s) and slope (-15 to 15º), using fuel beds of pine needles. Due to the test rig functioning constraints, back-wind upslope and wind-driven downslope fire could not be simulated. Weise and Biging (1997) also performed laboratory experiments under the joint effects of wind (-1 to 1 m/s) and slope (-17 to 17º) in fuel beds of vertical paper birch sticks mixed with aspen excelsior, for comparing the results of four fire spread models: CFBPS (Forestry Canada Fire Danger Group, 1992), McArthur's Mark V (Noble *et al.*, 1980), Rothermel (1972), and Pagni and Peterson (1973), using three methods for combining wind and slope (Albini, 1976; McAlpine *et al.*, 1991; Rothermel, 1972) yielding nine variants of the four basic models.

Another subject that gained the attention of some researchers was the development and testing of fire spread prediction systems. French *et al.* (1990) made a comparison of four methods for computing simulations of forest fires: three of them grid models (Kourtz and O'Regan, 1971; Frandsen and Andrews, 1979; Green, 1983) and the fourth (Anderson *et al.*, 1982) an analytical method, based on the Huygens' Principle. Ball and Guertin (1992) proposed

a raster (discrete propagation) based GIS system for fire growth using the Rothermel's (1972) model, and Catchpole *et al.* (1992) proposed a method for determining the proportion of the total perimeter and area burned for a specific range of Byram´s fire line intensity.

Some papers do not address a specific subject but instead aim to analyse and discuss several issues related with forest fires. For example, Cheney (1990) discussed several aspects related with the difficulty of describing and quantifying forest fires, concluding that Byram´s fire line intensity is useful to quantify and assess some fire characteristics and effects but should not be used to compare fires in fuel types that are structurally very different. Gill and Knight (1991) presented some extreme values of fire properties reported by other authors and discussed issues related with fire behaviour monitoring, concluding that when assessing fire behaviour, the use of instruments and methods that do not depend on the observer's subjectivity are preferable and that they should be chosen based on several aspects such as purpose, cost, and location of the measurement. Albini (1993) discussed some forest fires related aspects such as combustion, fire spread and growth, heat generation and fire intensity, fuel properties, and environmental factors.

Recent research and trends in forest fire behaviour modelling
In the last decade, research on forest fire behaviour continued growing and, despite the attention that empirical modelling continued having, in the last years we have been seeing a considerable increase of physical models that was responsible by the inversion of the tendency we had in the 90's of physical modelling losing share to empirical approaches and to other research. We continued having models based on the heat transfer between the flame and the unburned fuel, mostly based on radiative heat transfers with convection playing a secondary role or most of the times being ignored. For example, Vaz *et al.* (2004a) proposed a theoretical model based on a modular structure of sub-models for fire spread on level ground in the absence of wind, testing it against one laboratory experiment in a fuel bed of pine needles.

However, a new generation of physical models, incorporating the combustion reaction and the fire plume, was increasingly being chosen as the approach to simulate fire behaviour. Séro-Guillaume and Margerit (2002) derived a three-dimensional forest fire combustion model based upon global balance laws of mass, energy and momentum, like in the models proposed by Grishin (1997) and Larini *et al.* (1998). In Margerit and Séro-Guillaume (2002) three possibilities of reduction to two-dimension reaction diffusion models of the combustion model

16

were presented and the simplest reduction possibility is then used for obtaining numerical simulations of fire spread. Simeoni *et al.* (2001) proposed a theoretical model, following work from Balbi *et al.* (1999) and Morandini *et al.* (2000), for fire spread under the joint effects of wind and slope, testing the model against laboratory experiments from Ventura *et al.* (1998) that were described previously. Simeoni *et al.* (2003) improved that model by considering the buoyancy effect induced by combustion in the flaming zone. Morandini *et al.* (2002) proposed a two-dimensional physical model for fire spread under the combined effects of wind and slope, assuming they are independent and additive and again the experiments from Ventura *et al.* (1998) were used for validating the model. Morandini *et al.* (2005) merged the two previous approaches of Morandini *et al.* (2001) and Simeoni *et al.* (2003), proposing a non stationary model for fire spread under the joint effects of wind and slope, considering radiative and convective preheating ahead of the fire front. The authors performed laboratory tests of horizontal spread in still air for determining experimental parameters and used data from Ventura *et al.* (1998) for validating the model.

Like previously referred, semi-physical and empirical modelling continued to be the selected approach of many researchers. For example, Marsden-Smedley *et al.* (2001) developed an empirical model for the probability of fire extinguishment as a function of wind velocity, dead fuel moisture, and fuel load, using data from 156 field experiments on buttongrass moorland, and concluding that fires will self-extinguish easily in low productivity moorlands but in medium productivity moorlands the self-extinguishment will be much more restrictive. Nelson (2002) proposed a trigonometric method to combine the ambient wind velocity with an upslope component to derive an effective wind velocity and, using the Rothermel's (1972) fire spread model, tested it against laboratory experiments data from Weise (1993) that are also presented in Weise and Biging (1997). Sullivan *et al.* (2002) proposed a semi-physical method for determining the radiant heat flux from burning logs behind the fire, concluding with basis on field experiments that it provides reasonable estimates of the minimum time for the radiant heat flux to drop below the threshold values for pain and long-term survival. In Viegas (2002) the evolution of a linear fire line on a slope was analysed, using laboratory experiments under slope effect on fuel beds of pine needles and field experiments on shrub fuels, showing that the fire front tends to rotate and to become parallel to the slope gradient direction. The same author (Viegas, 2004a) also analysed fire spread under wind or slope effects, for assessing the existence

of a steady state of fire propagation for constant boundary conditions. Using laboratory experiments in fuel beds of pine needles of fire spread, caused by linear and point ignitions under favourable and contrary wind or slope effects, and of fire spread in a canyon test rig, concluded that, in the general situation of wind or slope fires, the existence of a steady state is not proved. In Viegas (2004b), using laboratory experiments in fuel beds of pine needles, a geometrical analysis of fire spread under the joint effects of wind and slope similar to that presented in Nelson (2002) was made. Streeks *et al.* (2005) analysed fire behaviour in mesquite-acacia shrublands in South Texas, based on three field experiments, comparing the data against the results from two fire behaviour prediction systems: *Behave* (Andrews *et al.*, 2003), *CSIRO* (McArthur, 1966, 1973; Cheney *et al.*, 1993, Cheney and Gould, 1995), and three shrubland fire behaviour models: Vega *et al.* (1998), Fernandes (2001), and Catchpole *et al.* (1998b). Following the work of Viegas (2002), Oliveras *et al.* (2006) analysed the existence of rotation of the fire line elements of line perimeter originated by a point ignition under slope or wind effects, based on 23 laboratory experiments in fuels beds of pine needles, in a wind tunnel (1-4 m/s) and in a slope test rig (0-40º), concluding that in point ignition fires there is a tendency for the flanks to become parallel to the maximum slope/wind direction. Higgins *et al.* (2008) proposed two empirical equations for computing the fire line intensity and two semi-physical equations for estimating the ROS of grassland fires, afterwards inputted into the Byram's (1959) fire line intensity equation. The parameters necessary to the four models were determined by statistical analysis of field experiments data from Trollope (1998) and the computed intensity results were compared against field experiments data from Williams *et al.* (1998) and Shea *et al.* (1996). Zhou *et al.* (2005) and Weise *et al.* (2005) developed a logistic regression model for predicting the probability of successful spread, based on laboratory experiments for determining the effects of wind, slope, moisture, and fuel characteristics in fuel beds of four chaparral species. Their final model correctly classified over 90% of more than 100 fires. Sun *et al.* (2006) performed experimental burns of three types of live and dead chaparral fuels in a cylindrical container, assessing parameters like the mass loss rate, flame height, and vertical temperature profile, and proposing power laws for the flame height as a function of the heat release rate.

Many other studies contributed for the knowledge of forest fire behaviour and related subjects, like Sullivan and Knight (2001) that proposed an equation for estimating the accuracy of the wind affecting the fire front based on a statistical analysis of wind velocity measurements

data, gathered during Project Vesta (1996-2001), using 20 grid displaced anemometers. Mendes-Lopes *et al.* (2003), based on the laboratory experiments of Ventura *et al.* (1998) previously described, assessed the flame characteristics, vertical temperature profile, and ROS data from a total of 192 laboratory experiments of fire spread under the joint effects of wind and slope, concluding that the ROS increases steeply with wind and slightly with slope and does not depend on wind velocity or slope for backing fires. Vaz *et al.* (2004b) proposed a method for estimating the radiation extinction coefficient of solid porous natural fuel beds and, using samples of pine needles, concluded that it produces better results than the standard formula. Butler (2006) assessed the effect of solar radiation on the fire ROS, based on 63 laboratory fire spread experiments in the absence of wind on a horizontal fuel bed of aspen excelsior, simulating solar radiation with halogen lamps and concluding that low magnitude surface incident irradiation, such as solar heating, can affect the ROS. Morandini *et al.* (2006) conducted a field experiment under wind conditions in Mediterranean shrub vegetation, assessing flame geometry, vertical temperature profile, and emitted radiation ahead of the fire front, concluding that fire behaviour and flame structure are very different from those at laboratory scale and that it is possible to measure thermodynamic quantities in the field, provided the wind characteristics, flame front temperature and emitted radiation are recorded successfully.

During fire propagation in a given fuel complex, in the general case we have to account for the joint effects of slope and wind. But we can consider that the fuel properties and topography are constant, at least for a given area of variable size. The same is not valid for the combustion process properties and atmospheric conditions that are constantly interacting and changing with time. Byram (1959) referred that, because of their storm characteristics, the behavior of high-intensity fires could be studied best from a meteorological point of view. For this reason, a thorough knowledge of the combustion process and its interaction with the atmosphere is probably the key for accurately predicting fire behaviour. The theoretical models that incorporate the combustion reaction and the fire plume address that part of the problem, provided that all the relevant phenomena are considered and correctly described. Despite the disadvantages in terms of complexity and high computational power demands, that many times is insufficient for providing real time simulations, those models do not have the same restrictions as empirical ones do when changing the parameters for which they have been developed. Those changes can be responsible for significant differences between predictions and actual rates of spread. However,

recent research in atmosphere-fire coupling, *i.e.* use of atmosphere simulation models for simulating the air flow dynamics caused by fire and feedback the results into the fire spread model, shows that, when considering fire effects on the wind flow dynamics, even simple empirical models seem to provide good results. This suggests that fire influence on the atmosphere is probably one of the major causes for the fire dynamic effects, being responsible for considerable discrepancy between predicted and observed fire behaviour, not only for empirical models but also for physical and semi-physical ones. It is curious, like *Carrier et al.* (1991) referred that, although convective heat transfers are frequently overlooked, many rapid fire spread events are associated with enhanced wind-aiding. After the pioneer work of Lopes *et al.* (1995), that to the present author's knowledge is the first work in atmosphere-fire coupling, many more arose. Linn *et al.* (2005) made an incorporation of discrete porous fuel beds, including canopy and understorey fuels, into a coupled atmosphere-fire behaviour model. The modelling framework is composed by the atmospheric model HIGRAD (Reisner *et al.*, 2000) and the theoretical wildfire behaviour model FIRETEC (Linn, 1997). The same model HIGRAD/FIRETEC is used in Linn *et al.* (2007) for studying the joint effects of inhomogeneous topography and wind, testing five topographies (flat terrain and four non-trivial topographies) combined with ambient wind velocities of 6 and 12 m/s, yielding ten simulations. In Mell *et al.* (2007) a three-dimensional coupled atmosphere-fire theoretical model for simulating fire spread over surface fuels on flat terrain was developed. The modelling approach is similar to that of multiphase models, like in Porterie *et al.* (1998), but allows simulations in three dimensions and due to computational constrains coarser grids are used. The model was tested against 16 field experiments on grassland fuels (Cheney *et al.*, 1993) for evaluating the ROS results and against 2 additional experiments for evaluating the behaviour of the entire fire perimeter. In Sun *et al.* (2009) coupled wildfire-atmosphere large eddy simulations of grassland fires, reported in Cheney and Gould (1995), were used to examine the differences in the ROS and area burnt by grass fires in two types of atmospheric boundary layer (ABL): buoyancy-dominated ABL or convective boundary layer (CBL) and roll-dominated ABL (RBL). The University of Utah's Large Eddy Simulation (UU-LES) model, proposed by Zulauf (2001), was used coupled with an operational empirically-based fire behaviour model (Forestry Canada Fire Danger Group, 1992), presented in Hirsch (1996). It was concluded that initially identical fire lines evolved differently

20

in the same ABL, with fire-induced convection appearing to be the main contributor to the variability in fire ROS and area burnt.

Current theoretical models accounting for flow dynamics are still not able to simulate real fire spread, due to the lack of incorporation of all the relevant phenomena and demand of huge computational power. Coupled atmosphere-fire models, even using semi-physical or empirical fire spread models, also require considerable computational power. Coen (2005) used coupled atmosphere-fire modelling simulation of the Big Elk Fire for assessing whether some factors that make simulations more computationally demanding, such as atmosphere-fire coupling and fine atmospheric model resolution, are needed for producing accurate predictions. The model uses an atmospheric model (Clark *et al.*, 2004) coupled with the Rothermel's (1972) model for USA fuel complexes or Noble *et al.* (1980) model for Australian fuel complexes, and a *BURNUP* type algorithm (Albini and Reinhardt, 1995; Albini *et al.*, 1995) for estimating the consumption of fuel mass with time. It is concluded that, although the atmosphere-fire feedback must be included for obtaining good estimations of fire growth, simulations with relatively coarse atmospheric resolution (grid spacing 100-500 m) can produce good results and can be performed over six times faster than real time on a single processor computer, whereas the simulations with fine atmospheric resolution would take more than eight times the real time. It is also concluded that atmosphere-fire interactions are observed at least up to 5 km from the fire.

Another approach to the problem is to incorporate wind flow dynamics in semi-physical or empirical models. Viegas and Pita (2004) analysed fire spread in canyons using laboratory experiments in fuel beds of pine needles and a field experiment in shrub fuels, concluding that the fire ROS is not constant, and proposed an analytical model that assumes elliptical growth of point ignition fires. Viegas (2005) proposed a semi-empirical model for fire spread in canyons, based on laboratory experiments in fuel beds of pine needles, and used it for the simulation of the ROS evolution of the South Canyon and Thirtymile fires, and in Viegas (2006) made a parametric study of the model.

In the last 70 years a considerable amount of research has been done on forest fire behaviour. However, a lot still has to be done in order to fully understand forest fire behaviour since nowadays fire behaviour prediction models are still unable of accurately estimate fire spread, at least at the field scale. In the author's opinion, a better description of the wind flow dynamics as influenced by fire, and account for the respective feedback effect, is the key for

major improvements of fire behaviour predictions, whether by including those effects in theoretical fire spread analysis or by coupling atmosphere dynamics with fire spread models. In that sense, atmosphere-fire coupling, using optimized atmospheric modelling techniques (Coen, 2005) together with simple fire spread models, seem to presently have some advantages when compared to theoretical models that attempt to solve the problem altogether and that currently still have prohibitive computational demands for simulating field scale fires faster than real time.

1.3. Present work

This work aims to develop a calculus algorithm for computing the fire perimeter evolution of a point ignition fire under the effect of wind or slope. For accomplishing this objective, a study of favourable and contrary wind or slope effects on surface fires spreading in fine fuels is made. Experimental parameters for some model equations proposed by other authors are determined, and original semi-physical and empirical models are developed, based on a comprehensive laboratory experimental program. Extension of the studied phenomena to field scale is also discussed.

Fire spread with favourable wind or slope is assessed, based on large scale experiments in order to minimize the scaling effect, performed in the facilities of the *Laboratório de Estudos sobre Incêndios Florestais* (*LEIF*) located in Lousã, Central Portugal. The focus given to wind or slope driven fires in forest fire behaviour research in general, and also in this work, is based on the practical interest of modelling fire behaviour in those conditions, particularly in fire fighting management. Reviewing previous work on fire behaviour we can find many studies on slope head fires (Van Wagner, 1968) and many more on wind headfires (Albini, 1981; Viegas and Neto, 1991; Viegas, 2004b). For this reason, the majority of fire behaviour simulators like *Behave* (Andrews *et al.*, 2003) and the *Canadian Forest Fire Behaviour Prediction System* (FCFDG, 1992) deal mainly with head or flank fires.

Understanding the importance of the fire ROS modelling, in this study great attention is given to the subject and parameters are determined for empirical model functions, previously presented by other authors like Rothermel (1972), for the dependence of the ROS on fuel moisture content for fire spreading with no wind or slope and for the dependence of the ROS on wind velocity or slope angle.

22

However, backing fires, *i.e.* fire spreading downslope or with contrary wind, are of practical interest as well because they can represent large sections of the fire perimeter. To the author's knowledge few studies were made with the purpose of studying backfire propagation. The well known Rothermel's (1972) model, that incorporates wind and slope effects, does not consider backfires and in the *Behave* fire simulator (Andrews *et al.*, 2003) the ROS for backfires is considered constant. Examples of backfire behaviour analysis are the work of Van Wagner (1988), Weise and Biging (1997), and Mendes-Lopes *et al.* (2003), all using laboratory experiments. This work aims to contribute to a better understanding of this type of behaviour, making an assessment of the ROS variation with contrary wind or slope and comparing the results with spread under no wind on level ground.

Despite the focus given to the ROS in forest fire research, due to its importance in operational application, it is shown, following the work of Viegas (2002), Oliveras *et al.* (2006), and Viegas *et al.* (2006b), that the concept of a single ROS value is not sufficient to describe the movement of a fire line in the general case. The experimental results presented here and also field experiments like those reported by Cheney *et al.* (1993) show that, even in cases where the fuel bed, the slope and the wind flow conditions are uniform and constant, the ROS changes from one point to the other of the fire line. This is called dynamic behaviour, *i.e.* the change in the fire spread properties over time even for constant boundary conditions (Viegas, 2004a). It was considered the existence of heat fluxes along the fire line that produce variations of the ROS. As a consequence of these fluxes, given the reactive nature of the fuel bed, the combustion reaction is modified and consequently the ROS changes from one point to another. This approach is analogous to that presented in Viegas (2005) in which it was shown that the fire induced convection could enhance the reaction combustion ahead of the fire line element, producing a change of the ROS and a continuous acceleration of the fire front that resulted ultimately in the so called fire eruption.

Resulting from the non-uniform ROS along the fire line, the concepts of fire line extension and rotation are introduced as a complement to describe the fire line movement and are shown to be responsible for the reduction of the fire line curvature. Wolff *et al.* (1991) referred to the curvature of the fire front and also attributed the phenomena to heat transfer mechanisms. The concept of fire line rotation was introduced by Viegas *et al.* (1994) as an alternative formulation to link the local and the global problems. Relevant considerations can be derived from the

analysis of the rotation movement of the fire line for the purpose of understanding the behaviour of a forest fire, namely the tendency of a fire flank to become a straight line and parallel to the main wind velocity or to the slope gradient. In Viegas *et al.* (1998), the case of a linear fire front in slope or wind driven fires was analysed, proposing a purely empirical model for the fire line rotation movement, based on laboratory experiments. In the present study the effects of wind and slope are considered to be equivalent and interchangeable, in the sense that it is assumed that in both cases, for a given fuel bed there is a reference value of the flow velocity that is univocally related to the flame geometry and ROS. The interaction between natural (slope induced) or forced (wind induced) convection and the fire front, the transverse convective flow in the reaction zone and its effect on the ROS are analysed. Analysing the fire line evolution by infrared imaging the fire line elements rotation and extension are assessed and a model, based on semi-empirical and empirical modelling, for predicting the fire line evolution of a point ignition fire under constant wind or slope is proposed. The model parameters are determined experimentally and a comparison is made with experimental laboratory results. The results are discussed and further research is proposed.

This thesis is organized as it follows: in Chapter 1 the problem of forest fires worldwide with focus on Portugal was discussed, a review on previous research was made, and the purpose of this work was presented; in Chapter 2 the approach to the problem is described and the mathematical model is developed considering the head fire, the flank fire, and the back fire, respectively; in Chapter 3 the experimental program is described, as well as the test rigs used, the procedures for preparing the fuel beds and for conducting the experiments, and how the data are processed; in Chapter 4 the experimental results are presented, the parameters for the empirical relationships proposed by other authors and for the present models are determined, and the models are tested against laboratory experimental data; in Chapter 5 conclusions are taken and future work is proposed.

2. Mathematical model

2.1. Problem analysis

In the present work, only surface fires spreading in uniform, homogeneous and of constant height fuel beds with a flaming front will be analysed and no marginal burning conditions will be considered.

Let us consider the perimeter of a fire originated by a point ignition spreading upslope or under constant wind. We can define the ROS R_h, R_f and R_b, associated to points H, F and B, corresponding to the most advanced parts of the head fire, flank fire and back fire, respectively (Figure 2.1a). It is here considered that points H and B have a translation with an O_0Y_0 component only, but with opposite directions, and that point F has a translation with a horizontal component only. In the general case, a given point in the fire line will have a translation composed by an O_0Y_0 and an O_0X_0 component. In the current analysis we will refer to the head fire as the movement of point H, to the flank fire where the fire line elements have a rotational velocity ω_f as the fire perimeter between H, exclusively, and F, inclusively, and to the back fire where the fire line elements have a rotational velocity ω_b as the fire perimeter between F, exclusively, and B, inclusively.
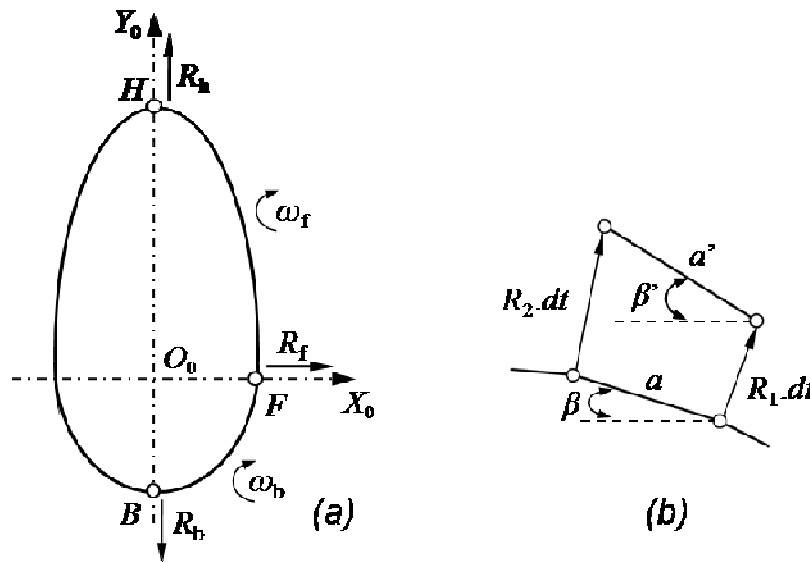

Figure 2.1 – (a) Schematic presentation of the perimeter of a fire originated by a point ignition spreading upslope or under constant wind. (b) Translation, extension and rotation of a linear fire line element between time steps t and $t' = t + dt$.

Although for constant boundary conditions and homogeneous fuel bed properties the fire perimeter evolution would be symmetrical in relation to the O_0Y_0 axis, the inability of preparing a perfectly homogeneous fuel bed and to assure constant and uniform boundary conditions, even for carefully prepared and made experiments with a high level of reproducibility, will result in small differences between the right and left sides of fire perimeter.

If we divide the fire perimeter in n fire line elements we have $n + 1$ points, each one spreading in a perpendicular direction to a tangent to the fire line in its vicinity with a given ROS that might or might not be the same at all points. The ROS in each point along the fire line will define the fire perimeter with time, that for being correctly described based on the evolution of all the individual fire line elements their length must be sufficiently small compared to the local radius of curvature of the fire line, so that the fire line element can be approximated by a straight line segment within a constant radius of curvature, but large enough to be of the order of the depth of the reaction zone in the fuel bed in order to be able to measure changes in its properties with sufficient accuracy. It is also required that the fire line elements are far from points with a sudden change of curvature or fuel bed properties, namely the edges of the fuel bed.

We can consider three cases regarding the overall shape of the fire line: straight, convex or concave (Figure 2.2).
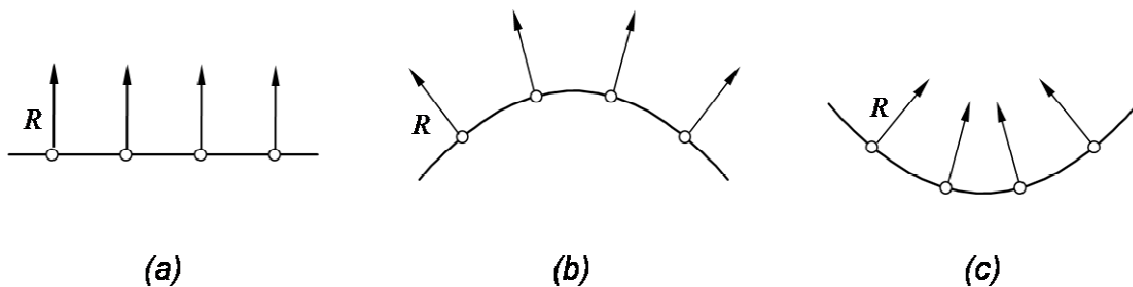

Figure 2.2 – (a) Straight fire line. (b) Convex fire line. (c) Concave fire line.

The fire line evolution will depend on the initial fire line shape and on the ROS of each point, in particular on the differences between the ROS of the points that define a fire line element. In all cases it will involve a translation and depending on the situation we can also have a length variation (extension/contraction) and a rotation (Table 2.1). In this analysis only straight and convex fire lines will be considered, in which the fire line elements in the most generic case

of different ROS in their ends, from one time instant to another, will suffer a translation, an extension and a rotation (Figure 2.1b).

Table 2.1 – Fire line evolution as a function of the initial shape and ROS in the ends of the fire line elements.

Fire line shape	ROS in the ends of the fire line elements	
	Equal	Different
Straight	TRA, - , -	TRA,EXT,ROT
Convex	TRA,EXT, -	TRA,EXT,ROT
Concave	TRA,CON, -	TRA,CON,ROT

TRA-Translation; EXT-Extension; CONT-Contraction; ROT-Rotation.

The only case that involves a pure translation is the case of a straight line with a uniform ROS field along the fire line. This is a very particular case of fire spread, corresponding to propagation on a uniform and homogeneous fuel bed with no wind on level ground. As this is a very rare situation in forest fires, in the general case the fire line evolution involves a composed movement of the fire line elements.

2.2. Head fire

Basic rate of spread

If we consider a forest fire started by a point ignition, spreading on a horizontal terrain with homogeneous and constant fuel bed properties and no ambient wind, the fire will spread with an approximately constant velocity with no preferential direction of propagation and the fire line will form a circle that maintains its centre but increases its radius over time. Theoretical analysis by Weber (1989) and experimental evidence referred in Viegas (2002) show that after an initial fire growth period the ROS settles at a practically constant ROS, as the curvature effect is minimized. The ROS of this fire line is found to be practically equal to the basic rate of spread R_0 that corresponds to the ROS of a linear fire front in the same fuel bed in no slope and no wind conditions and is considered to be a basic property of the fuel bed. As in Rothermel (1972), it will be considered that the basic ROS will depend on the fuel bed moisture content, assuming that the remaining fuel bed properties are kept constant:

$$R_0 = a_0.m_{\mathrm{f}}^3 + b_0.m_{\mathrm{f}}^2 + c_0.m_{\mathrm{f}} + d_0 \tag{2.1}$$

Wind or slope driven rate of spread

It is assumed that for a fuel bed the ROS of the fire line element is a function of the local flow velocity perpendicular to it, u_y, or slope angle α. Following previous work of Rothermel (1972), Oliveras *et al.* (2006) and Viegas (2005) it is considered that there is a unique relationship between them given by model functions of the type:

$$R_{h,u} = f_1(u_y) = R_0 . \left(1 + a_{1,u} . u_y^{b_{1,u}}\right) \tag{2.2}$$

$$R_{h,\alpha} = f_1(\alpha) = R_0 . \left(1 + a_{1,\alpha} . \alpha^{b_{1,\alpha}}\right) \tag{2.3}$$

The empirical form proposed in the second part of Eq. (2.2) and (2.3) follows Rothermel (1972) and was also used in Cheney *et al.* (1993), Beer (1993), and Viegas (2005). It is assumed that pairs of parameters $(a_{1,u} ; b_{1,u})$ and $(a_{1,\alpha} ; b_{1,\alpha})$ are dependent only on the fuel bed properties and can be determined experimentally for a given set of wind or slope experiments, respectively. Although the referred parameters are determined based on the ROS of the most advanced point of the head fire, in principle, the equations should remain valid for determining the ROS of any point in the flank fire, provided that the reference flow velocity, or its equivalent flow velocity associated to slope effect as will explained ahead, in the vicinity of that point is known, allowing to determine the value of the flow component perpendicular to a tangent to the fire line in the vicinity of that point. The reference flow velocity is given by:

$$\vec{u} = \vec{u}_0 + \vec{u}_i \tag{2.4}$$

Where u_0 is the general wind velocity (or its equivalent flow velocity associated to slope effect) that is assumed to be constant at all points; u_i is the local flow velocity induced by the fire that varies with x and y.

Despite the laboratory experiments here presented were made with great care, following a written protocol (Rossa, 2009), controlling and maintaining constant with reasonable accuracy the fuel load, fuel homogeneity and fuel bed bulk density, there were parameters, such as fuel moisture content that, although monitored, could not be maintained constant. In order to minimize the influence of some parameters that cannot be controlled and suffer slight variations from one experiment to another and to allow a better comparability between experiments, it shall be defined a non-dimensional ROS, R', given by the ratio between the absolute ROS and the

basic ROS tested in a fuel bed with the same overall properties that the one from the experiment made under wind or slope effects:

$$R' = \frac{R}{R_0} \tag{2.5}$$

Since R' represents the influence of wind or slope as a ratio of the fire ROS on a horizontal terrain without ambient wind, for a given fuel, one could expect small differences in the fuel bed properties from one experiment to another, under the same wind or slope, not to originate major differences in its value. Assuming that we can determine the value of R' using the model functions given by Eq. (2.2) and (2.3) for the case of wind driven or slope driven fires, respectively, if we determine experimentally the value of R_0 for a given fuel bed we can compute the position of a given point after a time interval dt, knowing its initial position s, using Eq. (2.6).

$$s' = s + R'.R_0.dt \tag{2.6}$$

Slope and wind equivalence

Despite some differences in the wind or slope effects on fire spread it will be considered here that there is equivalence between them in the sense that, for a given slope angle α, we can define an equivalent wind velocity u_{eq} that produces the same ROS value on a horizontal ground.

Following Rothermel (1983), from Eq. (2.2) and (2.3) we can easily obtain Eq. (2.7) that describes an equivalence curve based on parameters a_α and b_α that are obtained by combining a pair of parameters $(a_{1,u}; b_{1,u})$ with a pair of $(a_{1,\alpha}; b_{1,\alpha})$.

$$u_{eq} = \left(\frac{a_{1,\alpha}}{a_{1,u}}\right)^{\frac{1}{b_{1,u}}} . \alpha^{\frac{b_{1,\alpha}}{b_{1,u}}} = a_\alpha . \alpha^{b_\alpha} \tag{2.7}$$

2.3. Flank fire

Fire perimeter evolution

The model for the flank fire described in this section is based on the work of Viegas and Rossa (2009). For the sake of simplicity it is assumed that the terrain that is supporting the fuel bed is essentially flat with negligible curvature. Any change in terrain slope or curvature in the vicinity of the fire line element is considered to be sufficiently small so that we can treat the fire line as a two dimensional line and describe it in a Cartesian plane, as shown in Figure 2.3a. In the present

study it is assumed that the fire contour is represented by a convex line with its local centre of curvature always on the side of the already burned vegetation. Fire lines with concave sections require a different treatment that is beyond the scope of this study. In Figure 2.3a, it is defined a reference frame $X_0O_0Y_0$ that is fixed to the ground; its O_0Y_0 axis is parallel to the general wind velocity u_0 direction (or to the terrain slope gradient). There is a second reference frame X_1OY_1 associated with point P_1 ($P\equiv O$) that has its OY axis parallel to the local ROS vector $\vec{R}_1$. The angle between OX_1 and O_0X_0 axis is equal to β_1, as it is indicated in Figure 2.3a.

In order to predict the movement of the fire line we need to evaluate its propagation properties at different points along the fire line. Taking two generic points P_1 and P_2 of the fire line and assuming that the ROS of the fire at each point is given respectively by $\vec{R}_1$ and $\vec{R}_2$, after time step dt the location of these two points will be, respectively, P_1' and P_2' (Figure 2.3a).
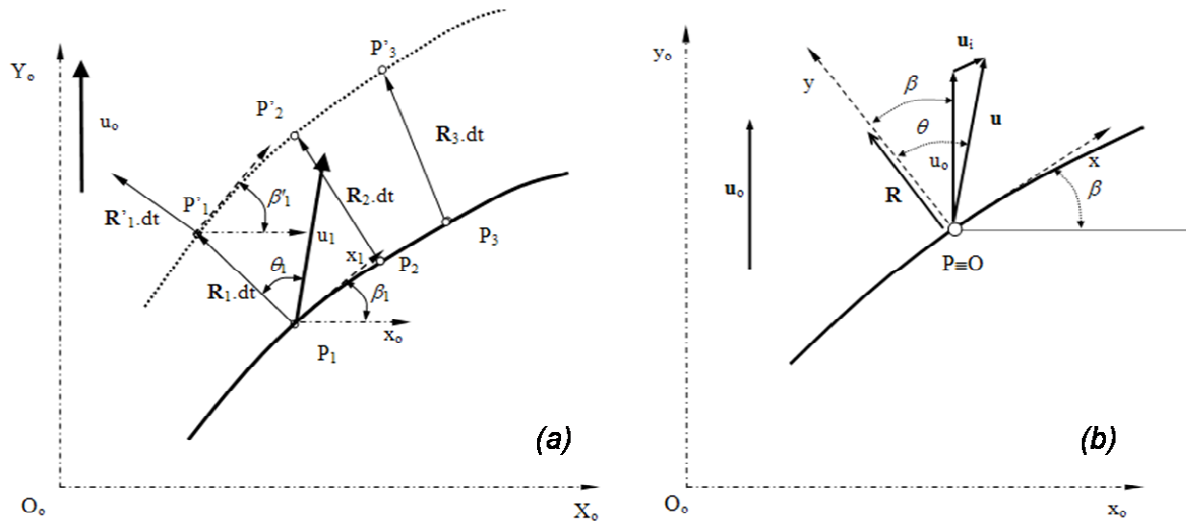

Figure 2.3 – (a) Schematic presentation of the evolution of flank fire perimeter at time steps t and $t'=t+dt$. (b) Schematic view of the local flow velocity u and ROS vector $\vec{R}$ and of the respective angles θ and β for the flank fire line.

We can write the following equations:

$$P'_1 = P_1 + R_1.dt \qquad (2.8)$$

$$P'_2 = P_2 + R_2.dt \qquad (2.9)$$

If points P_1 and P_2 are sufficiently close and if dt is small we can approximate the curved segments $\overline{P_1P_2}$ and $\overline{P_1'P_2'}$ by straight lines in order to analyse the elementary movement of the fire line. In this case the fire line element $\overline{P_1P_2}$ is parallel to the local OX axis.

Analysis of fire line extension

It will be defined the rate of relative extension of a fire line element as:

$$\varepsilon = \frac{a'-a}{a.dt} = \frac{1}{a}\cdot\frac{da}{dt} \tag{2.10}$$

In this equation a and a' are the initial and final length of the fire line element, respectively, during time step dt. The relative extension has the dimensions of a frequency $[\text{s}^{-1}]$. If we assume that it is reasonable for a given wind velocity or slope angle to consider an average rate of relative extension ε_{av}, the length of a fire line element after time step dt will be given by:

$$a' = a + \varepsilon_{av}.a.dt \tag{2.11}$$

Analysis of fire line rotation

Let us consider a generic point P of a flank fire line that is spreading in a boundary layer type flow uniform in relation to x and y coordinates but with a velocity profile along the OZ axis perpendicular to the plane XOY defined in Figure 2.3. It is assumed that there is a reference wind velocity u_0 that can be used to characterize the interaction between the wind flow and the fire front as it is shown in Figure 2.3b. One alternative situation is that of a fire on a constant slope α in which it has been previously considered to exist an equivalent wind velocity u_{eq}, defined in Eq. (2.7), that produces the same ROS value on a horizontal ground.

In the present work we are looking essentially to the flow parallel to the fuel bed. It is true that the presence of the reaction zone will induce a convective flow with a component perpendicular to the ground but it shall be neglected the role of this component, as we are essentially looking at the variations induced by the local flow along the fire line. This approach was also used in Viegas (2005) to derive the fire acceleration in a fire eruption and was adequate to put in evidence the role of the convective fluxes parallel to the ground, in spite of the very strong vertical convection that is certainly observed in such type of fires. In the case of a slope driven fire this convective flow will have two components: u_y that is perpendicular to the fire line

element, and u_x that is parallel to the fire line and will transport heat from the reaction zone to the unburned fuel; in the case of a wind driven fire there will be a general flow parallel to the ground and therefore to the fuel bed, with the same transport properties.

The transverse flow component u_x has a very important role in modifying the burning conditions in the fire line element that is adjacent to the one considered. In a manner similar to that considered in the fire induced acceleration, this transverse flow component will enhance the combustion reaction at the adjacent fire line element. As a result, the ROS of the fire front shall not be constant and uniform along its length and a rotation of the fire line is produced.

This process can be observed in fire lines at different scales and in a wide range of conditions. The well documented field experiments performed by Cheney *et al.* (1993) present good examples of fire lines that spread with a rotation movement that tends to align the fire line with the wind direction. The overall shape of the fire perimeter in those experiments is quite similar to the present ones (Figures 3.2a, 3.3a, 3.5 and 3.6) in spite of the differences in the order of magnitude of the scale.

We have already characterized the flow in the vicinity of the fire front by the reference flow velocity shown in Eq. (2.4). Having in mind Figure 2.3b it is considered that the local flow velocity u makes an angle θ with OY axis. The components of the flow velocity in the local reference frame are given by:

$$u_x = |\vec{u}|.\sin\theta \tag{2.12}$$

$$u_y = |\vec{u}|.\cos\theta \tag{2.13}$$

The flow angle θ must be close to β but in the general case $\theta \neq \beta$. A previous formulation of this model in Viegas (2005) was based on the assumption that $\theta = \beta$ but this is not applicable in the general case. The correct evaluation of θ would require a detailed dynamic analysis of the flow field in the vicinity of the fire line element. As this was not accomplished in the present study an approximation will be made of the parameters required to close the model.

It is derived an approximate form of computing the flank fire line elements rotational velocity ω_f to be used below, assuming that the fire line element can be approximated by a segment of a straight line as shown in Figure 2.4a. In this case $\vec{R}_1$ and $\vec{R}_2$ are parallel vectors. If the time interval dt is small the rotation angle $d\beta$ can be approximated by its tangent:

$$\omega_{\rm f} = \frac{d\beta}{dt} \approx \frac{tg(d\beta)}{dt} = \frac{dR}{dx} \tag{2.14}$$
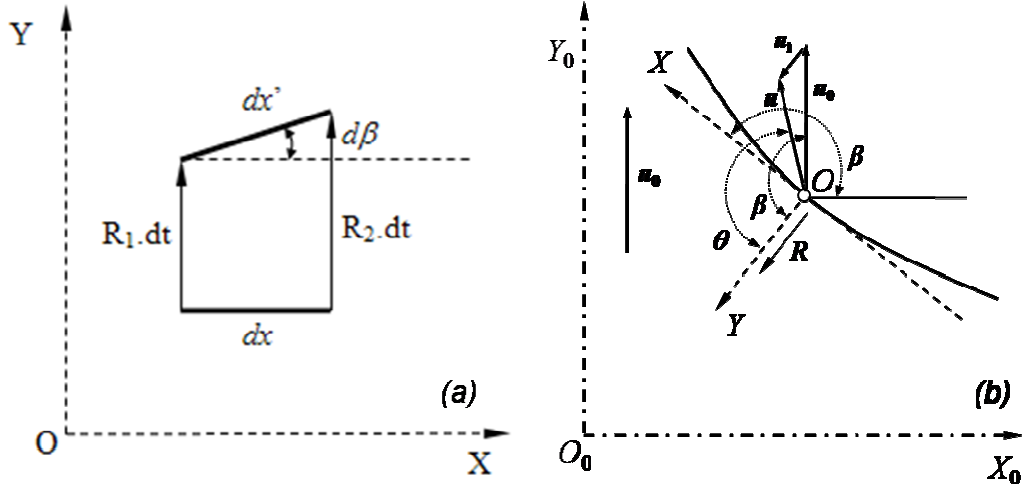

Figure 2.4 – (a) Infinitesimal rotation of a linear flank fire line element. (b) Schematic view of the local flow velocity u and ROS vector $\vec{R}$ and of the respective angles θ and β for the back fire line.

In Eq. (2.14) $d\beta$ is the angle of rotation of the fire line element during time step dt (Figure 2.4a). The rotational velocity $\omega_{\rm f}$ is a true angular velocity that has the units of [rad/s] or [°/s]. From Eq. (2.14) we can obtain:

$$\omega_{\rm f} = \frac{dR}{du_y} \cdot \frac{du_y}{dx} \tag{2.15}$$

From Eq. (2.2) we can derive the first factor on the right hand side of Eq. (2.15):

$$\frac{dR}{du_y} = R_0.a_{1,u}.b_{1,u}.u_y^{b_{1,u}-1} \tag{2.16}$$

Regarding the derivative of u_y with respect to x appearing in Eq. (2.15) it is reasonable to assume that the increase of the ROS along the fire line is associated with the transverse heat flux that is transported along the fire line by the local u_x component of the flow velocity. In line with the assumption that was made for Eq. (2.2) it shall be proposed a model:

$$\frac{du_y}{dx} = f_3(u_x) = a_3.u_x^{b_3} \tag{2.17}$$

Combining Eq. (2.16) and (2.17) with (2.15) it is possible to obtain the following analytical model to determine the fire line rotation velocity:

33

$$\omega_f = R_0.a_{1,u}.b_{1,u}.a_3.u_y^{\,b_{1,u}-1}.u_x^{\,b_3} \tag{2.18}$$

Using Eq. (2.12) and (2.13) we obtain:

$$\omega_f = R_0.a_{1,u}.b_{1,u}.a_3.u^{\,b_{1,u}-1+b_3}.(\cos\theta)^{(b_{1,u}-1)}.(\sin\theta)^{b_3} \tag{2.19}$$

This equation can also be written as:

$$\omega_f = R_0.a_{1,u}.b_{1,u}.a_3.u_y^{\,(b_{1,u}-1+b_3)}.(\tan\theta)^{b_3} \tag{2.20}$$

Knowing the angle β of a fire line element, that will vary in the range $0-90^\circ$, in a time instant t and the predicted rotational velocity ω during time interval dt we can easily compute the fire line element angle at time instant $t'=t+dt$:

$$\beta' = \beta + \omega \cdot dt \tag{2.21}$$

Parameters a_3 and b_3

From (2.19) and assuming that the flow velocity u is constant it is possible to determine the value of θ^* that maximizes the rotational velocity ω_{max}.

$$\frac{d\omega_f}{d\theta} = 0 \rightarrow \tan\theta^* = \left(\frac{b_3}{b_{1,u}-1}\right)^{\frac{1}{2}} \Leftrightarrow b_3 = (\tan\theta^*)^2.(b_{1,u}-1) \tag{2.22}$$

If the value of θ^* can be determined experimentally, from Eq. (2.22) we can estimate the value of b_3. Combining Eq. (2.22) with (2.20) we easily obtain the following expression for the maximum rotational velocity ω_{max}:

$$\omega_{f,max} = R_0.a_{1,u}.b_{1,u}.a_3.u_y^{\,(b_{1,u}-1+b_3)}.\left(\frac{b_3}{b_{1,u}-1}\right)^{\frac{b_3}{2}} \Leftrightarrow a_3 = \frac{\omega_{f,max}}{R_0.a_{1,u}.b_{1,u}}.u_y^{\,(1-b_{1,u}-b_3)}.\left(\frac{b_3}{b_{1,u}-1}\right)^{-\frac{b_3}{2}} \tag{2.23}$$

If, from experiments, we determine the value of ω_{max}, for a given value of u_y, from Eq. (2.23) we can determine a_3 in order to close the problem.

2.4. Back fire

Fire perimeter evolution

The model for the flank fire described in this section is based on the work of Rossa and Viegas (2009). For the back fire perimeter evolution study (Figure 2.1a) the same simplifying hypothesis

34

as for the flank fire are considered. It is also considered that the fire contour is represented by a convex line with its local centre of curvature on the side of the already burned vegetation. Again it will be considered a reference frame fixed to the ground $X_0O_0Y_0$ (Figure 2.3) and a local reference frame XOY (Figure 2.4b).

The resulting local flow velocity u defined in Eq. (2.4), as in the flank fire, will continue to have a transverse flow component $u_{x,b}$ that modifies the burning conditions along the fire perimeter, resulting in a variable ROS along the fire line elements length, and produces a rotation of the fire line. However, the parallel component to the OY axis $u_{y,b}$, will now have a negative contribution to the ROS vector $\vec{R}$ which explains the fact that the flame is tilted in the opposite direction of the fire spread. The combined effect of the back fire line extension and rotation tends to create a linear fire line perpendicular to the wind or maximum slope direction (Figures 3.2b, 3.3b, 3.7 and 3.8). Considering that the local flow velocity u makes an angle θ with OY axis, the local wind velocity components $u_{x,b}$ and $u_{y,b}$ will be given by:

$$u_{x,b} = |\vec{u}|.\sin\theta \tag{2.24}$$

$$u_{y,b} = -|\vec{u}|.\cos\theta \tag{2.25}$$

Again it will be considered that in the general case $\theta \neq \beta$ although in the present study we do not have enough data for a correct evaluation of θ. Since the model that shall be proposed below for estimating the fire line extension and rotation is purely empirical, at this point we do not need to determine the value of θ, like in the model proposed for the flank fire. As the fire line elements angle β is measured in relation to the reference axis O_0X_0 (Figure 2.3), having in mind the geometry of the back fire line perimeter, β will now vary in the range $90-180º$.

Analysis of fire line extension

For the back fire, the concept of rate of relative extension defined in Eq. (2.10) will also be used and from the experimental data analysis again it was considered that it is reasonable to estimate an average rate of relative extension ε_{av} for a given wind velocity or slope angle. The length of a fire line element after time step dt can be computed using Eq. (2.11).

Analysis of fire line rotation

Experimental data showed that the back fire line elements angle does not seem to follow the same evolution with time when compared with the flank fire line elements. The flank fire line elements rotational velocity, approximately described by Eq. (2.20), depends on the fire line element angle and has a value greater or equal to zero (Figure 4.13). On the contrary, the back fire line elements rotational velocity, despite also showing dependence on the fire line element angle, alternates between positive and negative values (Figures 4.23 to 4.26). This behaviour should probably be explained by the same reasons that cause the ROS of backfires to successively increase and decrease with contrary slope or wind and that will be explained later in section 4.1.4.

It will be shown also in section 4.1.4 that the back fire line elements rotational velocity alternates between positive and negative values. Having that in mind, there will be an angle for which we have a null rotational velocity. The data showed that, for each fire line element, the angle corresponding to a null rotational velocity β_{int} has a good linear dependence on the initial fire line element angle β_{ini}, *i.e.* the element angle at the initial time instant t_0.

$$\beta_{int} = m_\beta \cdot \beta_{ini} + b_\beta \tag{2.26}$$

The parameters of the linear dependence shown in Eq. (2.26) are a function of the fuel bed properties and of the test conditions (slope or wind tests). Experimental data suggests that it is reasonable to consider a set of fitting parameters for the entire range of tested slopes and another set for the entire range of wind velocities.

If we consider a linear dependence with a slope m_r between the rotational velocity ω_b and the back fire line elements angle β we can obtain Eq. (2.27):

$$\omega_b = m_r \cdot (\beta - \beta_{int}) \tag{2.27}$$

Using Eq. (2.27) we can easily determine a back fire line element rotational velocity ω_b and from Eq. (2.21) compute the fire line element angle at time instant $t' = t + dt$.

3. Experimental methodology

3.1. Experimental program

Overall information

The experimental program that supports the results presented in this work was conducted in the Laboratory of Forest Fire Research of the University of Coimbra, located in Lousã, and was divided into eight series of experiments using four test rigs that will be described below, in a total of 155 experiments. The main parameters of the experiments are given in Tables 3.2 to 3.5. Each test has an alpha-numerical reference indicating the type of experiment, the test rig in which it was made and the order of performance, separated by dashes. In Table 3.1 we have, for each series of experiments, the tests main features, like the parameters assessed and the type of monitoring that was made. When referring to a series of experiments (Table 3.6) and not an individual test, the alpha-numerical reference does not include the order of performance and is preceded by a two letter code indicating the fuel bed, defined in the beginning of section 3.3.

Types of experiments

Eight different alpha-numerical codes were defined according to the type of treatment to be made in each series of experiments (Table 3.1). The order of performance of the tests is added to this reference afterwards.

In the BS-MC1 experiments, the fire *basic rate of spread*, *i.e.* the ROS on horizontal ground with no wind, as a function of the fuel load and moisture content was studied.

In the FP-TC2 series, the *forward propagation*, in particular the ROS, of wind-driven fires was analysed and in the FP-DE4 experiments the same was done for slope-driven fires. In the FR-TC2 tests, the ROS of wind-driven fires was analysed and the *flank fire line rotation* was also assessed. In the FR-DE4 tests the same was done for slope-driven fires.

In the BP-DE1 experiments, the *backwards propagation*, in particular the ROS, of slope fires was analysed. In the BR-TC2 series, the ROS of wind backfires was studied and the *back fire line rotation* was also assessed and in the BR-DE4 tests the same was done for slope backfires.

3.2. Test rigs

Test rigs used

The dedicated experiments of fire propagation on level ground with no wind were made in the Combustibility Table MC1. For the fire propagation under the effect of slope the Combustion Table DE1 and the Canyon Table DE4 test rigs were used and for the propagation under the effect of wind the Combustion Tunnel TC2 was used. These last two test rigs are probably the largest experimental structures of its nature that exist in fire research laboratories.

Test rigs description

The Combustibility Table MC1 (Figure 3.1a) has a burn area of 1×1 m^2 with a fixed horizontal fuel bed and is used only for basic ROS experiments.

The Combustion Table DE1 (Figure 3.1b) has a burn area of 1.4×1.5 (L$\times$W) m^2 and can be tilted manually and positioned with geometrical angles varying in the range $0º < \alpha < 65º$ with 5º intervals.
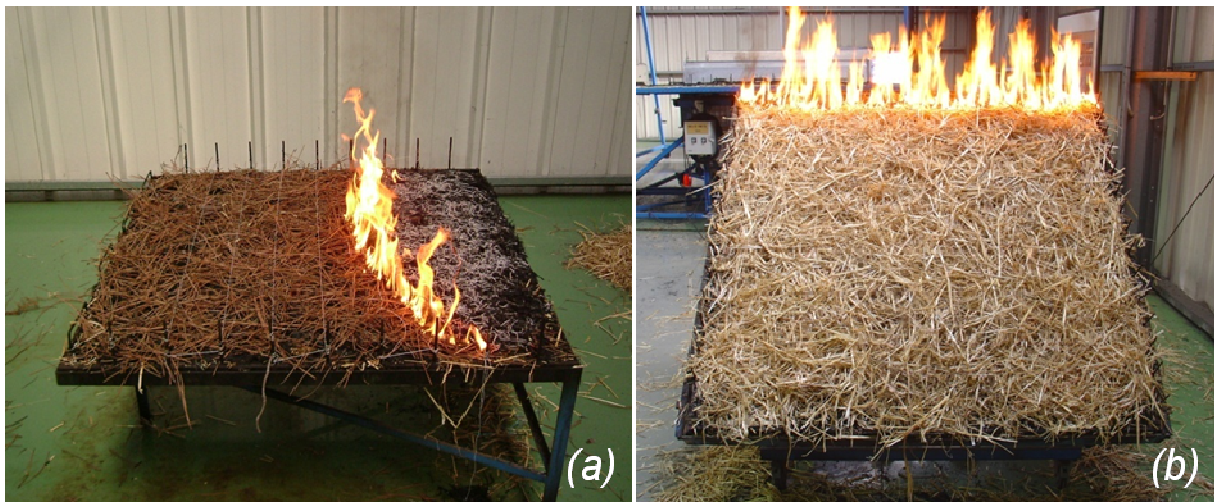
Figure 3.1 – (a) Experiment on the Combustibility Table MC1, ref.: BS-MC1-41, fuel bed: pine needles, fuel load: 0.6 kg/m^2. (b) Experiment on the Combustion Table DE1, ref.: BP-DE1-09, slope: -40º, fuel bed: straw, fuel load: 0.6 kg/m^2.

The Canyon Table DE4 (Figure 3.2) has two symmetrical faces of 4×6 m^2 each. These faces are driven hydraulically and can be positioned as a single slope or as a canyon with geometrical angles varying in the range 0º to 40º. In this study, only the slope configuration was used, forming a fuel bed on one face of the table of 6×3 m^2 for the FP-DE4 experiments, 3×4 m^2

for the FR-DE4 experiments (Figure 3.2a) and 2.5×3 m^2 for the BR-DE4 experiments (Figure 3.2b). The slope angle α could be varied continuously between 0º and 40º with a precision better than 0.5º.
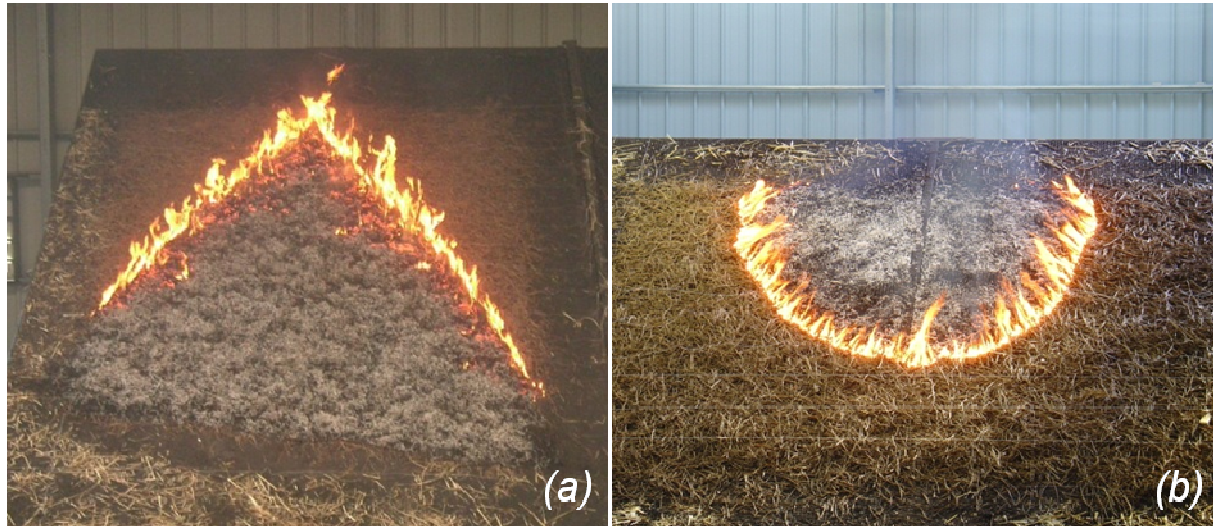
Figure 3.2 – Experiments on the Canyon Table DE4, fuel bed: pine needles, fuel load: 0.6 kg/m^2: (a) Ref.: FR-DE4-06, slope: 30º. (b) Ref.: BR-DE4-01, slope: -30º.

Figure 3.3 – Experiments in the Combustion Tunnel TC2, fuel load: 0.6 kg/m^2: (a) Ref.: FR-TC2-07, wind velocity: 2 m/s, fuel bed: pine needles. (b) Ref.: BR-TC2-04, wind velocity: -2 m/s, fuel bed: straw.

The Combustion Tunnel TC2 (Figure 3.3) has two axial fans of variable rotational velocity and the reference wind velocity above the fuel bed can be varied continuously between 0 and 5 m/s. The wind velocity calibration was made 3.7 m away from the air flow outlet, around half the typical fuel bed length used in most of the experiments, at 0.6 m high (estimation of a typical

mid-flame height, based on a visual assessment from previous experiments), with an *ALNOR 9870 Air Velocity Meter* (5 % flow velocity accuracy). The test section of the tunnel has a horizontal metallic structure to support the fuel bed, two vertical walls, and is open on the top. The test section area is 9×3 m^2 but the area of the fuel bed used was 6.5×1.3 m^2 for the FP-TC2 experiments, 5×2 m^2 for the FR-TC2 experiments (Figure 3.3a) and 2.5×2 m^2 for the BR-TC2 experiments (Figure 3.3b).

3.3. Fuel beds and procedures

Fuel beds

In the FP-TC2 and BS-MC1 experiments three types of fine fuel particles were used: dry straw (ST), *Pinus pinaster* dead needles (PN) and eucalyptus slash (ES), in order to simulate a flashy fuel and two slower burning fuels, respectively. In the remaining series of experiments only the straw and pine needles fuel beds were used. Great care was taken in the preparation of the fuel beds in all tests in order to assure consistency in the whole program as it is recognized that small variations in fuel bed properties are of paramount importance in assuring the reproducibility of a given laboratory experiment (Schuette, 1965).

Fuel loads

The fuel load used in the present tests was measured on a dry basis. In the FP-TC2 experiments fuel loads of 0.6 and 0.8 kg/m^2 were used and in the BS-MC1 experiments fuel loads of 0.6, 0.8 and 1.0 kg/m^2 were tested, allowing the fuel load effect assessment. In the remaining series of experiments only the 0.6 kg/m^2 fuel load was tested, like for example in the laboratory experiments reported in Van Wagner (1968). This value is similar to that of 0.5 kg/m^2 reported in Luke and McArthur (1978) as an average fuel load found in grasslands. Fuel loads of 0.5 kg/m^2 also correspond to the average value in the field experiments reported in Byram (1959) performed in mixtures of grass and pine needles.

Fuel moisture content was measured to determine the fuel weight necessary for each test using one or more samples in a fuel moisture analyzer *A&D MX-50* (0.1 % accuracy) that retrieved its value in about ten minutes. After weighing the required fuel in a scale *A&D HW-100KGL* (20 g accuracy) it was spread homogenously on the test rig, maintaining a regular fuel bed height between experiments with the same fuel in order to maintain constant bulk density.

Procedures

All tests were prepared according to a previously defined and written protocol adopted in our Laboratory for this type of experiments (Rossa, 2009). Fuel load, fuel homogeneity and fuel bed bulk density were controlled and maintained constant during the experiments without much difficulty, although in the FP-TC2 experiments the bulk density was not measured (Tables 3.2 to 3.5). On the contrary as fuel moisture content was not conditioned, varying as a function of the ambient air temperature and relative humidity, it had to be monitored carefully during the preparation and before each experiment. As the fuel was kept at indoor ambient conditions the fuel moisture content could change from one day to another and even during the same day from one test to another. In order to overcome this difficulty the fuel moisture content m_f was monitored as well as the air temperature and relative humidity (except for some experiments in the FP-TC2 series of experiments due to problems with the weather station). Also, the basic rate of spread R_0 was measured for each test in a separate experiment as described below.

Strings were stretched over the fuel bed at a constant spacing in order to determine the ROS by registering the time instant at which each string was broken by the advancing fire. The distance between strings varied between 10 and 50 cm, according to the test rig in use and the number of strings depended upon the size of the fuel bed. In general, in the series of experiments for which the expected ROS was higher, larger fuel beds with a higher number of strings were used. Except for the BR-TC2 experiments, where only three strings were used due to test rig design constraints, the number of strings was always above six. However, in those experiments it was chosen to determine the ROS by image processing, using the infrared images to determine the position of the most advanced part of the fire for a given time instant given that, in some experiments, the flame was much tilted backwards and did not burn the strings when passing below them.

In order to avoid any bias with some of the control parameters, tests were made randomly. Also, given that for achieving a careful preparation of the fuel bed in order to maximize the reproducibility of the tests, between the fuel weighing and the beginning of the experiment we could have a lag of over one hour, the fuel moisture content was measured just before starting the experiment.

In all the R_0 measurements the ignition was initiated by creating a near instantaneous line of fire, parallel to the strings, using a wool string soaked in a mixture of kerosene and petrol. In

the BP-DE1 experiments the second half of the burn area was used for determining the basic rate of spread R_0, after tilting the table back to 0º, whereas in the remaining experiments a separate fuel bed, with the same overall properties as the main one but with a smaller area of around 1×1 m², was prepared for each test for this purpose. For the DE4 test rig experiments, R_0 was determined using the left side of the table and for the TC2 experiments the initial section of the table was used for this purpose, except for the FP-TC2 experiments where the R_0 was measured using the MC1 test rig.

Regarding the main experiments, although the same process was used and also line ignitions were made, their positioning varied with the objectives of each series. In the FP-TC2, FP-DE4 and BP-DE1 experiments, where the head or backfire ROS analysis was the main objective, it was parallel to the strings. On the other hand, in the FR-TC2 and FR-DE4 experiments it was intended to analyze the occurrence of the flank fire line rotation and so an ignition was put making an angle of $\beta = 10º$ with the wind or slope gradient direction. Finally, in the BR-TC2 and BR-DE4 experiments both the backfire ROS and fire line rotation was to be assessed and so the ignition was placed along a 0.8 m line parallel to the wind or slope gradient direction at the centre of the fuel bed width.

Table 3.1 – Tests characteristics, parameters assessed and type of monitoring for each series of experiments.

	Tests characteristics					Parameter assessment					Image monitoring		
Series	Area (L×W) [m²]	Ign.[1] β [º]	Fav./Cont.[2] Wind/Slope	Fuel beds	Fuel loads [kg/m²]	R_0	Forw.[3] ROS	Flank Rot.[4]	Back.[5] ROS	Back.[5] Rot.[4]	Video Top	Video Side	IR Top
BS-MC1	1.0×1.0	0	—	PN/ST/ES	0.6/0.8/1.0	✓	—	—	—	—	—	—	—
FP-TC2	6.5×1.4	0	Fav. Wind	PN/ST/ES	0.6/0.8	✓	✓	—	—	—	—	—	—
FP-DE4	6.0×3.0	0	Fav. Slope	PN/ST	0.6	✓	✓	—	—	—	—	—	✓
FR-TC2	5.0×2.0	10	Fav. Wind	PN/ST	0.6	✓	✓	✓	—	—	✓	✓	✓
FR-DE4	4.0×3.0	10	Fav. Slope	PN/ST	0.6	✓	✓	✓	—	—	✓	✓	✓
BP-DE1	1.4×1.5	0	Cont. Slope	PN/ST	0.6	✓	—	—	✓	—	—	—	—
BR-TC2	2.5×2.0	90	Cont. Wind	PN/ST	0.6	✓	—	—	✓	✓	✓	✓	✓
BR-DE4	2.5×3.0	90	Cont. Slope	PN/ST	0.6	✓	—	—	✓	✓	✓	✓	✓

[1]Ignition line angle (0º - Perpendicular to wind/slope direction); [2]Favourable/Contrary; [3]Forward; [4]Rotation; [5]Backwards.

Test monitoring

In the experiments where the fire line rotation and extension occurrence was assessed, FR-TC2, FR-DE4, BR-TC2 and BR-DE4, images of the fire line evolution were recorded. Three cameras were used for this purpose: two video cameras and one infrared camera *Flir Systems ThermaCAM SC640* with a spectral range between 7.5-13.5 μm.

The infrared camera and one of the video cameras were used for recording images from the top of the tables (Figure 3.4a), in order to analyse the fire line shape evolution, and the other video camera was used for recording images from the side of the tables (Figure 3.4b) in order to measure flame length and flame angle. The analysis of these parameters is not considered in the present study.

In Figures 3.5 to 3.8, typical images taken by the infrared camera are shown. In the FP-DE4 experiments, infrared images from the top of the table were also recorded using an older model of infrared camera, although they were not analysed in this work.

Figure 3.4 – Image recording of the DE4 test rig: (a) Infrared and video images recording from the top of the table. (b) Video images recording from the side of the table.

3.4. Data processing

ROS computation

Two types of data were analyzed in the present work: the ROS data and the fire line evolution. The first refers to the ROS estimate of the most advanced part of the fire front that was usually made from the known times that the fire took to burn each string. In the BR-TC2 experiments, the infrared images were used instead of the strings to determine the backfire evolution due to the fact that, especially for the higher wind velocity experiments, the flame was so tilted backwards that it tended to pass below the strings without burning them immediately. In Figure 3.9, the plotting of the distance travelled by fire as a function of time for tests BS-MC1-31 and FR-DE4-03 is shown.

Figure 3.5 – Sequence of infrared frames for an experiment on the Canyon Table DE4, ref.: FR-DE4-06, slope: 30º, fuel bed: pine needles, fuel load: 0.6 kg/m². The time since ignition is indicated in each frame.

Figure 3.6 – Sequence of infrared frames for an experiment in the Combustion Tunnel TC2, Ref.: FR-TC2-07, wind: 2 m/s, fuel bed: pine needles, fuel load: 0.6 kg/m². The time since ignition is indicated in each frame.
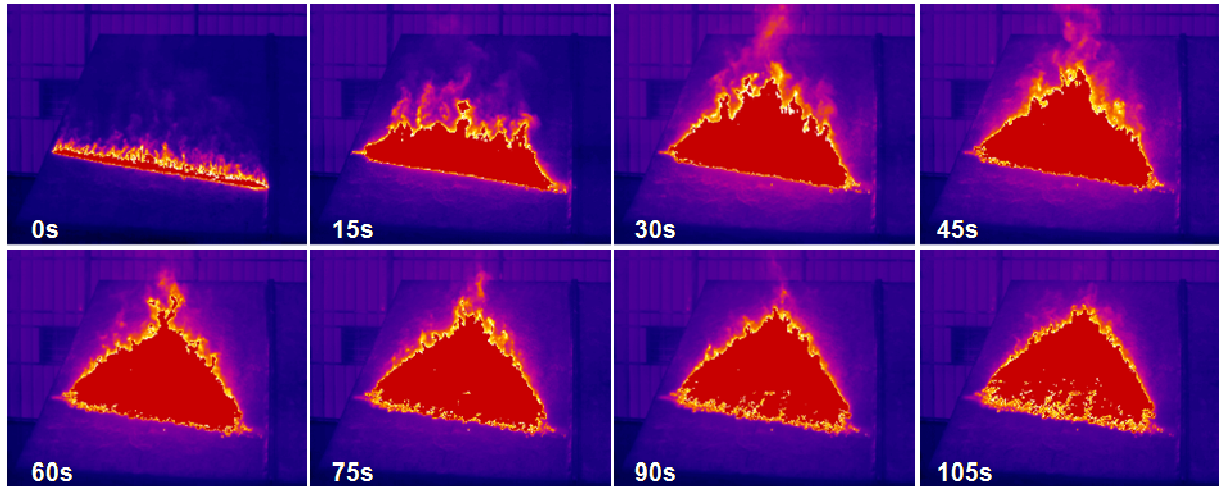

Figure 3.7 – Sequence of infrared frames for an experiment on the Canyon Table DE4, ref.: BR-DE4-03, slope: -30º, fuel bed: straw, fuel load: 0.6 kg/m². The time since ignition is indicated in each frame.

44

The value of the ROS for all tests was computed by linear fit using least squares error. For the basic ROS experiments the mean value of r^2 for was 0.996 with a standard deviation of 0.004 and always greater than 0.974. For the wind or slope driven experiments with higher ROS the correlation was obviously lower because the propagation was not so steady and so the plotting of the distance as a function of time was more scattered, yielding a minimum value of r^2 of 0.742 for the FP-TC2-94 experiment that corresponds to a fire propagation in a straw fuel bed, with a wind velocity of 3 m/s. However, the average value of r^2 for those experiments was 0.934, with a standard deviation of 0.065 which indicates an overall good correlation. The wind or slope backfires, like the R_0 experiments, have a slow and steady propagation and, as expected, yielded a high mean r^2 equal to 0.994 with a standard deviation of 0.006 and always greater than 0.973.
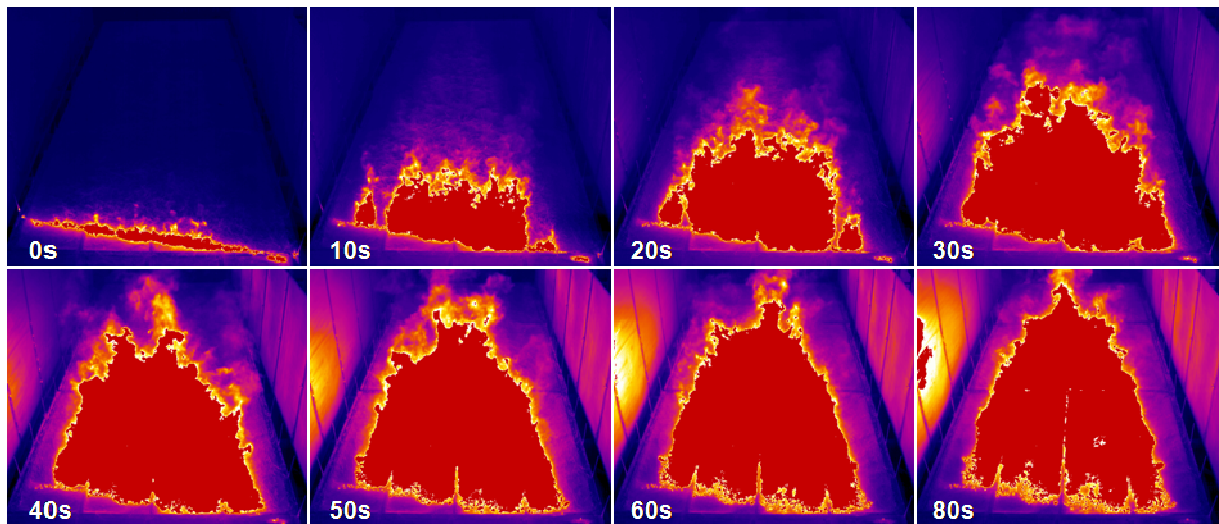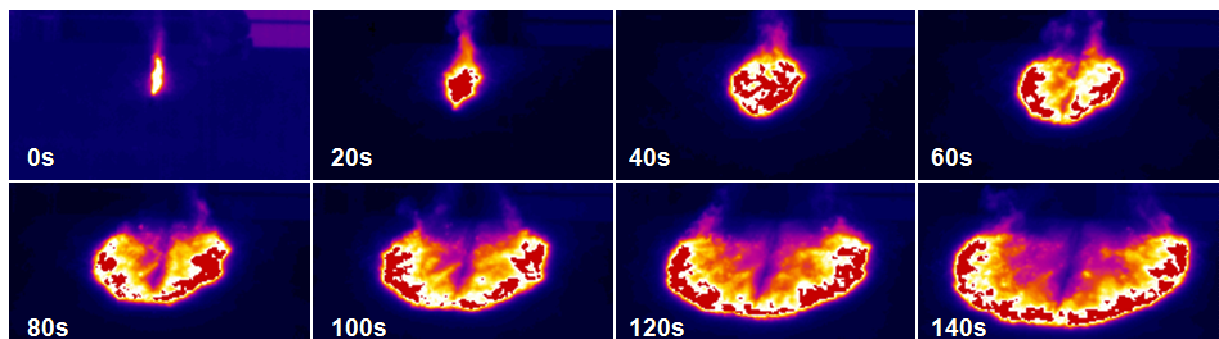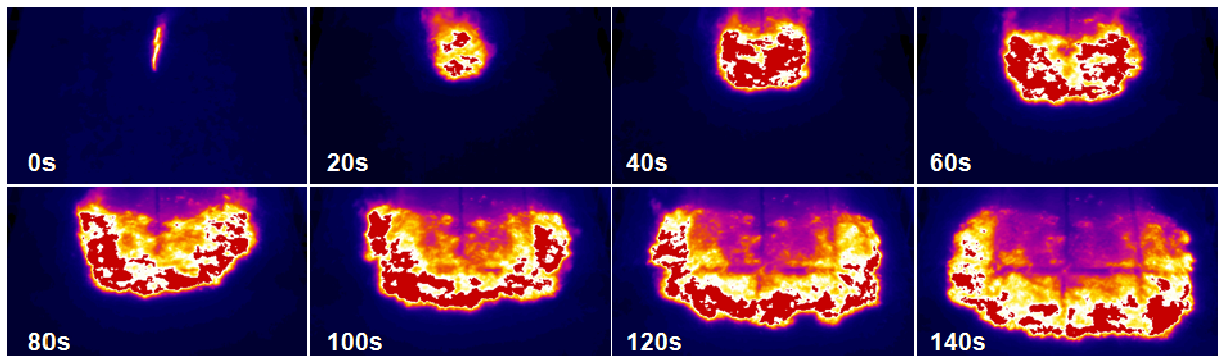

Figure 3.8 – Sequence of infrared frames for an experiment in the Combustion Tunnel TC2, ref.: BR-TC2-07, wind: -2 m/s, fuel bed: straw, fuel load: 0.6 kg/m². The time since ignition is indicated in each frame.
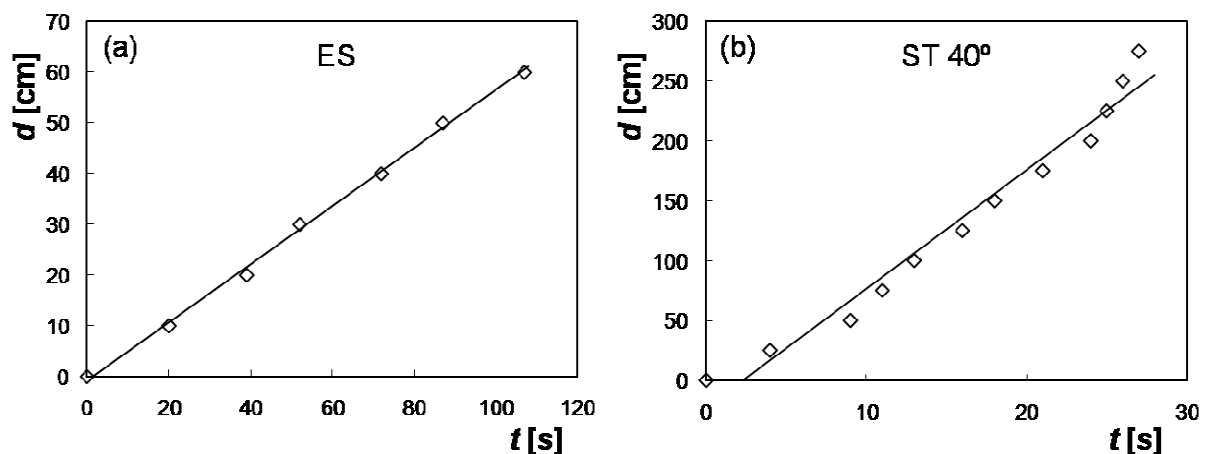
Figure 3.9 – Linear fit of the distance travelled by fire as a function of time (a) Test rig: Combustibility Table MC1, ref.: BS-MC1-31, fuel bed: eucalyptus slash, fuel load: 1.0 kg/m², fuel moisture: 4.6 %, computed basic ROS = 0.573 cm/s, r^2 = 0.997. (b) Test rig: Canyon Table DE4, ref.: FR-DE4-03, slope: 40°, fuel bed: straw; fuel load: 0.6 kg/m², fuel moisture: 12.8 %, computed ROS = 9.94 cm/s, r^2 = 0.971.

Table 3.2 – Parameters of the forward propagation experiments FP-TC2 in the combustion tunnel.

| Test parameters			Fuel bed data				Air conditions		ROS data		
Ref.	α [º]	u_0 [m/s]	Type	W [kg/m²]	m_f [%]	Bulk den. [kg/m³]	Temp. [ºC]	RH [%]	R_0 [cm/s]	R_h [cm/s]	R'_h
FP-TC2-97		1.0	straw	0.6	13.0	--	17.0	56	0.706	1.50	2.13
FP-TC2-100		1.5		0.6	11.7	--	17.5	49	0.698	3.10	4.45
FP-TC2-95		2.0		0.6	18.8	--	13.0	74	0.655	3.51	5.36
FP-TC2-98		2.5		0.6	15.4	--	15.5	62	0.531	5.00	9.42
FP-TC2-101		3.0		0.6	12.4	--	15.0	55	0.607	7.01	11.55
FP-TC2-94		3.5		0.6	12.9	--	15.5	74	0.686	8.34	12.15
FP-TC2-96		4.0		0.6	15.5	--	16.0	66	0.677	11.11	16.42
FP-TC2-99		4.5		0.6	13.2	--	13.0	59	0.660	17.64	26.74
FP-TC2-85		1.0	pine needles	0.6	13.5	--	20.5	70	0.265	0.93	3.52
FP-TC2-89		1.5		0.6	15.6	--	12.0	75	0.272	1.64	6.02
FP-TC2-111		2.0		0.6	15.5	--	21.0	71	0.302	2.34	7.75
FP-TC2-87	0	2.5		0.6	13.5	--	21.0	62	0.312	2.56	8.20
FP-TC2-110		3.0		0.6	13.4	--	23.0	62	0.292	3.44	11.81
FP-TC2-90		3.5		0.6	15.2	--	16.0	62	0.272	3.56	13.09
FP-TC2-86		4.0		0.6	14.0	--	19.5	66	0.272	3.93	14.47
FP-TC2-88		4.5		0.6	13.8	--	21.0	63	0.282	4.68	16.61
FP-TC2-50		1.0	eucalyptus slash	0.6	7.4	--	--	--	0.316	1.29	4.10
FP-TC2-48		1.5		0.6	7.2	--	--	--	0.276	1.60	5.79
FP-TC2-46		2.0		0.6	9.4	--	--	--	0.345	2.70	7.82
FP-TC2-51		2.5		0.6	7.4	--	--	--	0.344	4.65	13.54
FP-TC2-49		3.0		0.6	7.0	--	--	--	0.314	4.51	14.35
FP-TC2-44		3.5		0.6	6.9	--	--	--	0.290	5.53	19.05
FP-TC2-47		4.0		0.6	8.8	--	--	--	0.323	7.84	24.30
FP-TC2-45		4.5		0.6	6.9	--	--	--	0.290	7.45	25.67
FP-TC2-40		1.0	straw	0.8	10.4	--	--	--	0.643	1.87	2.91
FP-TC2-38		1.5		0.8	8.7	--	27.5	46	0.771	2.67	3.47
FP-TC2-42		2.0		0.8	10.4	--	--	--	0.792	4.07	5.14
FP-TC2-43		2.5		0.8	7.7	--	--	--	0.971	6.56	6.75
FP-TC2-37		3.0		0.8	8.6	--	23.5	68	0.771	6.23	8.09
FP-TC2-41		3.5		0.8	10.4	--	--	--	0.679	7.55	11.12
FP-TC2-103		4.0		0.8	13.7	--	11.0	77	0.626	10.61	16.95
FP-TC2-36		4.5		0.8	7.7	--	28.5	47	0.966	18.67	19.32
FP-TC2-79		1.0	pine needles	0.8	14.4	--	16.5	80	0.278	0.99	3.56
FP-TC2-68		1.5		0.8	13.6	--	--	--	0.298	1.48	4.94
FP-TC2-73		2.0		0.8	11.2	--	--	--	0.345	2.56	7.42
FP-TC2-70		2.5		0.8	12.6	--	--	--	0.300	2.86	9.52
FP-TC2-80	0	3.0		0.8	13.6	--	17.5	75	0.293	3.33	11.34
FP-TC2-74		3.5		0.8	12.4	--	--	--	0.317	3.91	12.34
FP-TC2-82		4.0		0.8	13.0	--	21.5	55	0.318	4.26	13.38
FP-TC2-81		4.5		0.8	12.7	--	20.5	63	0.347	5.81	16.75
FP-TC2-59		1.0	eucalyptus slash	0.8	6.9	--	--	--	0.406	1.43	3.53
FP-TC2-62		1.5		0.8	7.4	--	--	--	0.315	1.89	5.99
FP-TC2-52		2.0		0.8	8.7	--	29.0	34	0.363	2.82	7.76
FP-TC2-61		2.5		0.8	6.3	--	--	--	0.411	3.58	8.71
FP-TC2-60		3.0		0.8	6.1	--	30.0	20	0.518	5.96	11.51
FP-TC2-83		3.5		0.8	13.8	--	17.5	82	0.204	3.97	19.50
FP-TC2-65		4.0		0.8	5.2	--	--	--	0.535	13.00	24.29
FP-TC2-84		4.5		0.8	13.1	--	19.0	71	0.290	7.19	24.76

Table 3.3 – Parameters of the forward propagation experiments FP-DE4, FR-TC2, and FR-DE4, in the slope test rig and in the combustion tunnel.

Test parameters			Fuel bed data				Air conditions		ROS data		
Ref.	α [º]	u_0 [m/s]	Type	W [kg/m²]	m_f [%]	Bulk den. [kg/m³]	Temp. [ºC]	RH [%]	R_0 [cm/s]	R_h [cm/s]	R'_h
FP-DE4-01	10		straw	0.6	9.8	7.5	24.0	47	0.615	1.63	2.64
FP-DE4-04	20		straw	0.6	12.7	7.5	21.5	52	0.530	1.88	3.55
FP-DE4-03	30		straw	0.6	10.0	7.1	27.0	43	0.737	6.26	8.49
FP-DE4-02	40	0	straw	0.6	10.0	7.5	26.5	44	0.723	12.82	17.73
FP-DE4-07	10		pine needles	0.6	9.2	9.2	29.0	28	0.263	0.80	3.04
FP-DE4-05	20		pine needles	0.6	11.4	8.6	23.0	57	0.215	1.01	4.69
FP-DE4-08	30		pine needles	0.6	11.2	9.2	29.0	34	0.298	2.52	8.44
FP-DE4-06	40		pine needles	0.6	10.1	8.6	26.5	45	0.262	6.71	25.62
FR-TC2-06		1.0	straw	0.6	13.8	7.0	15.6	56	0.816	1.87	2.29
FR-TC2-03		2.0	straw	0.6	14.4	6.3	12.1	72	0.700	5.60	8.00
FR-TC2-05		3.0	straw	0.6	13.7	6.7	15.7	51	0.707	13.99	19.78
FR-TC2-04	0	4.0	straw	0.6	13.2	6.7	15.1	64	0.766	25.52	33.31
FR-TC2-09		1.0	pine needles	0.6	16.7	11.1	21.1	56	0.228	1.02	4.48
FR-TC2-07		2.0	pine needles	0.6	15.2	10.0	17.7	51	0.220	3.59	16.34
FR-TC2-10		3.0	pine needles	0.6	16.4	11.4	20.2	58	0.232	9.94	42.79
FR-TC2-08		4.0	pine needles	0.6	14.8	10.7	18.9	48	0.221	14.00	63.47
FR-DE4-02	10		straw	0.6	12.7	8.0	19.6	55	0.798	1.49	1.87
FR-DE4-05	20		straw	0.6	10.8	8.0	21.7	51	0.880	3.13	3.56
FR-DE4-01	30		straw	0.6	11.5	8.6	18.5	62	0.902	4.87	5.39
FR-DE4-04	40	0	straw	0.6	11.2	8.0	21.7	52	1.040	24.88	23.93
FR-DE4-08	10		pine needles	0.6	12.7	13.3	19.8	32	0.173	0.36	2.07
FR-DE4-09	20		pine needles	0.6	14.1	12.8	18.7	32	0.168	0.66	3.92
FR-DE4-06	30		pine needles	0.6	13.3	12.6	17.7	36	0.178	2.53	14.16
FR-DE4-07	40		pine needles	0.6	11.5	12.2	20.4	33	0.186	11.72	62.92

Fire line rotation and extension assessment

The second process refers to the infrared image analysis in order to obtain the fire line evolution contours. The first step in the image processing was the selection of the frames. The images were recorded with a time interval of 1 s, using a laptop connected to the infrared camera. Depending on the experimental conditions and the overall duration of each test, an adequate time interval *dt* was chosen, in order to have a reasonable number of frames to process and to have an adequate description of the evolution of the fire perimeter.

In the FR-DE4 and FR-TC2 experiments, as the ROS varied greatly with the tilt angle or wind velocity, the time step used depended on those parameters varying from 2 to 25 s for straw fuel beds and from 2 to 60 s for pine needles beds. In some cases, non uniform time intervals were used to describe the fire. On the other hand in the BR-DE4 and BR-TC2 experiments the fire spread the ROS did not vary much with the tilt angle and the time steps *dt* used for a given fuel bed were constant for all tests and equal to 20 and 60 s for straw and pine needles respectively.

Table 3.4 – Parameters of the backwards propagation experiments in the slope test rigs and in the combustion tunnel.

Test parameters			Fuel bed data				Air conditions		R0S data		
Ref.	α [º]	u_0 [m/s]	Type	W [kg/m²]	m_f [%]	Bulk den. [kg/m³]	Temp. [ºC]	RH [%]	R_0 [cm/s]	R_b [cm/s]	R'_b
BR-DE4-01	-10	0	straw	0.6	8.7	10.7	27.8	39	0.984	0.812	0.826
BR-DE4-04	-20		straw	0.6	10.4	8.0	25.5	46	0.802	0.691	0.862
BR-DE4-03	-30		straw	0.6	11.2	8.0	26.6	40	0.941	0.754	0.802
BR-DE4-05	-40		straw	0.6	8.5	8.6	30.5	34	1.163	0.938	0.807
BR-DE4-09	-10		pine needles	0.6	12.3	12.0	28.6	44	0.202	0.187	0.925
BR-DE4-07	-20		pine needles	0.6	12.4	12.2	26.0	49	0.236	0.183	0.776
BR-DE4-06	-30		pine needles	0.6	11.0	12.6	28.7	34	0.293	0.256	0.876
BR-DE4-08[3]	-40		pine needles	0.6	11.7	12.2	30.6	39	0.235	NV	NV
BR-TC2-14	0	-0.5	straw	0.6	8.9	9.0	32.0	36	0.855	0.939	1.099
BR-TC2-01		-1.0	straw	0.6	8.1	10.9	31.8	40	1.097	0.794	0.724
BR-TC2-04		-2.0	straw	0.6	9.5	10.0	32.2	39	0.783	0.765	0.977
BR-TC2-03		-3.0	straw	0.6	10.6	9.2	29.3	44	0.675	0.675	0.999
BR-TC2-02		-4.0	straw	0.6	7.7	9.2	32.3	40	0.776	0.545	0.702
BR-TC2-11[2]		-4.5	straw	0.6	11.1	7.1	25.4	57	0.889	DS	DS
BR-TC2-13		-0.5	pine needles	0.6	9.9	14.3	30.4	40	0.235	0.185	0.786
BR-TC2-06		-1.0	pine needles	0.6	13.7	12.0	24.9	54	0.233	0.204	0.875
BR-TC2-05		-2.0	pine needles	0.6	11.9	13.0	31.0	40	0.217	0.193	0.889
BR-TC2-07[1]		-3.0	pine needles	0.6	10.7	10.9	32.1	39	0.256	0.200	0.780
BR-TC2-08[1]		-4.0	pine needles	0.6	10.6	11.8	33.3	36	0.234	0.183	0.785
BR-TC2-10[2]		-4.5	pine needles	0.6	13.5	11.8	33.0	37	0.254	DS	DS
BP-DE1-08	-5	0	straw	0.6	11.2	9.4	16.3	54	0.904	0.832	0.921
BP-DE1-05	-10		straw	0.6	11.2	10.0	20.7	38	1.050	0.737	0.702
BP-DE1-12	-15		straw	0.6	9.6	9.1	22.2	33	1.027	0.786	0.765
BP-DE1-10	-20		straw	0.6	10.9	9.5	22.1	39	0.926	0.688	0.743
BP-DE1-01	-25		straw	0.6	12.8	9.7	18.3	43	1.087	0.716	0.659
BP-DE1-11	-30		straw	0.6	9.9	9.4	22.2	34	0.959	0.703	0.733
BP-DE1-03	-35		straw	0.6	10.0	9.0	21.3	38	1.130	0.825	0.730
BP-DE1-09	-40		straw	0.6	11.2	10.9	19.2	47	0.922	0.721	0.781
BP-DE1-07	-45		straw	0.6	13.8	9.8	14.1	59	0.947	0.616	0.650
BP-DE1-04	-50		straw	0.6	12.2	9.4	21.2	37	1.012	0.816	0.807
BP-DE1-06	-55		straw	0.6	11.2	8.7	12.6	64	0.909	0.674	0.742
BP-DE1-19	-5		pine needles	0.6	14.6	12.5	18.3	71	0.251	0.193	0.768
BP-DE1-22	-10		pine needles	0.6	14.3	12.5	17.3	50	0.214	0.183	0.855
BP-DE1-17	-15		pine needles	0.6	14.0	12.5	18.5	67	0.261	0.170	0.652
BP-DE1-20	-20		pine needles	0.6	15.9	12.2	16.1	66	0.179	0.148	0.825
BP-DE1-23	-25		pine needles	0.6	14.6	13.0	16.4	46	0.190	0.176	0.924
BP-DE1-15	-30		pine needles	0.6	14.4	13.0	18.1	66	0.210	0.206	0.983
BP-DE1-21	-35		pine needles	0.6	15.0	11.8	17.1	55	0.228	0.189	0.829
BP-DE1-16	-40		pine needles	0.6	14.4	13.3	19.6	64	0.204	0.181	0.887
BP-DE1-14	-45		pine needles	0.6	13.7	12.5	15.9	70	0.224	0.196	0.876
BP-DE1-25[3]	-50		pine needles	0.6	14.4	13.0	16.6	44	0.202	NV	NV
BP-DE1-18[3]	-55		pine needles	0.6	14.6	12.0	18.4	71	0.189	NV	NV

[1]Fire put out after parallel ignition to the wind. Perpendicular ignition was made afterwards.
[2]Fire did not spread because it was put out with wind.
[3]Non-validated ROS experiment due to spotting inside the fuel bed.

For each experiment, after selecting the frames to analyse, using CAD software, the contours of the fire line for each frame were drawn and corrected to represent orthogonal projections of the fire contours to a plane parallel to the camera lens, using the software

developed by Gonçalves (2000). In the FR-DE4 and FR-TC2 experiments, as the selected temperature amplitude in the infrared camera was in the range -40 ℃ to 120 ℃, the image of the head fire zone in some frames was affected by the presence of the fire plume hot gases. In order to address this situation, the video images were used as a complement to determine the position of the fire line. In the BR-DE4 and BR-TC2 experiments the selected temperature amplitude was in the range 0 ℃ to 500 ℃ and there was no problem.

Table 3.5 – Parameters of the basic ROS experiments.

Test		Fuel bed data			Air conditions		R0S
Ref.	Type	W [kg/m²]	m_f [%]	Bulk den. [kg/m³]	Temp. [ºC]	RH [%]	R_0 [cm/s]
FP-TC2-25	straw	0.6	7.5	--	27.5	37	0.897
FP-TC2-28		0.6	6.9	--	34.0	26	0.793
FP-TC2-102		0.6	18.2	--	9.5	82	0.455
BS-MC1-39		0.6	8.3	7.1	--	--	0.967
BS-MC1-45		0.6	8.2	7.5	--	--	1.337
BS-MC1-51		0.6	7.3	7.5	--	--	1.328
FP-TC2-36		0.8	7.7	--	28.5	47	0.966
FP-TC2-39		0.8	8.7	--	27.5	46	0.796
BS-MC1-05		0.8	6.3	8.9	--	--	1.227
BS-MC1-09		0.8	6.1	8.9	--	--	1.242
BS-MC1-13		0.8	5.8	7.6	--	--	1.419
BS-MC1-23		1.0	7.2	7.7	--	--	1.234
BS-MC1-29		1.0	7.0	8.3	--	--	1.232
BS-MC1-35		1.0	6.7	9.1	--	--	1.313
FP-TC2-85	pine needles	0.6	13.5	--	20.5	70	0.265
FP-TC2-108		0.6	16.9	--	8.5	70	0.218
FP-TC2-109		0.6	16.3	--	15.0	67	0.225
BS-MC1-41		0.6	8.4	7.5	--	--	0.371
BS-MC1-47		0.6	7.8	7.5	--	--	0.429
BS-MC1-53		0.6	7.3	7.5	--	--	0.391
FP-TC2-69		0.8	12.8	--	21.5	78	0.258
FP-TC2-71		0.8	12.2	--	--	--	0.316
FP-TC2-72		0.8	12.7	--	--	--	0.286
BS-MC1-03		0.8	6.6	7.0	--	--	0.519
BS-MC1-11		0.8	5.9	7.6	--	--	0.593
BS-MC1-17		0.8	5.3	7.0	--	--	0.610
BS-MC1-21		1.0	7.4	8.7	--	--	0.553
BS-MC1-27		1.0	7.3	8.3	--	--	0.539
BS-MC1-33		1.0	5.8	8.7	--	--	0.559
FP-TC2-32	eucalyptus slash	0.6	6.6	--	31.0	32	0.367
BS-MC1-37		0.6	7.6	8.0	--	--	0.318
BS-MC1-43		0.6	6.3	8.6	--	--	0.367
BS-MC1-49		0.6	5.7	7.5	--	--	0.402
FP-TC2-63		0.8	6.6	--	--	--	0.436
FP-TC2-64		0.8	6.0	--	29.0	23	0.663
BS-MC1-01		0.8	5.3	7.6	--	--	0.597
BS-MC1-07		0.8	4.7	8.4	--	--	0.589
BS-MC1-15		0.8	4.4	7.6	--	--	0.581
BS-MC1-19		1.0	5.8	8.3	--	--	0.524
BS-MC1-25		1.0	5.5	8.3	--	--	0.596
BS-MC1-31		1.0	4.6	9.1	--	--	0.573

Table 3.6 – Average parameters and standard deviation for the forward and backwards series of experiments.

Ref.	m_f [%]	ST Dev. [%]	Bulk den. [kg/m³]	ST Dev. [kg/m³]	Temp. [ºC]	ST Dev. [ºC]	RH [%]	ST Dev. [%]	R_0 [cm/s]	ST Dev. [cm/s]
ST-FP-TC2	14.1	2.34	--	--	15.3	1.65	62	9.0	0.652	0.0581
ST-FP-TC2-0.8	9.7	2.01	--	--	22.6	8.05	60	15.5	0.777	0.1331
ST-FR-TC2	13.8	0.27	6.68	0.274	14.6	1.70	61	9.2	0.747	0.0547
PN-FP-TC2	14.3	0.95	--	--	19.3	3.55	66	5.0	0.283	0.0167
PN-FP-TC2-0.8	12.9	0.98	--	--	19.0	2.38	68	11.4	0.312	0.0244
PN-FR-TC2	15.8	0.62	10.81	0.616	19.5	1.49	53	4.6	0.225	0.0059
ES-FP-TC2	7.6	0.95	--	--	--	--	--	--	0.312	0.0252
ES-FP-TC2-0.8	8.4	3.25	--	--	23.9	6.54	52	29.5	0.380	0.1124
ST-FP-DE4	10.6	1.39	7.39	0.221	24.8	2.53	47	4.0	0.651	0.0975
ST-FR-DE4	11.6	0.82	8.14	0.286	20.4	1.59	55	5.0	0.905	0.1006
PN-FP-DE4	10.5	1.02	8.90	0.381	26.9	2.84	41	12.8	0.260	0.0342
PN-FR-DE4	12.9	1.11	12.74	0.451	19.2	1.20	33	1.9	0.176	0.0077
ST-BP-DE1	11.3	1.27	9.5	0.59	19.1	3.40	44	10.5	0.988	0.077
ST-BR-DE4	9.7	1.29	8.8	1.29	27.6	2.15	40	4.9	0.972	0.149
PN-BP-DE1	14.5	0.57	12.6	0.48	17.5	1.18	61	10.2	0.214	0.026
PN-BR-DE4	11.9	0.63	12.3	0.26	28.5	1.89	42	6.5	0.241	0.038
ST-BR-TC2	9.3	1.34	9.2	1.25	30.5	2.74	43	7.5	0.846	0.143
PN-BR-TC2	11.7	1.60	12.3	1.19	30.8	3.09	41	6.6	0.238	0.015

For each test, an image similar to those shown in Figures 3.10 and 3.11, that correspond to tests made in the Canyon Table DE4 with favourable or contrary slope respectively, was obtained. Although the fire line evolution was more irregular in the experiments with favourable or contrary wind, as it can be seen in Figures 3.6 and 3.8, the fire line contour evolutions are similar to those shown in Figures 3.10 and 3.11.

In these figures, we have *p* contours corresponding to *p-1* time steps of the analysis. In the initial line, at $t = t_0$, we chose *n* points that define *n-1* fire line segments referred as S_i with *i* varying from 1 to *n-1*. The initial segments were chosen at the centre of the ignition fire line in order to minimize edge effects. The length of the initial fire line elements was chosen to be around 5 % of the ignition line length that in the FR-DE4 and FR-TC2 experiments was approximated by the fuel bed width, corresponding to 15 cm for the Canyon Table and 10 cm for the Combustion Tunnel. In the BR-DE4 and BR-TC2 experiments that corresponded to 4 cm for both test rigs. A larger distance would minimize the description of the fire perimeter, on the contrary a smaller distance would result in a poor definition of the fire line element orientation and size, given the non regular shape of the fire perimeter in many situations of fire spread as was described in Viegas (2007b). As a rule, three fire line segments were chosen in FR-DE4 and FR-TC2 tests although in some cases more points were considered. In tests BR-DE4 and BR-TC2, given the existence of a symmetry axis in the initial fire perimeter, segments from the right

50

and left sides were considered and referred as S_{iR}, S_{iL} respectively. The centreline segment was referred as S_{CL}. For BR-DE4 tests, a centreline element and four segments from each side were usually considered. Given the fuel bed of the BR-TC2 tests was narrower, the fire line elements reached the fuel bed limits more rapidly and, for this reason, besides the centreline element five segments from each side were usually considered in order to increase the amount of data.

The tangent direction to the fire line contour at each point P_i is determined by geometric construction; from this a perpendicular line is drawn to define the ROS direction and to determine the point P'_i corresponding to the position of point P_i at time $t' = t+dt$. This process was repeated for each time step as shown in Figures 3.10 and 3.11. The coordinates x_i, y_i of each point were determined using the CAD software and were then used to determine the various parameters analysed in this study.

For each segment S_i (Figure 3.12) it was determined successively:

- The length $a_{i(i+1)}$ and $a'_{i(i+1)}$ at time t and at time $t+dt$ respectively.
- The fire line extension ε.
- The rate of spread R_i and R_{i+1} at points P_i and P_{i+1} at the ends of the fire line segment.
- The average rate of spread at the midpoint of the fire line segment.
- The average angle of inclination $\beta_{i(i+1)}$ and $\beta'_{i(i+1)}$ at time t and at time $t+dt$ respectively.
- The rotational velocity ω.

For the FR-DE4 and FR-TC2 tests were also determined:

- The normal component R_{in} and $R_{(i+1)n}$ of the ROS respectively at points P_i and $P_{(i+1)}$ perpendicular to the straight fire line element $a_{i(i+1)}$.
- The characteristic flow velocity u_y perpendicular to the fire line element.
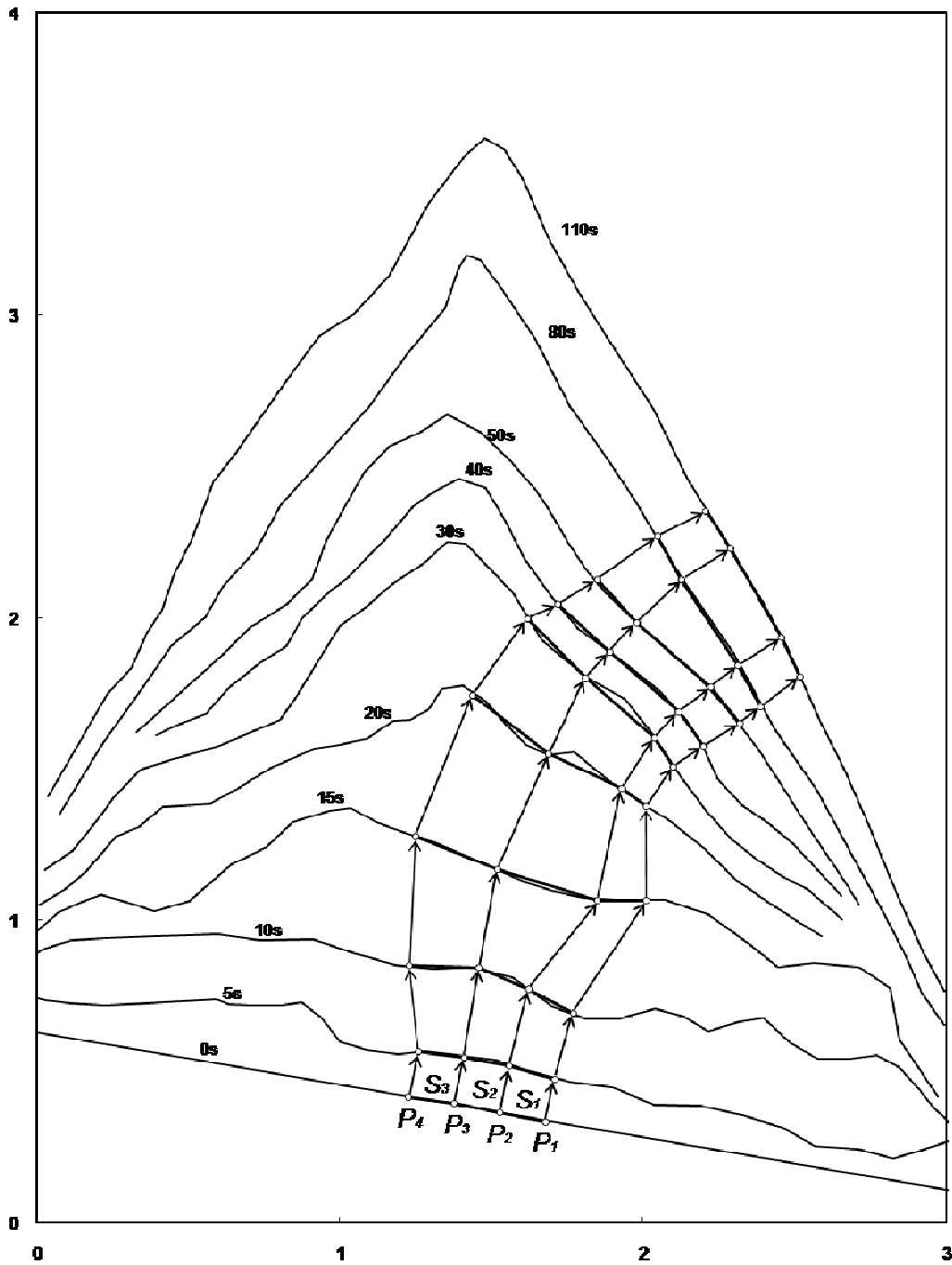
Figure 3.10 – Fire line contours and point evolution with time for an experiment on the Canyon Table DE4, ref.: FR-DE4-06, slope: 30°, fuel bed: pine needles, fuel load: 0.6 kg/m². Burn area dimensions in [m].
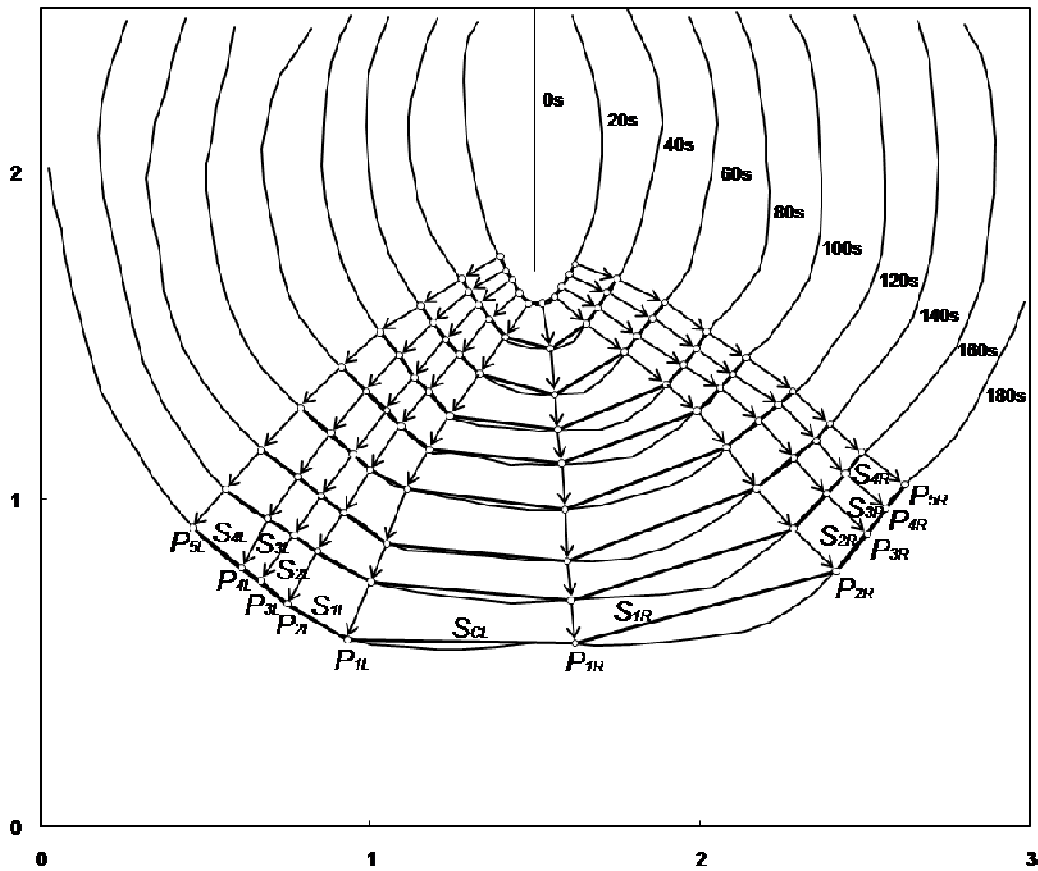
Figure 3.11 – Fire line contours and point evolution along time for an experiment on the Canyon Table DE4, ref.: BR-DE4-03, fuel bed: straw, slope: -30°, fuel load: 0.6 kg/m^2. Burn area dimensions in [m].
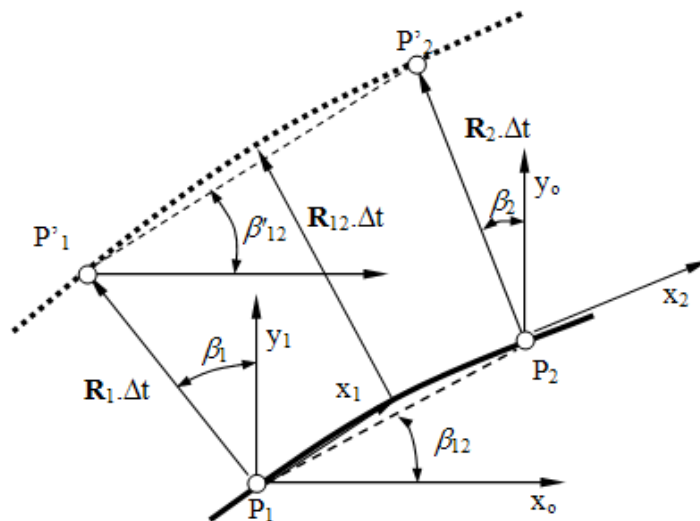
Figure 3.12 – Schematic description of the elements used to determine the components of the model from experimental fire perimeters.

4. Results and discussion

4.1. Analysis of fire line spread

4.1.1. Basic rate of spread

Fuel load and fuel moisture effects

The experimental results for the basic ROS, R_0, as a function of fuel moisture content for straw, pine needles and eucalyptus slash are plotted in Figures 4.1 and 4.2a. For the three types of fuel the data suggests that, for the range of tested fuel moisture, the obtained ROS is independent of the fuel load, since for a given moisture content the R_0 results do not exhibit significant differences between them nor a trend for higher or smaller values depending on the fuel load. Having in mind this consideration, for each fuel, the entire set of data for all fuel loads (Tables 3.2 to 3.5) was considered for obtaining a best fit of the polynomial law given by Eq. (2.1), yielding the parameters presented in Table 4.1. The corresponding curves are plotted in Figures 4.1 and 4.2.
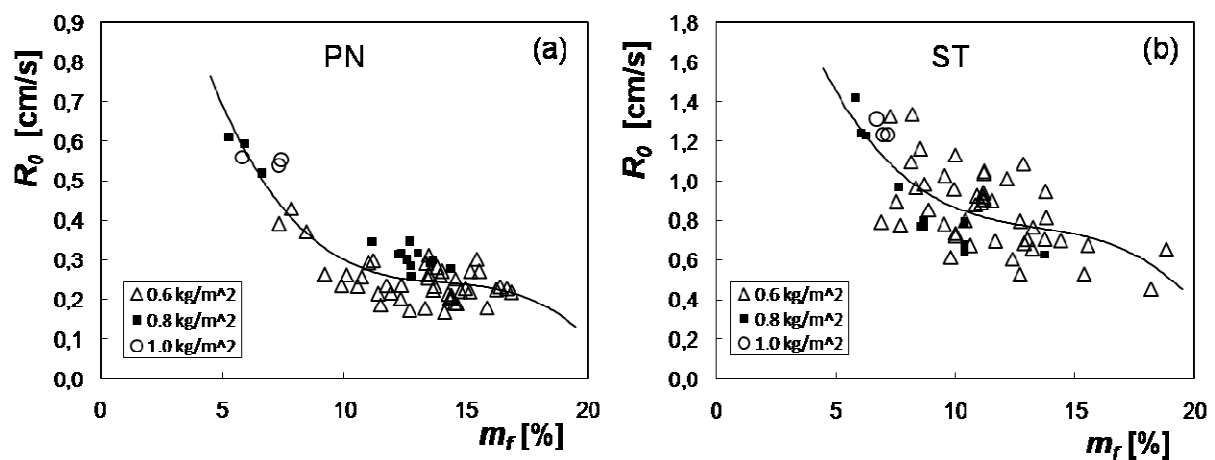
Figure 4.1 – Basic ROS as a function of fuel moisture from single test burns, fuel loads: 0.6, 0.8 and 1.0 kg/m², fitting parameters for Eq. (2.1) presented in Table 4.1: (a) Pine needles tests. (b) Straw tests.

As we can see, straw has higher scattering in terms of ROS when compared with both pine needles and eucalyptus slash. This is explained by the difficulty of providing fuel with very similar properties over a long period of time which will have consequences in terms of the burning properties of the individual fuel particles and also on the bulk density of the fuel beds. In Table 4.1 we can also find some statistical data regarding the fitting curves. For computing the

standard deviation it was assumed that for a given fuel moisture the ROS values would follow a normal distribution around the mean value that was considered to be the obtained value by the prediction curves. The error was estimated so that, considering the number of experiments, a ROS value would be predicted within a 95% level of confidence.
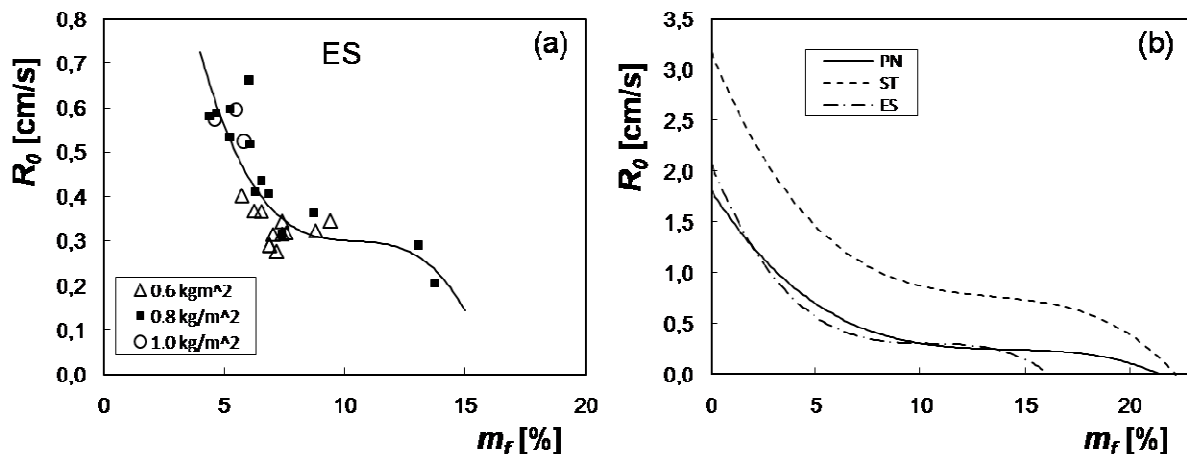
Figure 4.2 – Basic ROS as a function of fuel moisture from single test burns, fuel loads: 0.6, 0.8 and 1.0 kg/m², fitting parameters for Eq. (2.1) presented in Table 4.1: (a) Eucalyptus slash tests. (b) Fitting curves for pine needles, straw and eucalyptus slash fuel beds.

Table 4.1 – Parameters for Eq. (2.1) for R_0 as a function of the fuel moisture content for each fuel bed.

Fuel bed	Parameters							
	n_{exp}	a_0	b_0	c_0	d_0	r^2	[1]ST Dev. [cm/s]	[2]Error [cm/s]
Pine needles	64	-5.29E-04	0.0225	0.322	1.808	0.792	0.074	0.019
Straw	63	-8.92E-04	0.0358	0.500	3.173	0.493	0.155	0.039
Eucalyptus slash	28	-1.53E-03	0.0479	0.504	2.071	0.699	0.095	0.036

[1]The ST Dev. was computed considering the predicted value as the mean and accounting for n_{exp}.
[2]The error was estimated for a prediction within a 95 % level of confidence ($2 \times$ ST Dev.$\times n_{exp}^{-1/2}$).

Solving the equations for a null value of R_0 we can estimate a fuel moisture of extinction of around 22.2 %, 21.4 %, and 16.1 % for pine needles, straw, and eucalyptus slash respectively (Figure 4.2b). Using data from Anderson (1964) for ponderosa pine needles for obtaining a best fit of the polynomial law given by Eq. (2.1) we obtain around 18 %. Marsden-Smedley *et al.* (2001) present data for buttongrass moorlands indicating that for low wind velocities we begin to observe non-sustaining fires above dead fuel moisture of approximately 20 %. For fire spread in eucalypt fuels under calm wind conditions McArthur (1967) presents values of around 15 % for the fuel moisture corresponding to a null rate of spread. One must have in mind that a comparison between data from these authors and those presented here must be done carefully,

56

because there could be differences due to the particular fuel species being sampled and method used for the fuel moisture analysis. Also, further experiments should be made for higher fuel moisture contents in order to verify the validity of the estimated fuel moistures of extinction. Nevertheless, there is a general reasonable agreement between the present results and those from other sources. For conditions of marginal burning the data can be rather scattered and the modelling of the threshold value that defines if the fire will sustain or not as a function of the fuel moisture content is better described by probability functions instead of deterministic ones (Marsden-Smedley *et al.*, 2001; Zhou *et al.*, 2005).

4.1.2. Head fire

Eruptive fire behaviour

When analysing the plotting of the distance travelled by fire as a function of time it was verified that for the slope experiments up to 20º the slope of the line *x(t)*, that gives the ROS between two points, remains fairly constant during fire spread but with high inclinations of 30 or 40º, like shown in Figure 3.9b, it is usual to observe a slight increase in the ROS with time (Viegas, 2004). This is a consequence of the fire dynamic behaviour, *i.e.* the changing of fire spread properties over time even for constant boundary conditions, caused by a convective heat flow along the fire line. An extreme consequence of the dynamic fire behaviour is the eruptive fire behaviour (Viegas, 2005 and 2006), a sudden increase in the fire velocity caused by the wind flow feedback effect, that occurs in long very inclined hills and especially in canyons (Viegas and Pita, 2004). It can also occur under high steady winds but due to the wind velocity natural variability it is not so likely to happen. On the other hand, also for high inclinations, as the initial line ignition spreads upslope, the head fire gets narrower diminishing the heat received by radiation from the fuel ahead of the most advanced part of the fire line. Cheney and Gould (1995) referred to the importance of the fire line width on the ROS. The narrowing of the head fire after the line ignition opposes to the fire tendency to accelerate and, since for slope-driven fires caused by line ignitions the increase in the ROS usually takes place in longer fuels beds than those used here (up to 6 m) after the head fire reaches a more or less constant triangular shape, it was considered that the ROS remained constant during each experiment.

In the combustion tunnel experiments, for a given rotation frequency of the fans, the flow velocity tends to decrease as the fire moves away from the fans, as it was verified during the

tunnel calibration referred previously, not allowing the fire to increase the velocity like in the high tilted slope tests.

Fuel load

In Figure 4.3 we can see the results for the ROS of the most advanced part of the head fire R_h and in Figure 4.4 we have the results for the non-dimensional ROS R_h', obtained for the wind driven or slope driven head fires. As for each experiment the ROS on level ground in the absence of wind R_0 was determined, the ROS corresponding to a null wind velocity or null slope was considered to be the average of the R_0 for that series of tests.
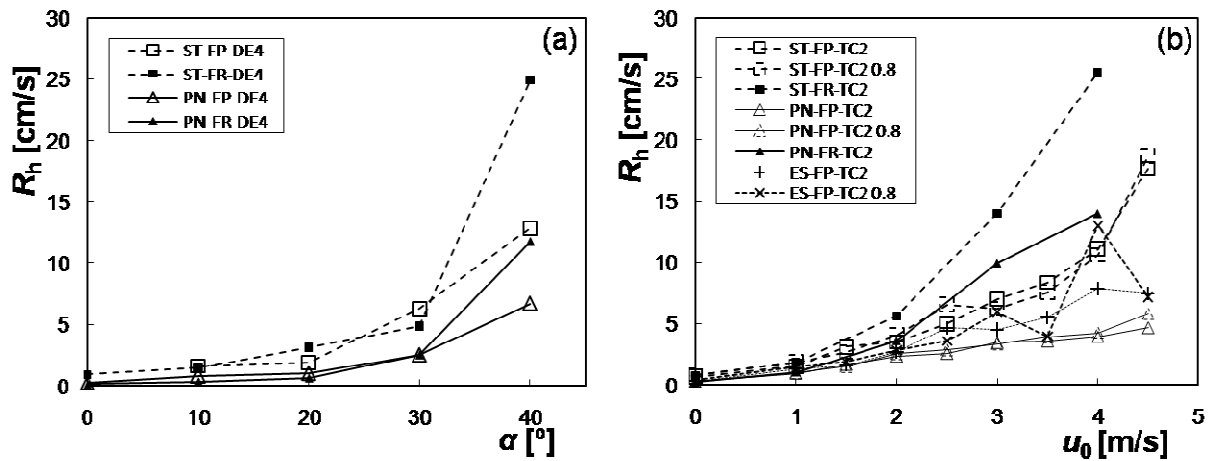
Figure 4.3 – ROS results from single test burns, except for a null wind velocity or null slope where the average of the R_0 for that series of tests was considered: (a) As a function of slope, fuel beds: straw and pine needles, fuel load: 0.6 kg/m². (b) As a function of wind velocity, fuel beds: straw, pine needles and eucalyptus slash, fuel loads: 0.6 and 0.8 kg/m².

As the non-dimensional ROS, R_h', represents a ratio between the fire absolute ROS under the influence of wind or slope and the ROS on a horizontal terrain without ambient wind, for the same fuel bed, one could expect small differences in the fuel bed properties from one experiment to another under the same wind or slope not to originate major differences in its value. This is particularly important given the impossibility to control certain parameters, namely fuel moisture content.

It is easy to observe in Figures 4.3 and 4.4 that for slope angles greater than 20° and wind velocities greater than 1.5 m/s significant differences exist between some series of experiments, even for the same fuels and very similar fuel bed arrangement. When trying to identify their cause, according to the results for the wind driven fires shown in Figures 4.3b and 4.4b, the fuel

load does not seem to have a significant influence on the ROS. As can be seen in the results, for the absolute and non-dimensional ROS, for the six series of FP-TC2 experiments that correspond to testing the wind velocity effect on three different fuels and for two fuel loads, for each fuel there are no significant differences in the results for the tested fuel loads. Thus, for each fuel, the entire set of data for the two tested fuel loads was considered for obtaining a best fit of the polynomial law given by Eq. (2.2), yielding the parameters presented in Table 4.2.
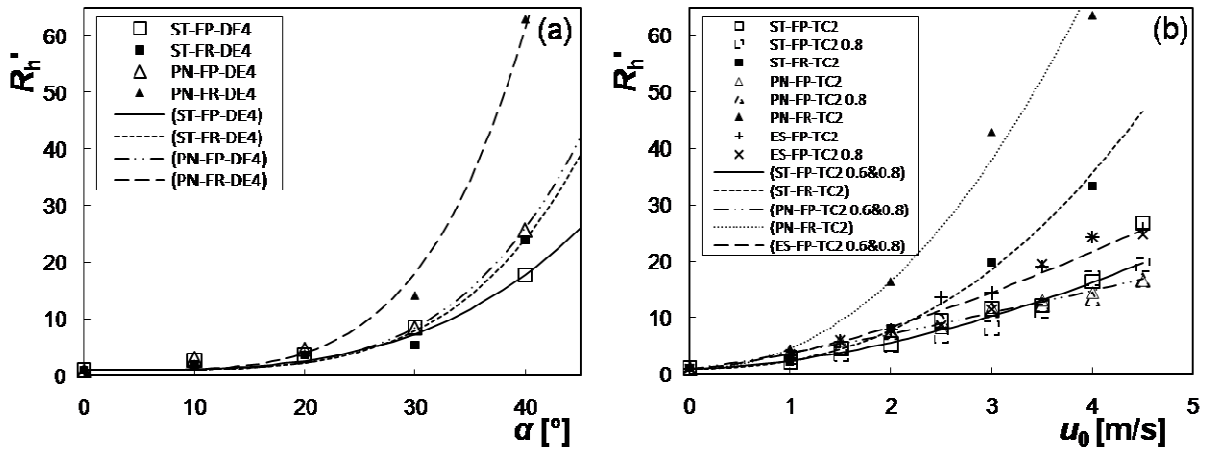
Figure 4.4 – Non-dimensional ROS results from single test burns: (a) As a function of slope, fuel beds: straw and pine needles, fuel load: $0.6 \, \text{kg/m}^2$, fitting parameters for Eq. (2.3) presented in Table 4.3. (b) As a function of wind velocity, fuel beds: straw, pine needles and eucalyptus slash, fuel loads: 0.6 and 0.8 kg/m^2, fitting parameters for Eq. (2.2) presented in Table 4.2.

The statistical data regarding the standard deviation and the error was estimated having in mind the same considerations as for the basic ROS experiments. It should be noted that, at least for the series where only four tests were made, we are dealing with a relatively small sample and the standard deviation would have been estimated more accurately if n_{exp} - 1 was considered instead of the total number of experiments. However, for the sake of performing the same analysis for all the experiments, n_{exp} was considered instead.

Table 4.2 – Parameters for Eq. (2.2) for the wind driven fires for data series.

Data series	n_{exp}	$a_{1,u}$	$b_{1,u}$	r^2	[1]ST Dev. [cm/s]	[2]Error [cm/s]
PN-FP-TC2 0.6&0.8	16	2.701	1.178	0.983	0.603	0.301
PN-FR-TC2	4	3.544	2.135	0.995	3.794	3.794
ST-FP-TC2 0.6&0.8	16	1.398	1.724	0.955	2.040	1.020
ST-FR-TC2	4	1.326	2.353	0.998	1.303	1.303
ES-FP-TC2 0.6&0.8	16	2.630	1.487	0.968	1.573	0.787

[1]The ST Dev. was computed considering the predicted value as the mean and accounting for n_{exp}.

[2]The error was estimated for a prediction within a 95 % level of confidence ($2 \times$ST Dev.$\times n_{exp}^{-1/2}$).

The fuel load effect on the ROS is not consensual in the literature. The present results agree with those from Cheney *et al.* (1993) but for example Luke and McArthur (1978) and Cheney (1981) report that the ROS increases nearly linearly with the fuel load. On the other hand, Thomas (1971) reports that it varies inversely with loading, the same dependence drawn theoretically by Fleeter *et al.* (1984). Based on the present work, for wind or slope aided and also level ground propagation, at least for fine fuel beds maintaining a constant bulk density and having tested three different fuel beds, the ROS does not seem to depend on the fuel load.

Regarding the slope driven fires, the best fit of the polynomial law given by Eq. (2.3) obtained using least square error yielded curves that for values of α above 30º had significant differences between the predicted R_h' values and those obtained by experiments. For this reason a visual fit was obtained instead, yielding the parameters presented in Table 4.3. Given the similarities between wind and slope effects on fire spread, in principle, the fuel load independence of the ROS should be observed also in slope driven head fires.

Table 4.3 – Parameters for Eq. (2.3) for the slope driven fires for each data series.

Data series	n_{exp}	$a_{1,\alpha}$	$b_{1,\alpha}$	[1]ST Dev. [cm/s]	[2]Error [cm/s]
PN-FP-DE4	4	4.50E-06	4.210	1.541	1.541
PN-FR-DE4	4	6.00E-06	4.370	2.217	2.217
ST-FP-DE4	4	6.00E-05	3.400	1.065	1.065
ST-FR-DE4	4	4.00E-06	4.220	1.452	1.452

[1]The ST Dev. was computed considering the predicted value as the mean and accounting for n_{exp}.

[2]The error was estimated for a prediction within a 95 % level of confidence ($2 \times$ST Dev.$\times n_{exp}^{-1/2}$).

Fuel bed width

Analysing the R_h results, one might be tempted to conclude that there was some effect of the fuel bed width on the ROS, given the series of experiments ST-FR-TC2 and PN-FR- TC2, with wider fuel beds, exhibit higher values of ROS when compared with others made with the same fuel but having lower average m_f values and higher average R_0. However, making the same analysis in the DE4 test rig results, where all the experiments had the same fuel bed width, again the ST-FP-DE4 and PN-FR-DE4 series have higher ROS when compared with the other experiments made with the same fuel and where the average m_f was lower in both cases and the average R_0 was lower for the pine needles. Therefore, the fact that the ST-FR and PN-FR series of experiments consistently exhibit higher R_h values in both test rigs appears not to be related with an eventual effect of the fuel bed width, but rather with other factors affecting the combustibility.

Fuel moisture and fuel bed combustibility

When comparing the R_h values of the two FP-TC2 series of experiments in the wind tunnel, for a given fuel (Figure 4.3b), we can see that the ROS does not seem to be very affected by the differences in the average fuel moisture content. This probably can be explained by the small variation in the R_0 velocity for values of m_f around $10 - 15$ % (Figures 4.1 and 4.2) that could indicate a similarity in the combustibility properties for that range.

However, the FR-TC2 and FR-DE4 results for both straw and pine needles do not corroborate this assumption. Nevertheless, the fact that R_h values are higher for both fuels and for experiments made in different test rigs, when compared with the other corresponding experiments, seems to exclude differences in the fuel properties and an eventual factor related with the test rig as a cause for the difference in the results. This is a strong indicator that the cause for the observed differences is external to the fuel bed.

Although each experiment in the series was performed in a random order to avoid any bias in the results, each series of experiments was made usually within $4 - 5$ days to minimize the variations in the ambient conditions. In Table 3.6 we can see that in general, for a series of experiments, the standard deviation for each controlled parameter is usually low. This is very important to assure consistency between the results of a given series and we can see that the higher R_h values in the FR-TC2 and FR-DE4 experiments were observed, regardless of the test rig or fuel used, reinforcing the idea that it most likely had something to do with parameters external to the fuel bed, that will be discussed below.

One parameter that could have had been responsible for such results is the ambient air stability inside the laboratory. It is clear that fire spread is influenced by fire-atmosphere interactions (Coen, 2005; Linn *et al.*, 2007; Sun *et al.*, 2009) and the laboratory facilities height is around 8 m, which should be sufficient to observe significant differences in the air temperature vertical profile, although at this point the author does not have data to support this hypothesis. Another parameter that could have had a significant influence is the mean radiative temperature of the surrounding surfaces that, in principle, can have considerable variations for a given air temperature and that influences the fire and fuel bed radiative losses. Butler (2006) analysed the effect of solar radiation on the ROS of fires spreading on level ground in the absence of wind, concluding that low magnitude surface incident irradiation, such as solar heating, can affect the ROS of a fire burning through a bed of fine dead woody fuels. It is of great importance to

identify the causes of the observed differences in fire behaviour, so we can know *a priori* the set of conditions for which a pair of values of (a_1, b_1), associated with the functions defined in Eq. (2.2) and (2.3), for a given fuel bed combustibility is valid. Future work is intended to be done in order to address this problem.

Slope equivalent wind

As referred in Chapter 2, it shall be considered that for a given slope angle α we can define an equivalent wind velocity u_{eq} that produces the same ROS value on a horizontal ground. This equivalence was established only between series of wind driven and slope driven fires tests made in the same period, so that the fuel beds combustibility similarity was maximized by having similar ambient parameters.

As can be seen in Figure 4.5, for both fuel beds, the equivalence curves obtained are very similar, despite the differences between the FP and FR data series results (Figure 4.4). This suggests that, as long as the wind driven and slope driven fires are spreading under the same overall conditions, the equivalence between them should yield similar equivalence curves. For each fuel bed the entire set of data was then combined for obtaining a best fit of the power law shown in Eq. (2.7) yielding the parameters presented in Table 4.4.
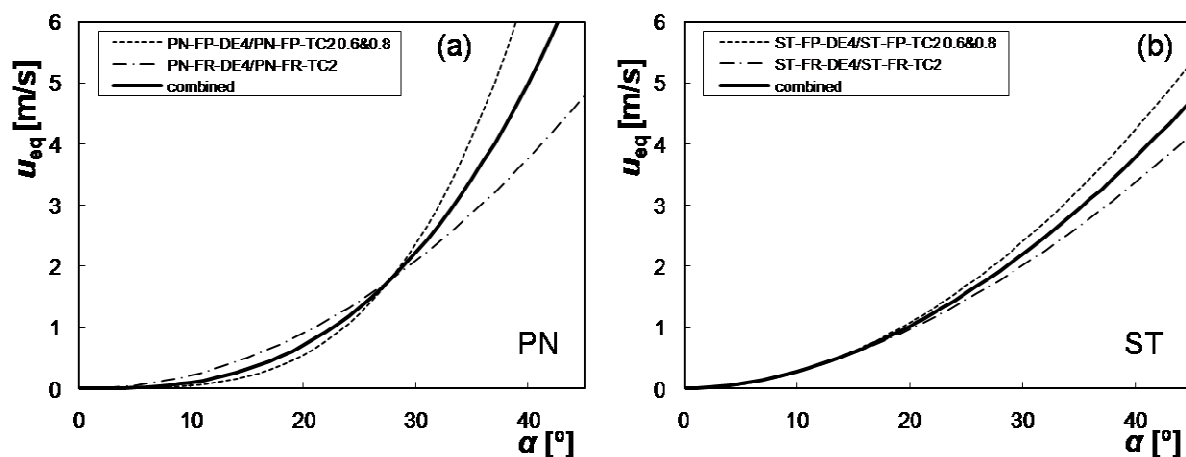
Figure 4.5 – Slope equivalent wind, fitting parameters for Eq. (2.7) presented in Table 4.4: (a) Pine needles tests. (b) Straw tests.

Table 4.4 – Parameters for Eq. (2.7) for slope equivalent wind for each fuel bed.

Fuel bed	a_α	b_α	r^2
Pine needles	1.57E-04	2.811	0.914
Straw	3.63E-03	1.883	0.997

4.1.3. Flank fire

Fire line extension rate

The results for the flank fire described in this section are based on the work of Viegas and Rossa (2009). In Figures 4.6 and 4.7, the fire line elements relative extension ε as a function of time, for the experiments FR-DE4 and FR-TC2, is shown. Although the data is scattered we can observe a tendency for higher extension rates for the fire line elements inclination angles β in the range 0-45°. In a few situations, especially for low tilt angles or wind velocities and in the beginning of the experiments, when the angle β was small, it sometimes became negative. However that corresponds to an unstable situation and those points were not considered.
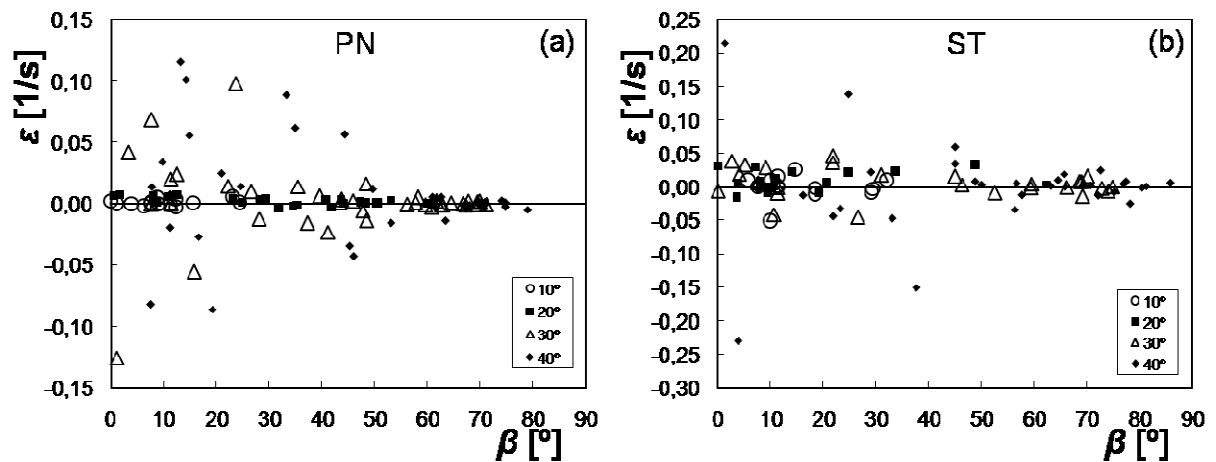
Figure 4.6 – Flank fire line elements relative extension ε as a function of the fire line element inclination angle β for the slope tests, fuel load: $0.6\,\mathrm{kg/m^2}$: (a) Pine needles fuel beds. (b) Straw fuel beds.
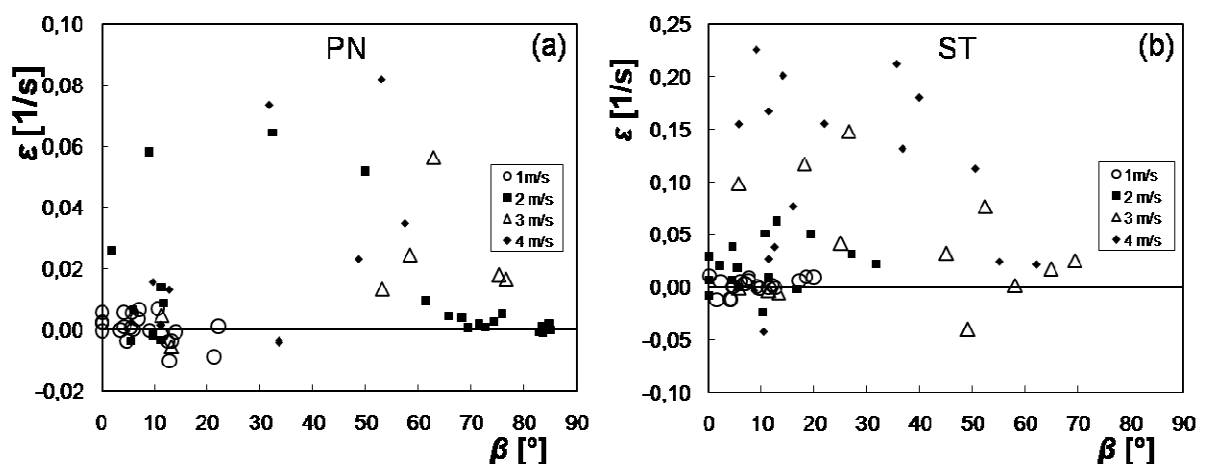
Figure 4.7 – Flank fire line elements relative extension ε as a function of the fire line element inclination angle β for the wind tests, fuel load: $0.6\,\mathrm{kg/m^2}$: (a) Pine needles fuel beds. (b) Straw fuel beds.

Analysing the relative extension data obtained, during the testing of the model, it was concluded that it is reasonable to consider an average value of this parameter for a given fuel and slope angle or wind velocity. It was therefore computed the relative extension average values ε_{av} for each case. The results of ε_{av} obtained for pine needles and straw, as a function of α or u_0 are shown in Figures 4.8 and 4.9, respectively.

We can observe that the fire line elements relative extension ε_{av} variation with α or u_0 can be well described by a linear fit given in Eq. (4.1). The parameters obtained from the fit for pine needles and straw fuel beds for the wind or slope tests are shown in Table 4.5.

$$\varepsilon_{av} = m_\varepsilon \cdot \alpha + b_\varepsilon \qquad (4.1)$$
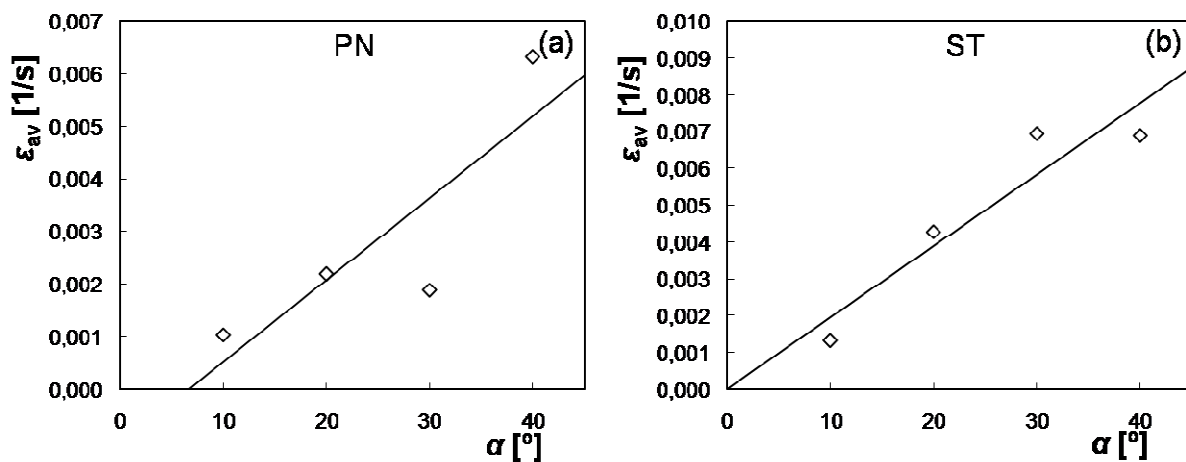
Figure 4.8 – Results from single test burns for the flank fire line elements average relative extension ε_{av} as a function of the test rig tilt angle α for the slope tests, fuel load: $0.6\,kg/m^2$: (a) Pine needles fuel beds. (b) Straw fuel beds.
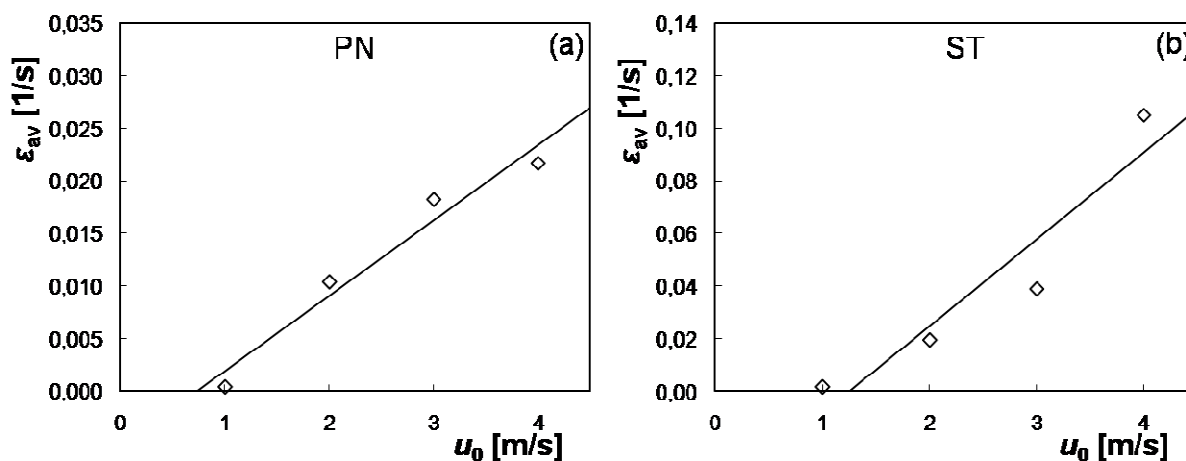
Figure 4.9 – Results from single test burns for the flank fire line elements average relative extension ε_{av} as a function of the reference wind flow velocity u_0 for the wind tests, fuel load: $0.6\,kg/m^2$: (a) Pine needles fuel beds. (b) Straw fuel beds.

Table 4.5 – Parameters for Eq. (4.1) for the flank fire line elements relative extension rate for each fuel bed.

Fuel bed	Slope tests			Wind tests		
	m_ε	b_ε	r^2	m_ε	b_ε	r^2
Pine needles	1.56×10^{-4}	-1.03×10^{-6}	0.724	7.17×10^{-3}	-5.23×10^{-3}	0.959
Straw	1.94×10^{-4}	5.29×10^{-6}	0.880	3.30×10^{-4}	-4.13×10^{-2}	0.888

Evaluation of a_3 and b_3

Using the equivalence between wind and slope, as described above, we can determine the perpendicular flow velocity u_y as a function of the inclination angle β for each fire line element and the results are shown in Figure 4.10. As the analysis of the slope tests was easier to perform, in the following it shall be presented the results obtained for the four slope tests and for only one wind test, corresponding to the maximum wind velocity (4 m/s) for each fuel.
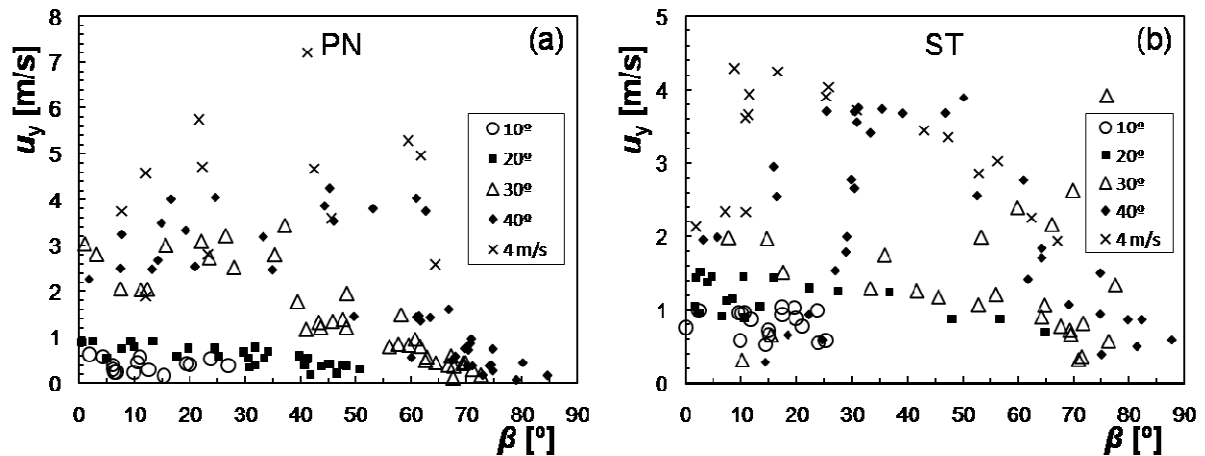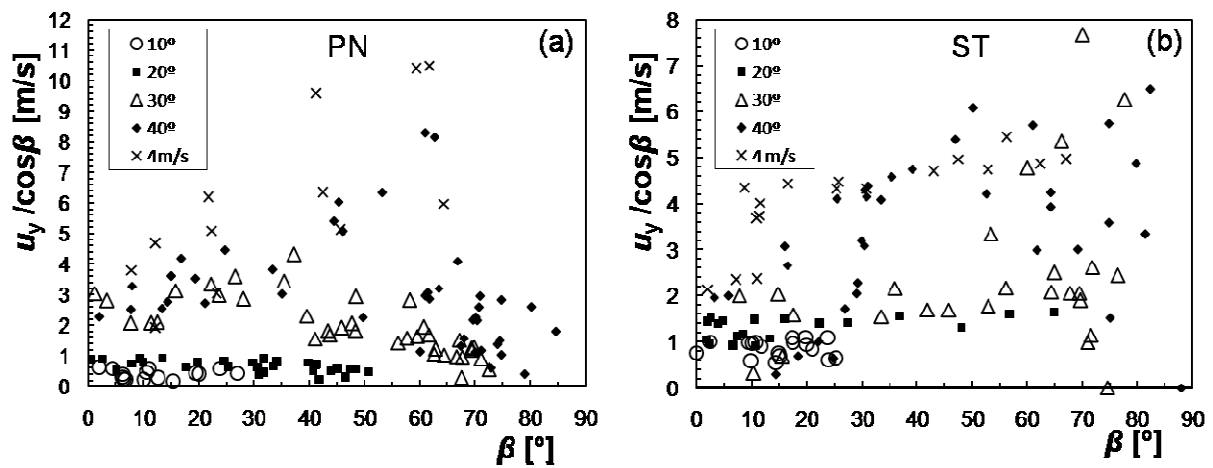

Figure 4.10 – Distribution of the perpendicular flow velocity u_y as a function of the flank fire line element inclination angle β, fuel load: $0.6 \, \text{kg/m}^2$: (a) Pine needles tests. (b) Straw tests.

As it can be seen in this figure the characteristic flow velocity u_y for each value of u_0 (corresponding to a slope angle or to a reference wind velocity) is fairly constant, although its value decreases for $\beta > 50°$. The average value of u_y and its standard deviation were computed for each case and are given in Table 4.6.

In order to use the present model we need to check the fact that the flow velocity u remains constant in a given test as this condition was assumed in the derivation of Eq. (2.22). As the flow angle θ was not measured it will be computed an approximate value u' defined by:

$$u' = \frac{u_y}{\cos \beta} \tag{4.2}$$

The values of u' for all tests are shown in Figure 4.11. As can be observed in these plots, for $\alpha < 30°$ the value of u' is practically constant as it was assumed in the derivation of (2.22). On the other hand, for $\alpha = 40°$ or $u_0 = 4$ m/s the value of u' increases with β, especially in the tests with pine needles. The average value of u' and its standard deviation were computed for each case and are given in Table 4.6.

In order to estimate the values of the two parameters a_3 and b_3 associated with function f_3 defined in Eq. (2.17), for each test with a relatively constant value of u, pairs of values of β^* and ω_{max} determined experimentally were used. It must be noted that the values of β^* are just surrogate values of θ^* therefore this estimate is only a first order approximation of those two parameters. The results obtained are shown in Table 4.6.

Figure 4.11 – Distribution of the approximate local flow velocity u' as a function of the flank fire line element inclination angle β, fuel load: 0.6 kg/m^2: (a) Pine needles tests. (b) Straw tests.

Fire line rotational velocity

The results obtained for the rotational velocity as a function of the inclination angle β of fire line elements in the set of tests that were analyzed are shown in Figures 4.12 and 4.13. In each figure, the curves of ω_f given by the Eq. (2.20) were plotted, using the parameters that were determined in Table 4.6 and the values of u that are indicated in each case. In these figures, the lower values of u were generally used to describe the data points corresponding to the higher values of β in accordance with was observed in Figure 4.11.

Despite of the scattering of the data, that is in part justified by the fact that we are using β as a surrogate of θ, in general terms the shapes of the curves given by the present model are in

accordance with the distribution of the data points, allowing the use of the present model to estimate a first approximation of the rotational velocity of the fire line elements as a function of their orientation angle β and of the other parameters involved in the model.
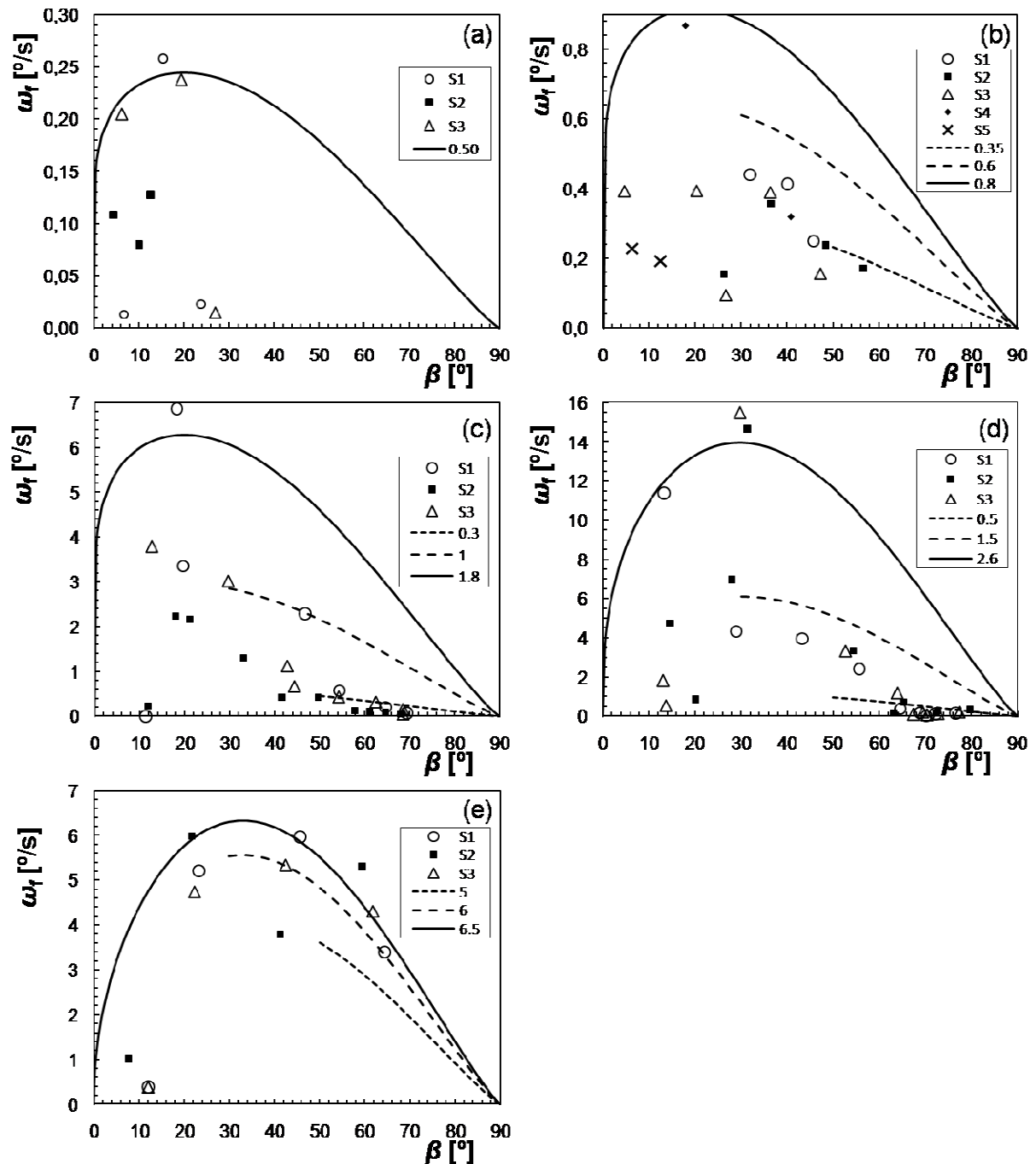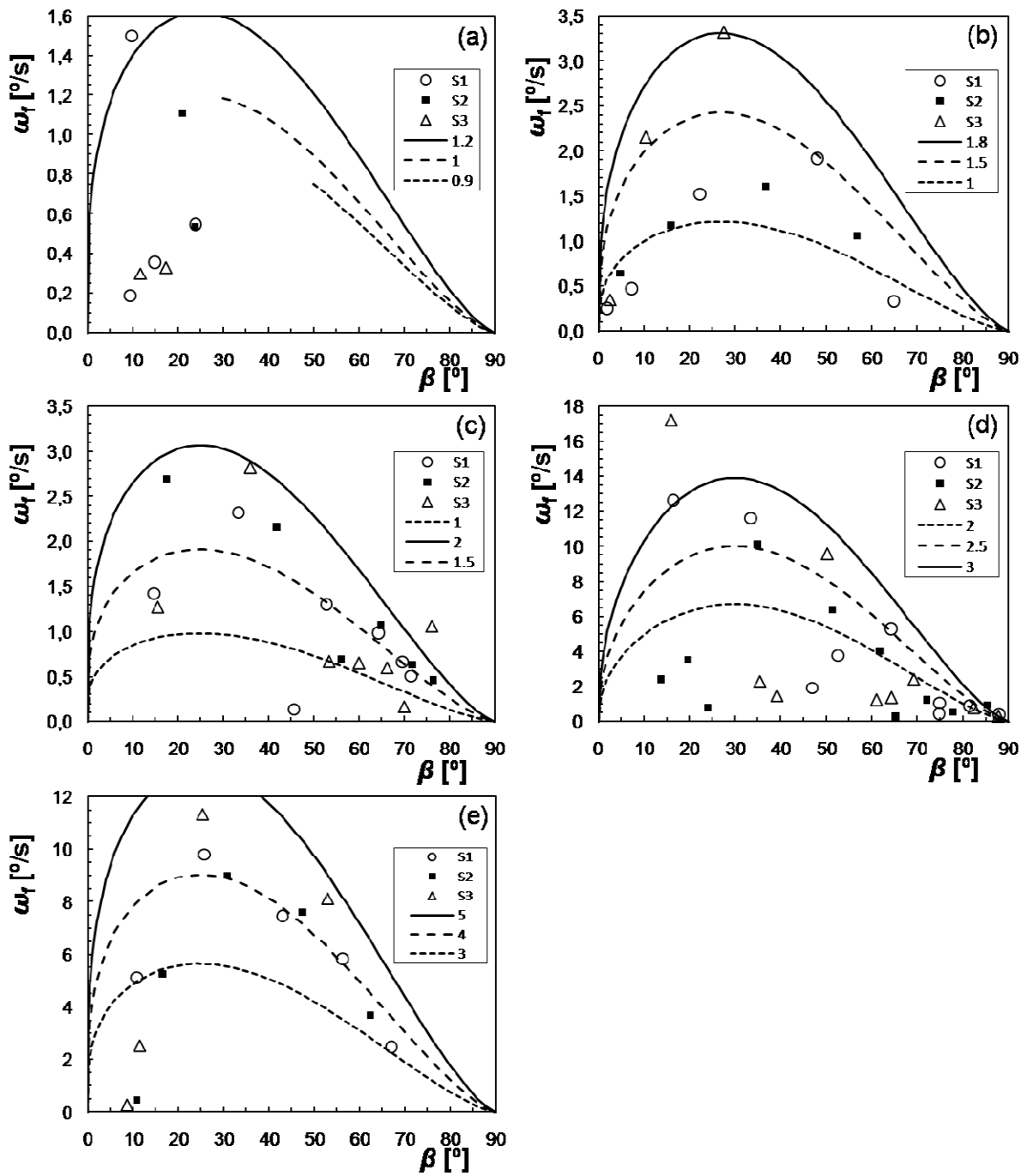

Figure 4.12 – Distribution of the rotational velocity ω_f of a flank fire line element as a function of the fire line inclination angle β for pine needles fuel beds for four slope angle tests and for one wind test, fuel load: 0.6 kg/m^2: (a) 10° (b) 20° (c) 30° (d) 40° (e) 4 m/s. The curves correspond to the present model for the values of the local flow u that are indicated in the legend.

Figure 4.13 – Distribution of the rotational velocity ω_f of a flank fire line element as a function of the fire line inclination angle β for straw fuel beds for four slope angle tests and for one wind test, fuel load: 0.6 kg/m^2: (a) 10° (b) 20° (c) 30° (d) 40° (e) 4 m/s. The curves correspond to the present model for the values of the local flow u that are indicated in the legend.

Table 4.6 – Parameters of the flow properties and model parameters for Eq. (2.20) for each fuel bed.

		u_y [m/s]		u' [m/s]		β^* [º]	$\omega_{f,max}$ [º/s]	b_3	a_3 [º]
Pine needles									
Reference u_o		Aver.	St. Dev.	Aver.	St. Dev.				
α [º]	10	0.39	0.14	0.40	0.15	20	0.26	0.15	57.2
	20	0.57	0.21	0.66	0.18	20	0.87	0.15	120.8
	30	1.43	1.02	1.97	0.93	20	6.86	0.15	275.9
	40	1.84	1.39	3.02	1.80	30	16.50	0.37	357.8
u_o [m/s]	4	4.30	1.48	6.06	2.79	33	6.60	0.48	30.6
Straw									
Reference u_o		Aver.	St. Dev.	Aver.	St. Dev.				
α [º]	10	0.82	0.18	0.86	0.18	25	1.6	0.29	71.1
	20	1.15	0.24	1.28	0.25	27	3.3	0.35	75.5
	30	1.34	0.83	2.93	3.18	25	3.3	0.29	58.1
	40	2.08	1.20	3.64	2.56	30	17.0	0.45	128.2
u_o [m/s]	4	3.27	0.78	4.10	0.95	25	12.0	0.29	57

4.1.4. Back fire

Rate of spread

The results for the back fire described in this section are based on the work of Rossa and Viegas (2009). In Figure 4.14 we have the ROS results for the wind or slope backfires and in Figure 4.15 we have the non-dimensional ROS for the same experiments. It is easy to see that for the tested slope angles and wind velocities, for each fuel bed, the R_b values are in the same range.
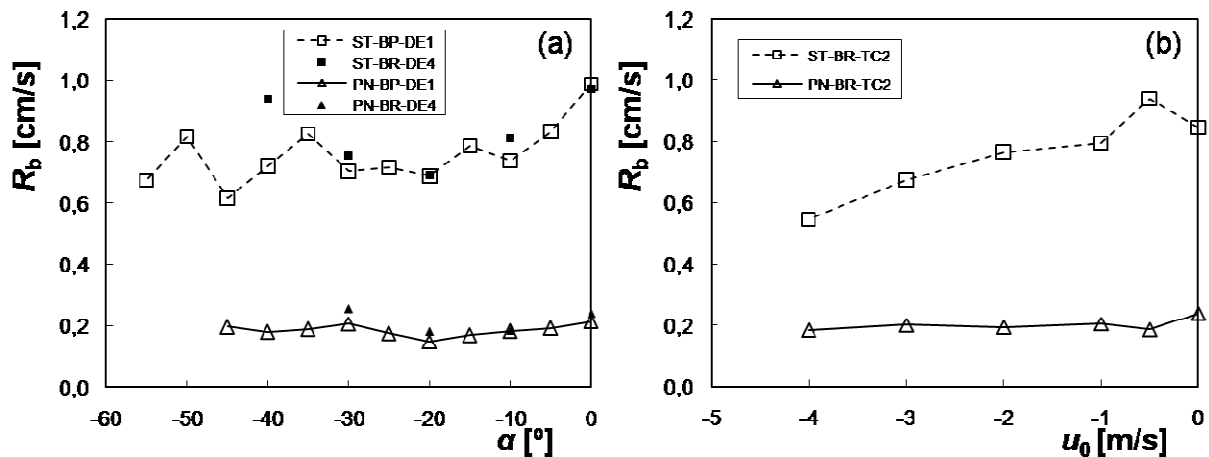
Figure 4.14 –ROS results from single test burns, except for a null wind velocity or null slope where the average of the R_0 for that series of tests was considered, fuel beds: pine needles and straw, fuel load: 0.6 kg/m²: (a) As a function of slope. (b) As a function of wind velocity.

The first group of contrary slope experiments performed in the test rig DE4, which aimed to analyse the ROS and also the fire line shape, includes a total of eight tests, four using straw and four using pine needles fuel beds, in a range of slopes varying from $-40° < \alpha < -10°$ with 10° intervals. Regarding the non-dimensional ROS results (Figure 4.15), for both fuels, it appeared that R_b' had a value slightly lower than 1, but more or less constant over the range of tested slopes. However, in order to study back fire propagation for a wider range of slopes (up to -60°) a new group of experiments was planned. It was decided to use an angle interval $\Delta\alpha = 5°$ and given the high number of experiments to perform (a total of 22 experiments, 11 for each fuel) a smaller test rig was used (test rig DE1) and only ROS results were assessed.

Although the test rig DE1 allowed for angles over -60° it was verified that for $\alpha < -45°$ for pine needles and $\alpha < -55°$ for straw, spotting started to occur due to falling embers. For this reason the results obtained for angles out of the referred range are not presented. Van Wagner (1988) also reported slides of burning material for $\alpha < -45°$ for experiments with pine needles fuel beds.
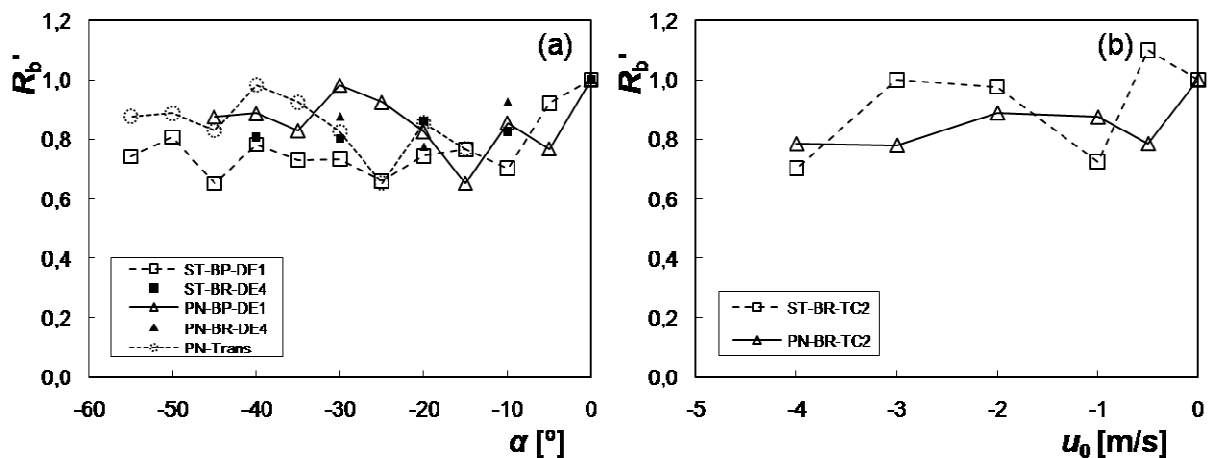
Figure 4.15 – Non-dimensional ROS results from single test burns, fuel beds: pine needles and straw, fuel load: 0.6 kg/m²: (a) As a function of slope. The dotted line corresponds to a translation of the data for pine needles with a displacement of 15°. (b) As a function of wind velocity.

Looking at the results in Figure 4.15, one is tempted to conclude that for backfires spreading in both fuels the value of R_b' is constant but a more careful analysis shows that the backfire velocity has an oscillatory evolution over the range of analysed slopes. It is interesting to notice that the oscillation pattern is similar for both fuels. This can be easily observed if, in the graphic shown in Figure 4.15a, we translate the points relative to the backfire propagation

velocity in pine needles by 10º to the left, *i.e.* the velocity that actually corresponds to -5º would correspond to -15º and there forth. Doing this we can see that the ROS values are very similar but also that their minimum and maximum values occur with exactly the same interval for both fuels.

In order to estimate the relative error of the measurements, the cases for which there was more than one test with the same slope and fuel, were analysed, although tests were performed either in DE1 or DE4. The fact that experiments were made in different test rigs, and table DE1 is significantly smaller than DE4, should not be a cause of differences in spread characteristics because, for laboratory back fires, scale effects are not as relevant as for head fires. On one hand, for contrary wind or slope fires, flames are smaller than for head fires. On the other hand, due to the curvature of the fire perimeter, heat tends to diverge from the most advanced part of the fire to the sides, as opposed to head fires where heat tends to be transported along both sides of the fire line converging to the head fire and making fire line width an important parameter to consider. The maximum difference on the values of R_b' for straw and for pine needles was respectively 18 % and 12 %. The amplitude of the oscillation of R_b' values for different slope angles in the range $-40º < \alpha < -25º$ for straw (ST-DE1) and for pine needles (PN-Trans) was, respectively, 18 % and 51 %. This means that the amplitude of oscillation for straw is of the same order of the maximum estimated relative deviation in the estimation of R_b', but for pine needles the oscillation is over four times that difference. Considering that the results are obtained from single test burns, that each experiment in the data series was performed in a random order to avoid any bias and that the oscillation pattern is similar for both fuels we have a good indication that it should not be a consequence of random variance in the measurements.

Although in the case of wind backfires (Figure 4.15b) the oscillatory behaviour of R_b' is not so clear, it appears to follow a similar pattern. Since higher wind velocities cannot be used, because fire spread is not sustained, to better understand the ROS evolution over the possible range of wind velocities, further tests must be performed for wind velocities in between those already used.

Van Wagner (1988) reported results of laboratory experiments on contrary slopes in fuel beds of *Pinus resinosa* needles and both Mendes-Lopes (2003) and Viegas (2004a) present results on contrary wind or slope, also from laboratory experiments but in fuel beds of *Pinus pinaster* needles. In the first two cases, despite both authors present ROS for contrary slope or

wind inferior to those obtained on level ground or in the absence of wind, respectively, which agrees well with the present data in qualitative terms, it is difficult to make an adequate comparison between results, since we do not have access to a R_0 value for each experiment. In the last case, the results for the slope backfires have reasonable agreement with those here presented, although the agreement is not so good for the wind backfires. One explanation for the discrepancy in the wind backfires could be the R_0 tests, since the author concluded that for determining R_b' values it is of paramount importance to perform the R_0 and R_b tests with an interval of no more than few minutes. Having a considerable interval between those tests could imply to be comparing fuel beds with different combustibility properties, not only because of the fuel bed moisture content but also because of the ambient parameters.

A possible explanation for the oscillation of the fire ROS is the balance of heat transfer by radiation and convection at the fire line. It is commonly accepted that, for fire spread on level ground, flame radiation plays a secondary role to the radiation inside the fuel bed. In fact, Frandsen and Schuette (1978) reported that the rate of burning of excelsior was the same for fire burning downward in a basket or spreading horizontally through a fuel bed. Of course that, in the case of wind or slope back fires either ambient wind or induced wind flow will have a negative contribution, explaining the slight decrease of ROS. However if we consider that radiation inside the fuel bed, for contrary wind or slope, is similar when compared with a level ground spread and that the decrease in the ROS is due exclusively to the diminishing of convective heat transfer, we should expect a constant decrease of the ROS with decreasing wind or slope. As that does not happen it is probable that radiation over the fuel bed has a role and may be responsible for the observed phenomenon.

Radiation over the fuel bed is greatly dependent on flame geometry, namely on its inclination angle and length, that are influenced by the local flow properties: as we tilt the table the air entrainment increases causing the enhancement of the combustion reaction and of the buoyancy forces which cause the flame to become more vertical, but the increase of the air velocity also forces the flame to tilt backwards. The balance between these two effects seems to produce an oscillatory evolution of the ROS with decreasing slope or flow velocity.

Pictures of the flame geometry for back fires with different slope angles are shown in Figure 4.16 to support the assumption that flame radiation has some influence in the ROS

oscillations. Based in those pictures, the author considers that flame geometry seems to have some influence in radiative heat transfer to the unburned fuel bed.

Figure 4.16 – Flame geometry and non-dimensional ROS as a function of slope for tests in the range $0° \leq \alpha \leq 40°$. The variation of the flame geometry for different slope angles can be observed, fuel bed: straw, fuel load: $0.6 \, \text{kg/m}^2$.

Comparing the flame for horizontal spread and -10° we can see that the later, although not very different in length, is more tilted backwards. The reduction in the view factor between the flame and the fuel bed causes a decrease in the heat transfer by radiation and therefore a decrease in the ROS, which corresponds to a local minimum in the graphic (Figure 4.15a). When comparing the flame for -20° with the one for -10° we can see that the first has a slightly smaller tilt backwards but a significantly higher flame length, which allows for an increase of the transferred radiation and explaining the increase in the ROS. For -25° when compared with -20°, we can see both an increase in the flame tilt backwards and a decrease in the flame length which causes a new decrease in the ROS and justifies another local minimum in the graphic. Then for -35° and -40°, when compared with -25°, respectively, we can see first an increase in the flame length and a very similar tilt, and afterwards a decrease in the backwards tilt, which explains the successive increase in the ROS. It must be said that the behaviour that is illustrated in these pictures was consistent in each test and for each configuration the properties that were described

above were practically the same for the duration of the test. Nevertheless, a correct assessment of the flame geometry requires a detailed evaluation of fire spread, using several time frames, for the situations here presented. For that reason the theory here proposed is just a preliminary approach that needs further research, intended as future work.

Fire line extension rate

In Figures 4.17 to 4.20, displaying results from the experiments BR-DE4 and BR-TC2, we have the back fire line elements relative extension ε, defined in Eq. (2.10), as a function of the fire line element inclination angle β for the slope and wind tests and for pine needles and straw fuel beds.
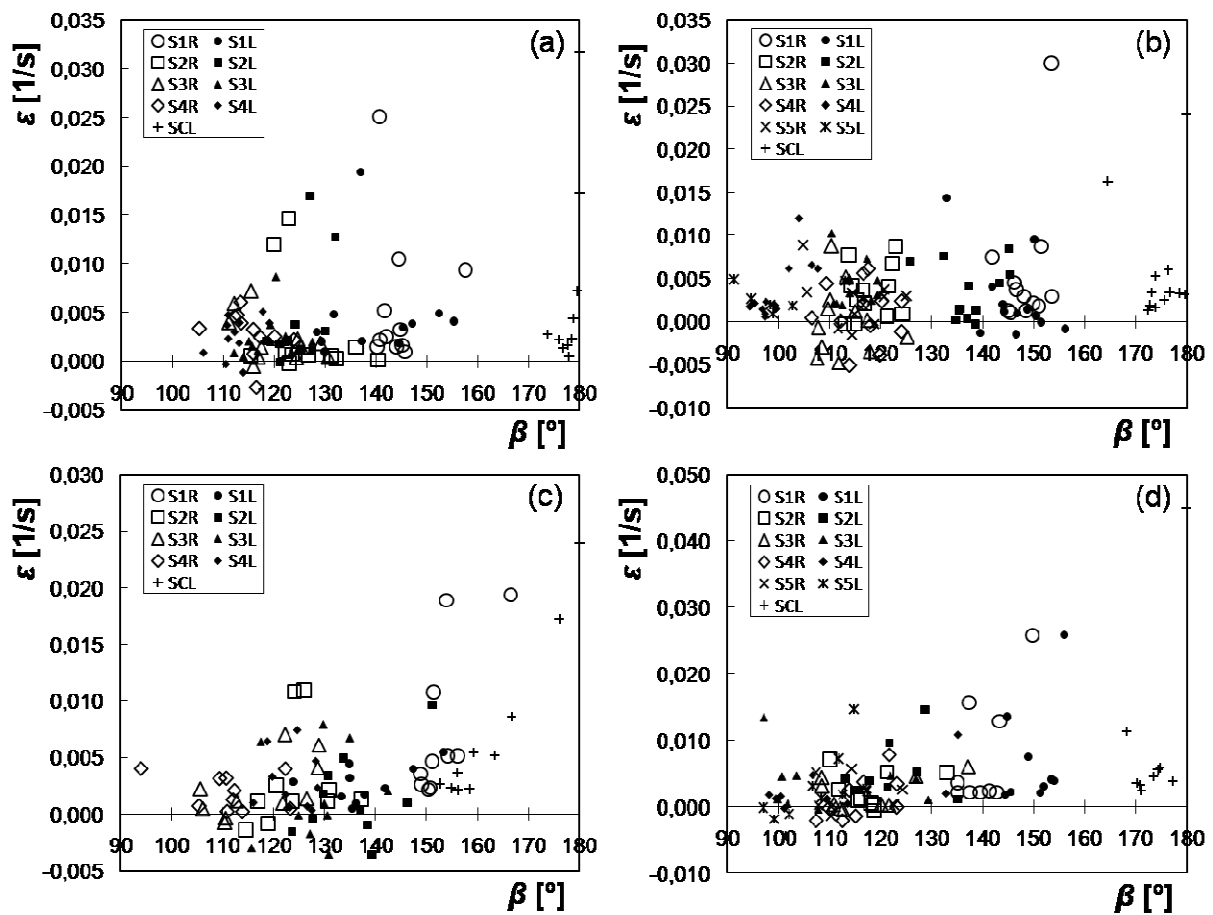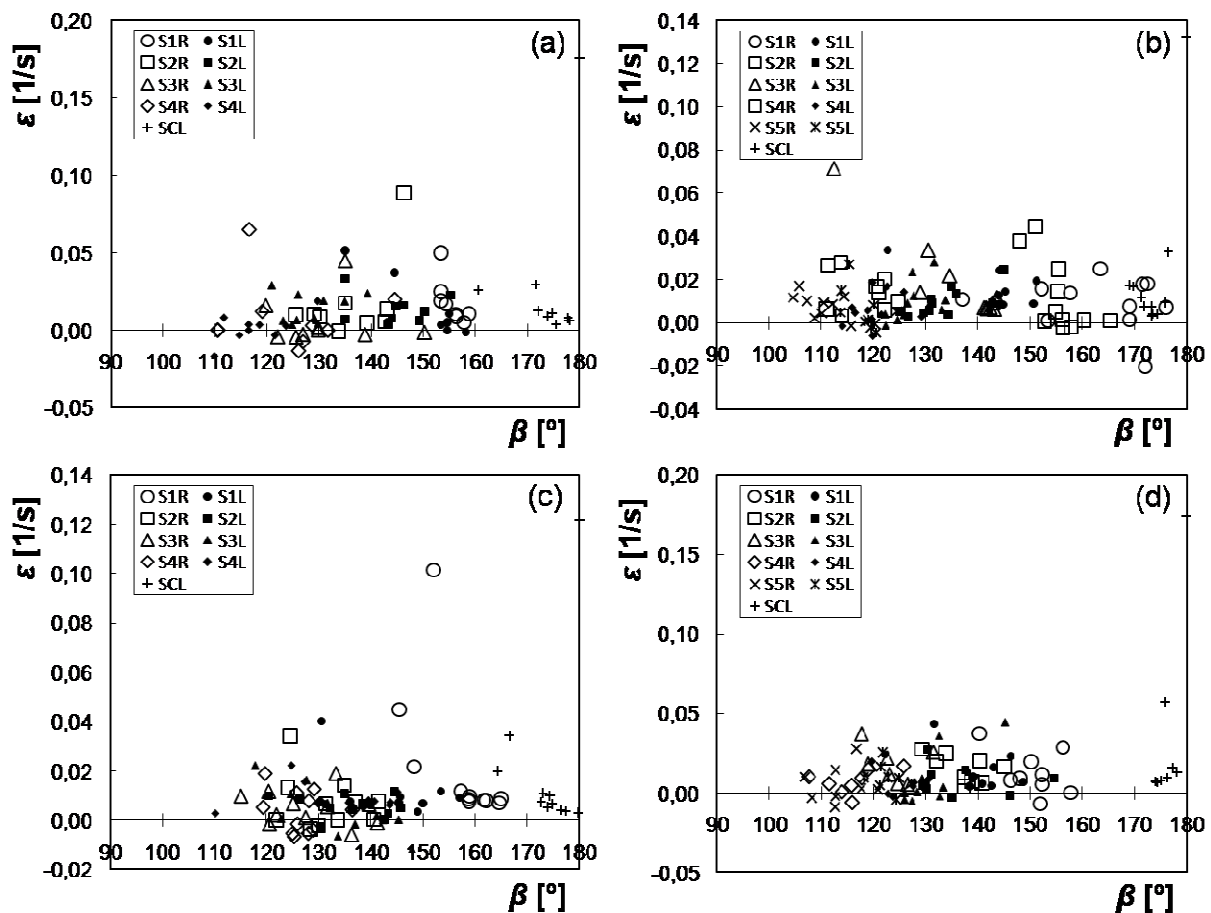

Figure 4.17 – Back fire line elements relative extension ε as a function of the fire line element inclination angle β for the slope tests, fuel bed: pine needles, fuel load: 0.6 kg/m^2: (a) 10º (b) 20º (c) 30º (d) 40º.

We can observe a tendency for higher rates of extension for inclinations angles around 135º. However, as the data is very scattered, it was concluded that it is reasonable for each slope or wind test to compute an average relative extension ε_{av} for a given fuel and slope angle or wind

74

velocity, instead of trying to define a function that would consider an increase from 90 to 135°
and then a decrease from 135° to 180°.

The relative extension distribution as a function of the fire line element inclination angle
for the wind tests is much more scattered than for the slope tests. This is explained by the highly
irregular shape of wind back fires perimeter, especially for high contrary winds, due to the flame
turbulence. From the fire line shape analysis it was easy to conclude that in global terms the fire
line evolution follows the same pattern as for the contrary slope fires. However, the fire
perimeter has rapid changes in short periods of time and for these tests it was not always easy to
find a section of the fire line that maintained a regular evolution with time. For this reason, in
some tests a smaller amount of segments was analysed.

Figure 4.18 – Back fire line elements relative extension ε as a function of the fire line element inclination angle β
for the slope tests, fuel bed: straw, fuel load: 0.6 kg/m^2: (a) 10° (b) 20° (c) 30° (d) 40°.

The results for the average relative extension ε_{av} of the fire line elements as a function of the slope angle α or the wind velocity are shown in Figure 4.21 and Figure 4.22, respectively.
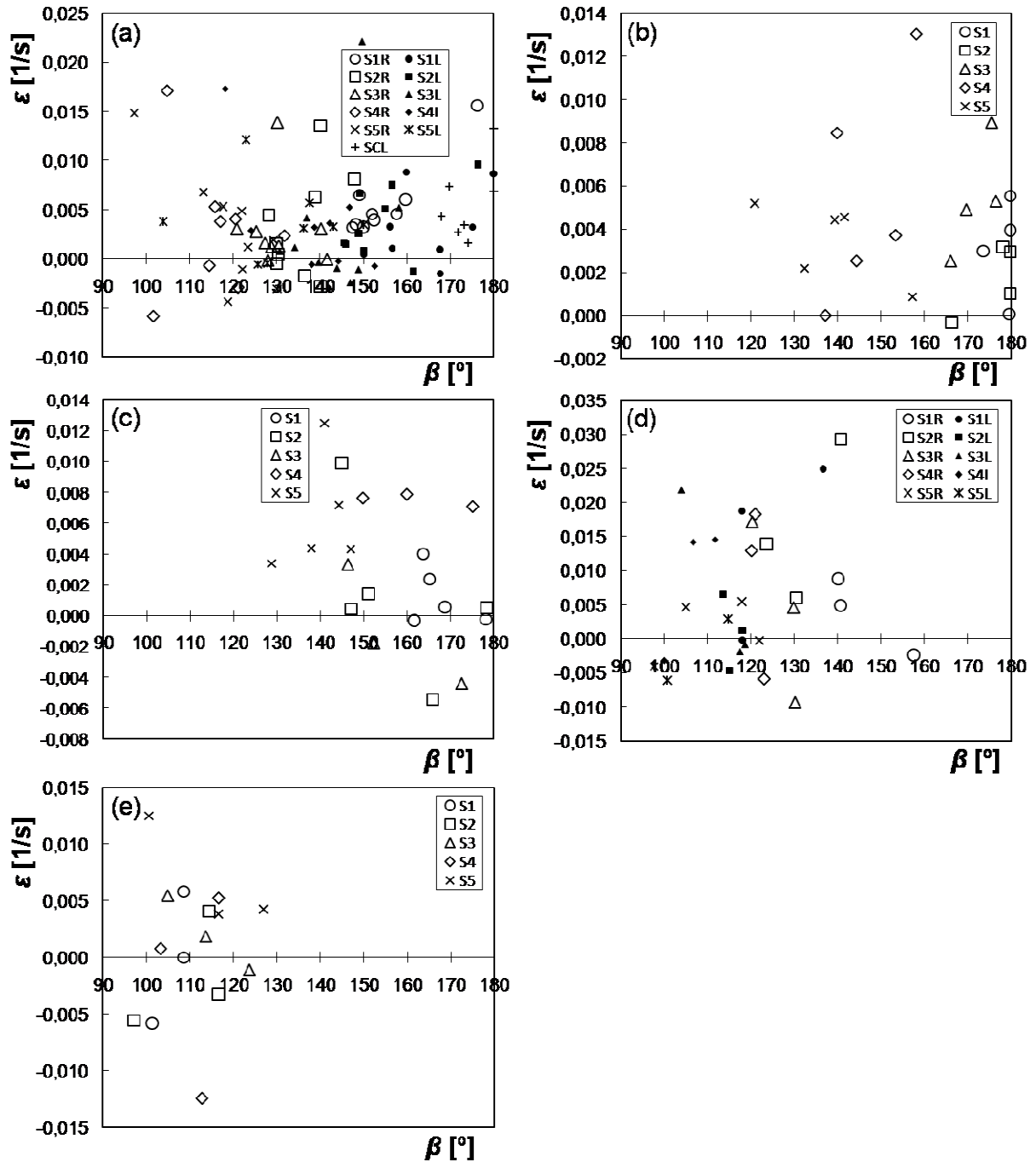

Figure 4.19 – Back fire line elements relative extension ε as a function of the fire line element inclination angle β for the wind tests, fuel bed: pine needles, fuel load: 0.6 kg/m^2: (a) 0.5 m/s (b) 1 m/s (c) 2 m/s (d) 3 m/s (e) 4 m/s.
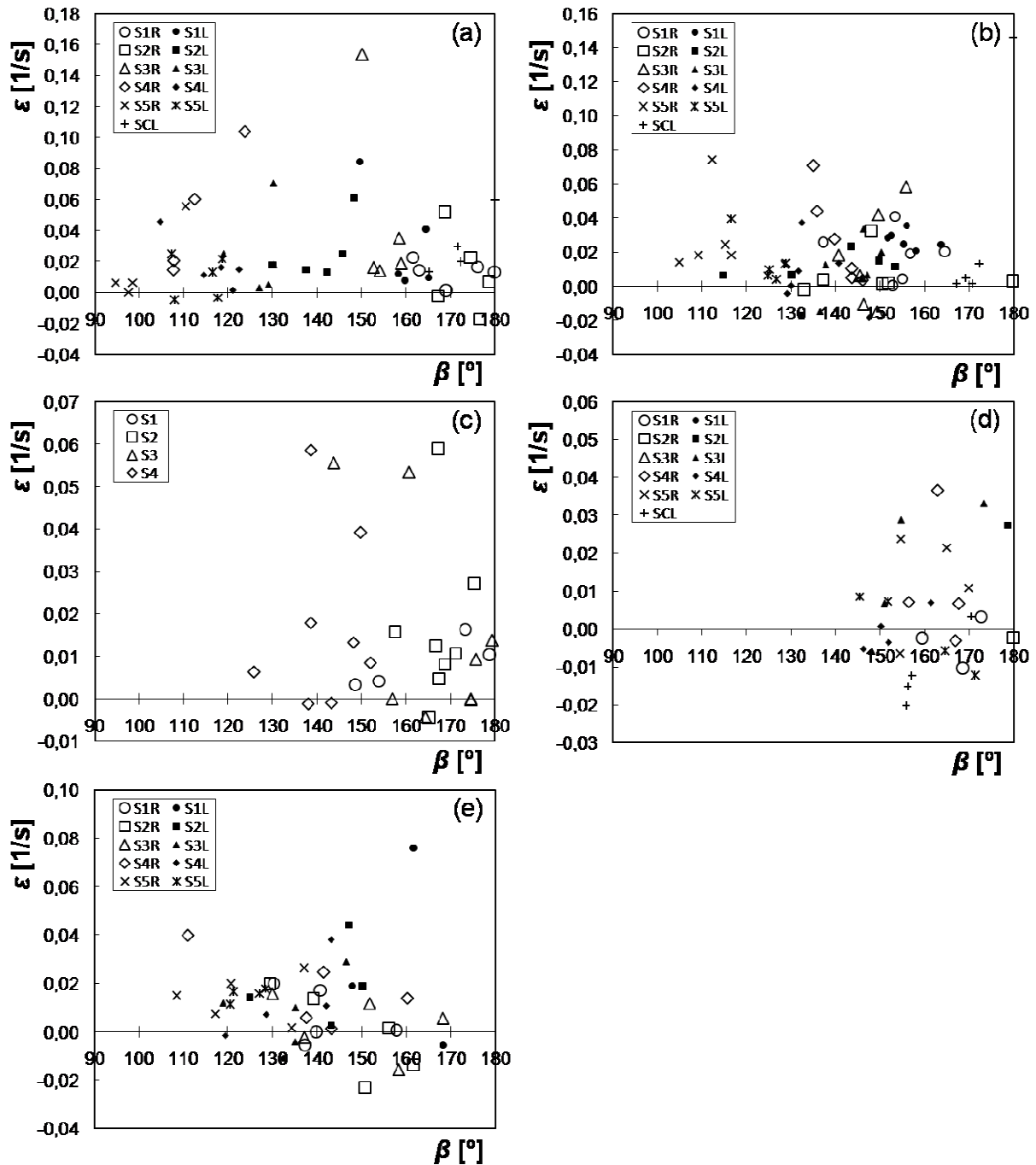
Figure 4.20 – Back fire line elements relative extension ε as a function of the fire line element inclination angle β for the wind tests, fuel bed: straw, fuel load: 0.6 kg/m^2: (a) 0.5 m/s (b) 1 m/s (c) 2 m/s (d) 3 m/s (e) 4 m/s.

The variation of the of ε_{av} value with the slope angle or wind velocity follows the same pattern for all cases, except for the wind backfires in pine needles fuel beds where the -0.5 and -3 m/s tests appear as outliers. This is easy to understand because back fire spread in pine needles

fuel beds is very slow and for that reason more irregular when compared with straw, adding to the fact that, as previously referred in the wind tests the fire line evolution is already very irregular. In the remaining situations the relative extension decreases up to $\alpha = -30°$, for the slope tests, and $u_0 = -3$ m/s, for the wind tests, increasing afterwards.
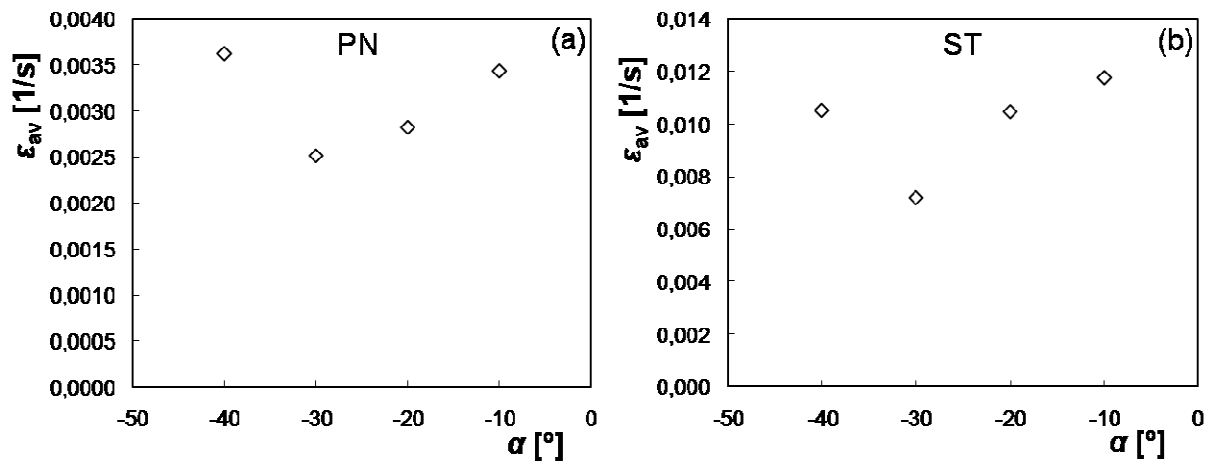

Figure 4.21 – Results from single test burns for the back fire line elements average relative extension ε_{av} as a function of the test rig tilt angle α for the slope tests, fuel load: 0.6 kg/m^2: (a) Pine needles fuel beds. (b) Straw fuel beds.
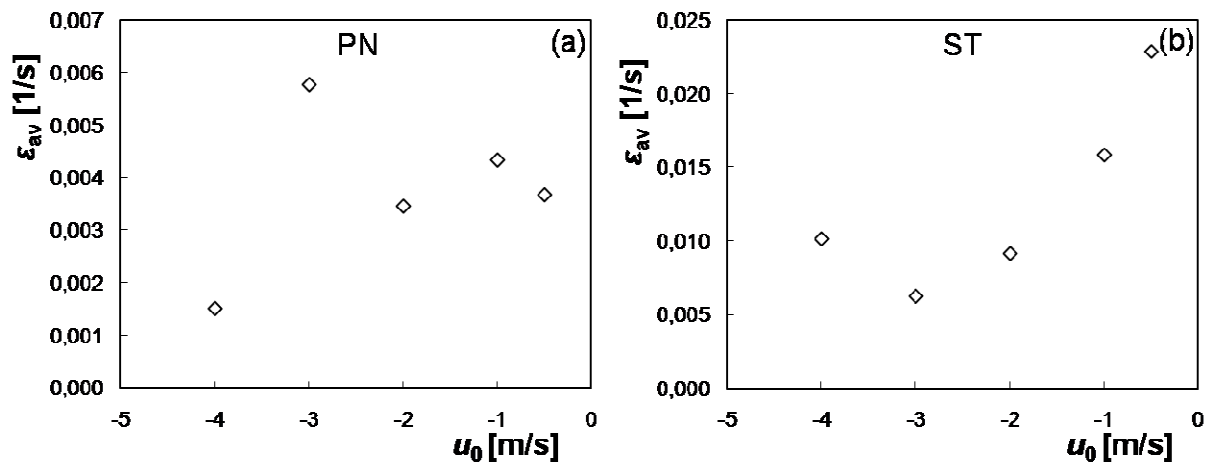

Figure 4.22 – Results from single test burns for the back fire line elements average relative extension ε_{av} as a function of the wind velocity u_0 for the wind tests, fuel load: 0.6 kg/m^2: (a) Pine needles fuel beds. (b) Straw fuel beds.

Fire line rotational velocity

In Figures 4.23 to 4.26 we have the rotational velocity ω_b of a back fire line element as a function of the fire line inclination angle β for the slope and wind tests as a function of the segment angle in a given time instant, for pine needles and straw fuel beds. Despite the scatter,

78

the data suggests that ω_b varies linearly with β, assuming positive and negative values. This behaviour is attributed to the same phenomena, previously referred, that causes the R_b' oscillation with contrary wind velocity or slope angle, given that the local flow along a back fire line element changes with the element orientation angle and influences the ROS of each point of the element.
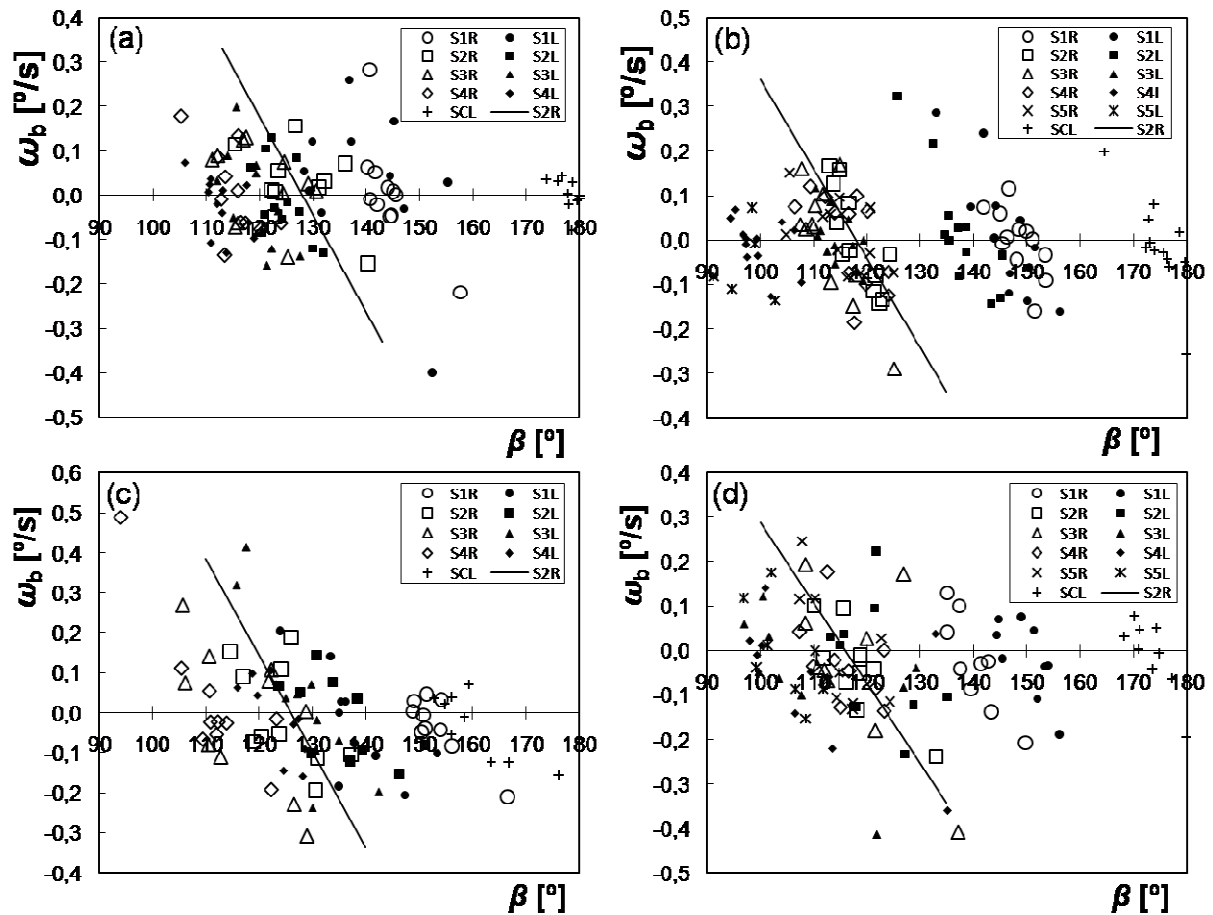

Figure 4.23 – Distribution of the rotational velocity ω_b of a back fire line element as a function of the fire line inclination angle β for the slope tests, fuel: pine needles, fuel load: $0.6\,\text{kg/m}^2$: (a) 10° (b) 20° (c) 30° (d) 40°. The line corresponds to the linear fit for the rotational velocity of the segment S_{2R}.

Segments from the left and right sides of the fire line perimeter were considered but, as the results did not exhibit any difference between the two sides, an analysis was made for the entire set of data. Straight lines, following Eq. (2.27), were adjusted to each set of points corresponding to a given segment, like the example shown for slope tests for segment S_{2R} in Figures 4.23 and 4.24. Horizontal or near horizontal fire line elements occasionally attain angles over 180°,

resuming afterwards to angles below that value. However, those elements have lower rotational velocities, as can be seen from the results figures, and tend to remain horizontal.

It was found that the slope, m_r, of the various trendlines was more or less constant, for each fuel, for all segments analysed in the range of tested slopes, and for the segments analysed in the range of tested wind velocities. This means that the segments rotation in backwards spreading fires seems to depend essentially on the fuel bed properties. For that reason, for the slope experiments, the value of m_r for each fuel was considered to be the average of the obtained values for each segment for each tested slope. The same procedure was done for the wind results and the corresponding parameters are presented in Table 4.7.

Each segment has an inclination angle that corresponds to a null rotational velocity β_{int} that has a reasonable correlation with the segment angle at the beginning of each experiment β_{ini}, as it is shown in Figures 4.27 and 4.28.
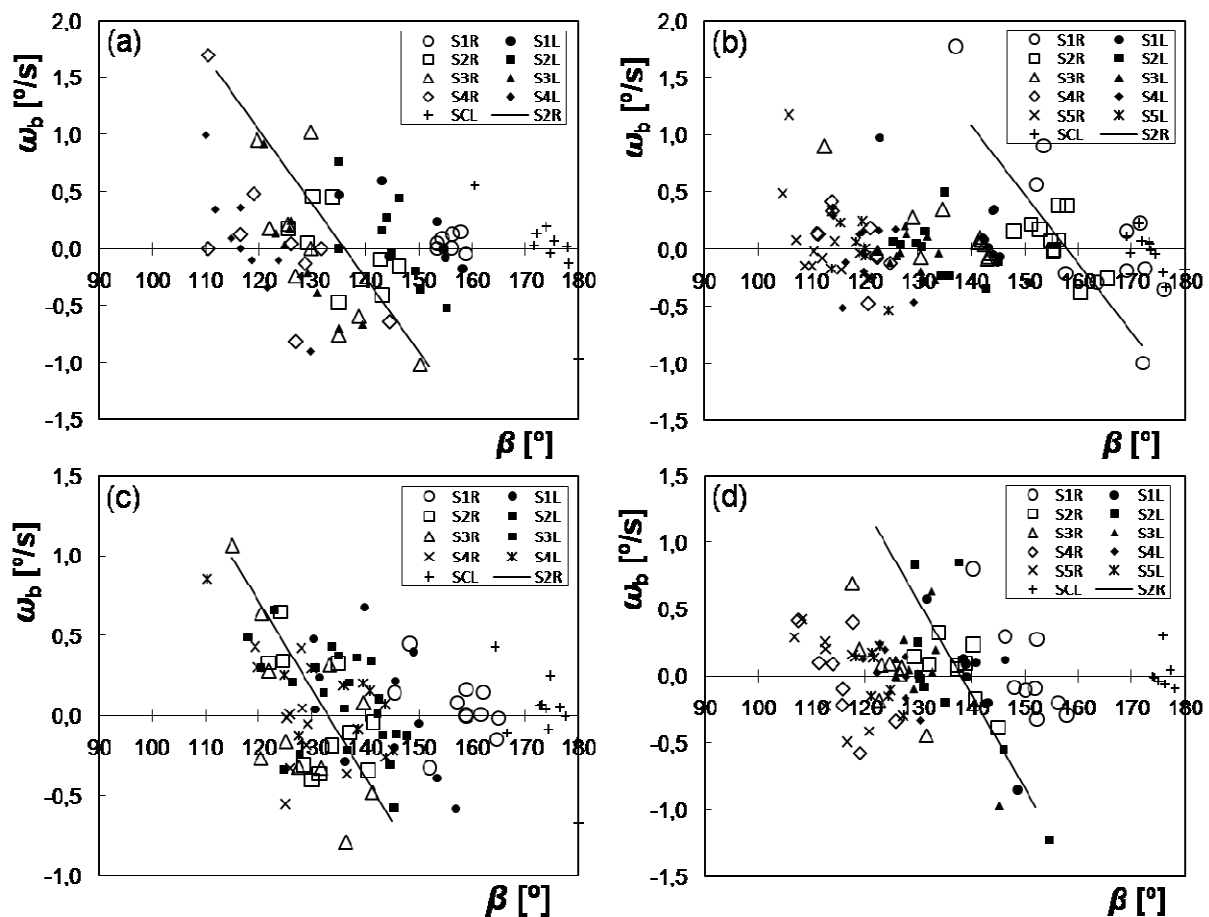

Figure 4.24 – Distribution of the rotational velocity ω_b of a back fire line element as a function of the fire line inclination angle β for the slope tests, fuel: straw, fuel load: 0.6 kg/m^2: (a) 10° (b) 20° (c) 30° (d) 40°. The line corresponds to the linear fit for the rotational velocity of the segment S_{2R}.
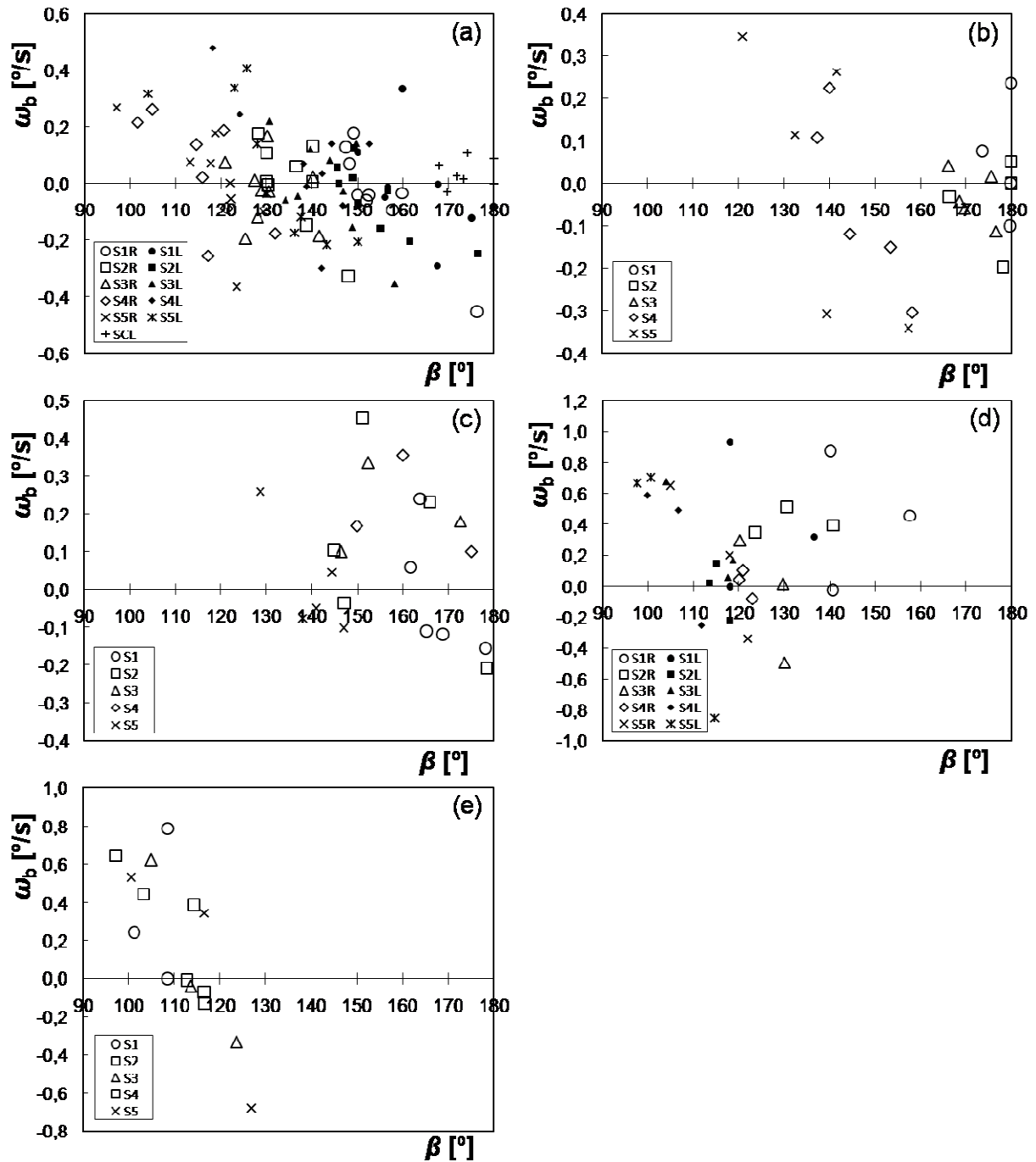
80

Figure 4.25 – Distribution of the rotational velocity ω_b of a back fire line element as a function of the fire line inclination angle β for the wind tests, fuel: pine needles, fuel load: $0.6\,\mathrm{kg/m^2}$: (a) $0.5\,\mathrm{m/s}$ (b) $1\,\mathrm{m/s}$ (c) $2\,\mathrm{m/s}$ (d) $3\,\mathrm{m/s}$ (e) $4\,\mathrm{m/s}$.

The angle β_{int} depends essentially on the fuel bed properties and after plotting β_{int} against β_{ini} for a given fuel we can determine the parameters for Eq. (2.26) by linear regression, for the range of tested slopes or wind velocities. The correlation coefficient r^2 was always above 0.77

and the determined parameters are presented in Table 4.7. Computing the value of β_{int} and using Eq. (2.27) and Eq. (2.21), we can estimate a fire line segment rotational velocity and the angle after a given time interval.
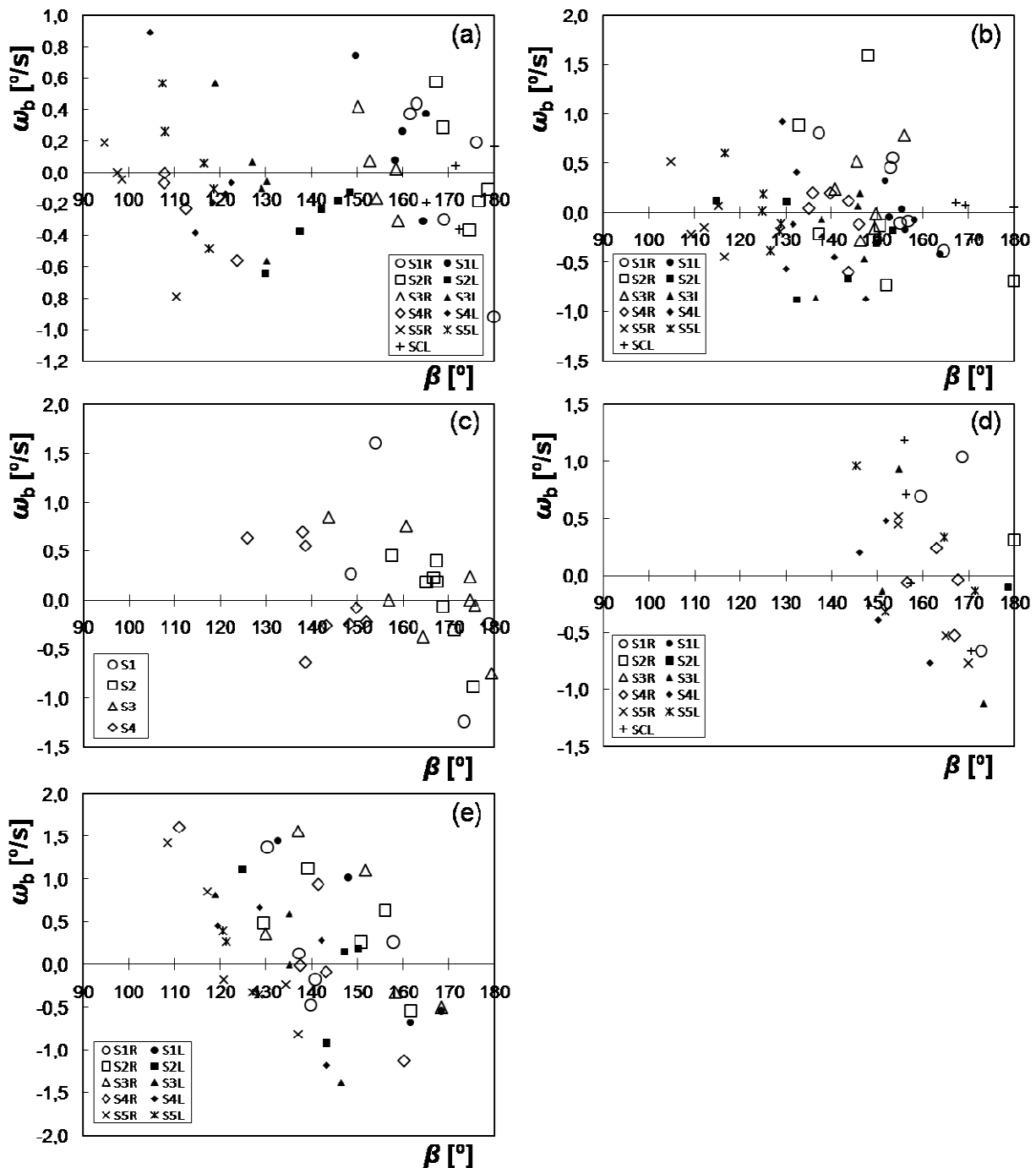

Figure 4.26 – Distribution of the rotational velocity ω_b of a back fire line element as a function of the fire line inclination angle β for the wind tests, fuel: straw, fuel load: $0.6\,kg/m^2$: (a) $0.5\,m/s$ (b) $1\,m/s$ (c) $2\,m/s$ (d) $3\,m/s$ (e) $4\,m/s$.
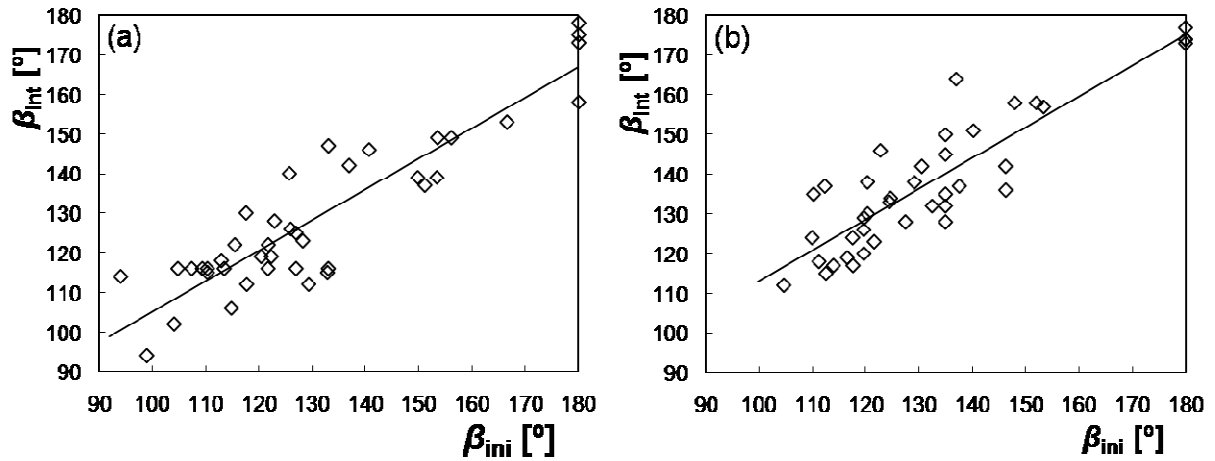
Figure 4.27 – Results from single test burns for the back fire line elements angle corresponding to a null rotational velocity β_{int} as a function of the fire line initial inclination angle β_{ini} for the slope tests, fuel load: 0.6 kg/m², fitting parameters for Eq. (2.26) presented in Table 4.7: (a) Pine needles fuel beds. (b) Straw fuel beds.

Figure 4.28 – Results from single test burns for the back fire line elements angle corresponding to a null rotational velocity β_{int} as a function of the fire line initial inclination angle β_{ini} for the wind tests, fuel load: 0.6 kg/m², fitting parameters for Eq. (2.26) presented in Table 4.7: (a) Pine needles fuel beds. (b) Straw fuel beds.
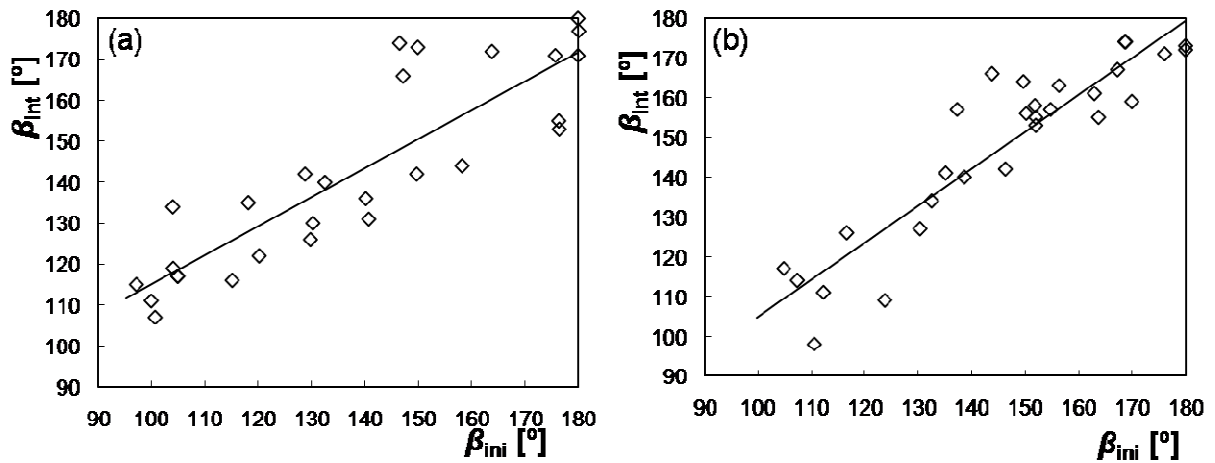
Table 4.7 – Parameters for Eq. (2.26), and (2.27), for the back fire line elements rotation for each fuel bed.

Fuel bed	Slope back fires				Wind back fires			
	m_β	b_β	r^2	m_r	m_β	b_β	r^2	m_r
Pine needles	7.72×10^{-1}	27.91	0.821	-2.4×10^{-2}	7.07×10^{-2}	44.47	0.773	-3.30×10^{-2}
Straw	7.77×10^{-1}	35.38	0.792	-6.40×10^{-2}	9.33×10^{-1}	11.8	0.885	-6.2×10^{-2}

4.2. Simulation model

4.2.1. Validation tests and data processing

Experiments

For the purpose of validating the fire line evolution prediction models developed previously, two large-scale experiments were made. As already referred, the general behaviour of the slope tests and the wind tests is the same. However, as in the wind tests the fire line is more irregular, making the fire perimeter analysis more difficult, it was chosen to use slope tests for the models validation. The experiments simulate a point ignition fire under the effect of slope (Figures 4.29 and 4.30) because, although for the purpose of model development the fire line evolution analysis was divided in forward propagation and backwards propagation, the objective was to be able to predict the entire fire perimeter evolution under the effect of slope or wind.

In nature, the most inclined slopes are usually in the range 30-40º and it is in these situations that many forest fires related accidents occur. For this reason, it was decided to make the experiments with a 30º slope angle for two different fuel beds. The methodology used is similar to the one described in Chapter 3 but the main features of the experiments will be described below. The experiments were named FL-DE4 followed by a dash and the number indicating the order of performance. This alpha-numerical reference follows the same pattern used in the remaining experimental program. The tests main features are shown in Table 4.8. In Tables 4.9 and 4.10 we have the tests main parameters and ROS data, respectively.

Test rig and fuel beds

The test rig used was the Canyon Table DE4 (Figures 3.2, 4.29 and 4.30), previously described in section 3.2, forming a fuel bed of $5\times3\,\text{m}^2$ on one face of the table.

As in the experiments made for the models development, dry straw and *Pinus pinaster* dead needles fuel beds with a fuel load of 0.6 kg/m² were used. The fuel bed preparation followed the same steps described in section 3.3.

Procedures

Again, fuel homogeneity and fuel bed bulk density were controlled and fuel moisture content was monitored, before the fuel bed preparation and before each experiment, with simultaneous

register of the air temperature and relative humidity. The basic rate of spread R_0 was also measured for each test in a separate experiment.

Thirteen strings were stretched over the fuel bed in order to determine the head fire ROS and six were used in order to determine the backfire ROS, placed with a distance of 25 cm between them. Also, in these experiments, three strings parallel to the slope direction were placed in the right half of the fuel bed with a spacing of 40 cm. However, for reasons that will be explained below, the lateral ROS was computed using the infrared images for determining the position of the fire line for a given time instant, like in the BR-TC2 experiments.

Like in all the other DE4 test rig experiments, the R_0 was determined using the left side of the table on a separate fuel bed with the same overall properties as the main one and the fire was initiated by a line ignition, parallel to the strings. In the main experiments, the ignition was made using a piece of cotton placed at the centre of the fuel bed width at a distance of 1.625 m from the bottom of the test rig (Figures 4.29 and 4.30).

Table 4.8 – Tests characteristics, parameters assessed and type of monitoring for the FL-DE4 experiments.

Tests characteristics						
Series	Area (L×W) [m²]	Ign.[1]	Fav./Cont.[2] Slope		Fuel beds	Fuel load [kg/m²]
FL-DE4	5.0×3.0	Point	Fav.&Cont. Slope		PN/ST	0.6
Parameter assessment					Image monitoring	
R_0	Forw.[3] ROS	Flank Rot.[4]	Back.[5] ROS	Back.[5] Rot.[4]	Video Top	Video Side	IR Top
✓	✓	✓	✓	✓	✓	✓	✓

[1]Type of ignition; [2]Favourable/Contrary; [3]Forward; [4]Rotation; [5]Backwards.

Test monitoring

In these experiments, as the fire perimeter evolution was to be assessed, like in the experiments where images of the fire line evolution were recorded, three cameras were used: one video camera for recording images from the top of the table (Figure 3.4a), one video camera for recording images from the side of the table (Figure 3.4b) and one infrared camera for recording images from the top of the table (Figure 3.4a). Also, pictures like those shown in Figures 4.29 and 4.30 were taken with constant time interval. In Figures 4.31 and 4.32, sequences of images taken by the infrared camera are shown.
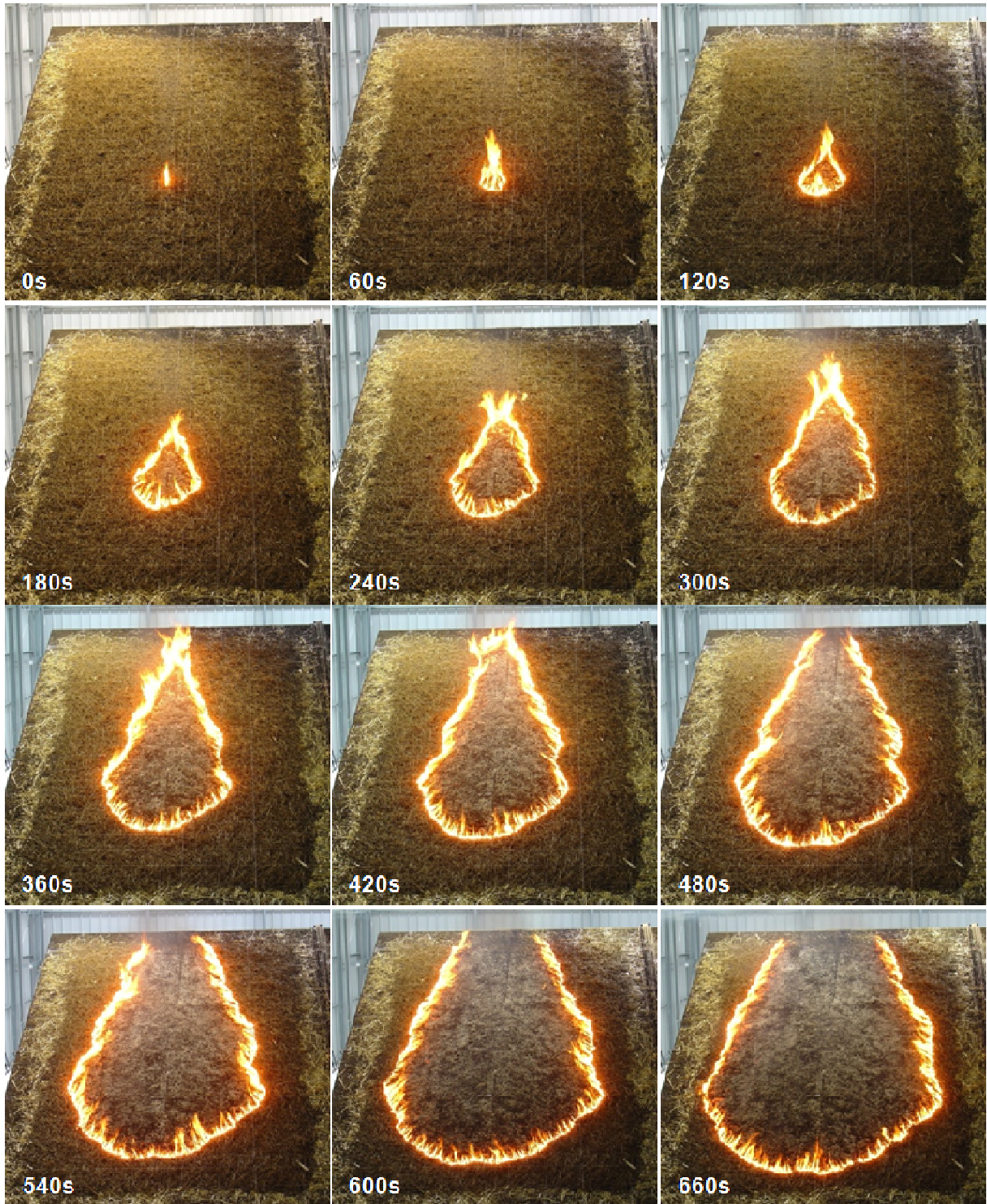
Figure 4.29 – Sequence of pictures for the experiment FL-DE4-02 on the Canyon Table DE4, fuel bed: pine needles, fuel load: $0.6\,\mathrm{kg/m^2}$, slope: 30º. The time since ignition is indicated in each picture.

Figure 4.30 – Sequence of pictures for the experiment FL-DE4-01 on the Canyon Table DE4, fuel bed: straw, fuel load: 0.6 kg/m², slope: 30º. The time since ignition is indicated in each picture.
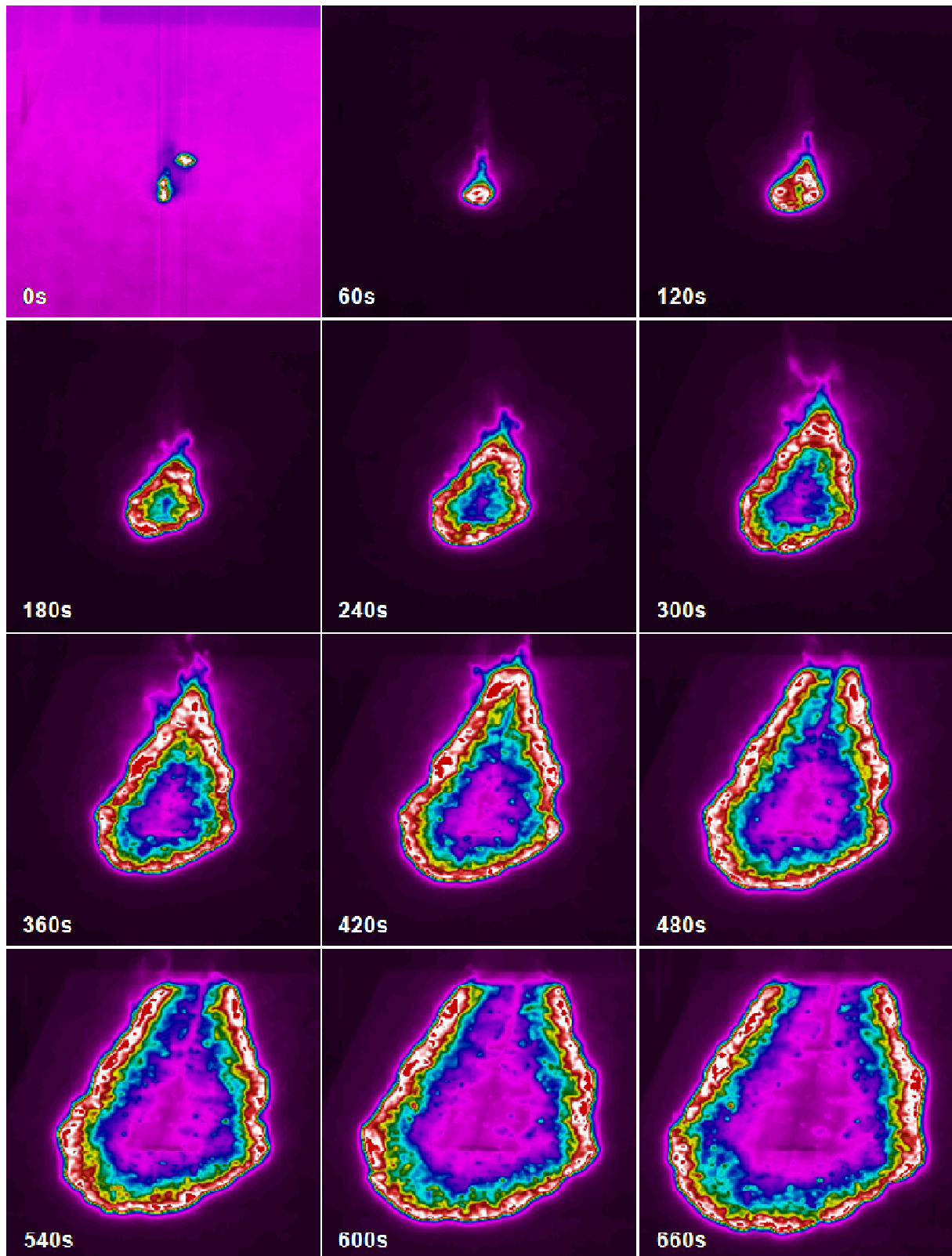
Figure 4.31 – Sequence of infrared frames for the experiment FL-DE4-02 on the Canyon Table DE4, fuel bed: pine needles, fuel load: 0.6 kg/m², slope: 30º. The time since ignition is indicated in each frame.
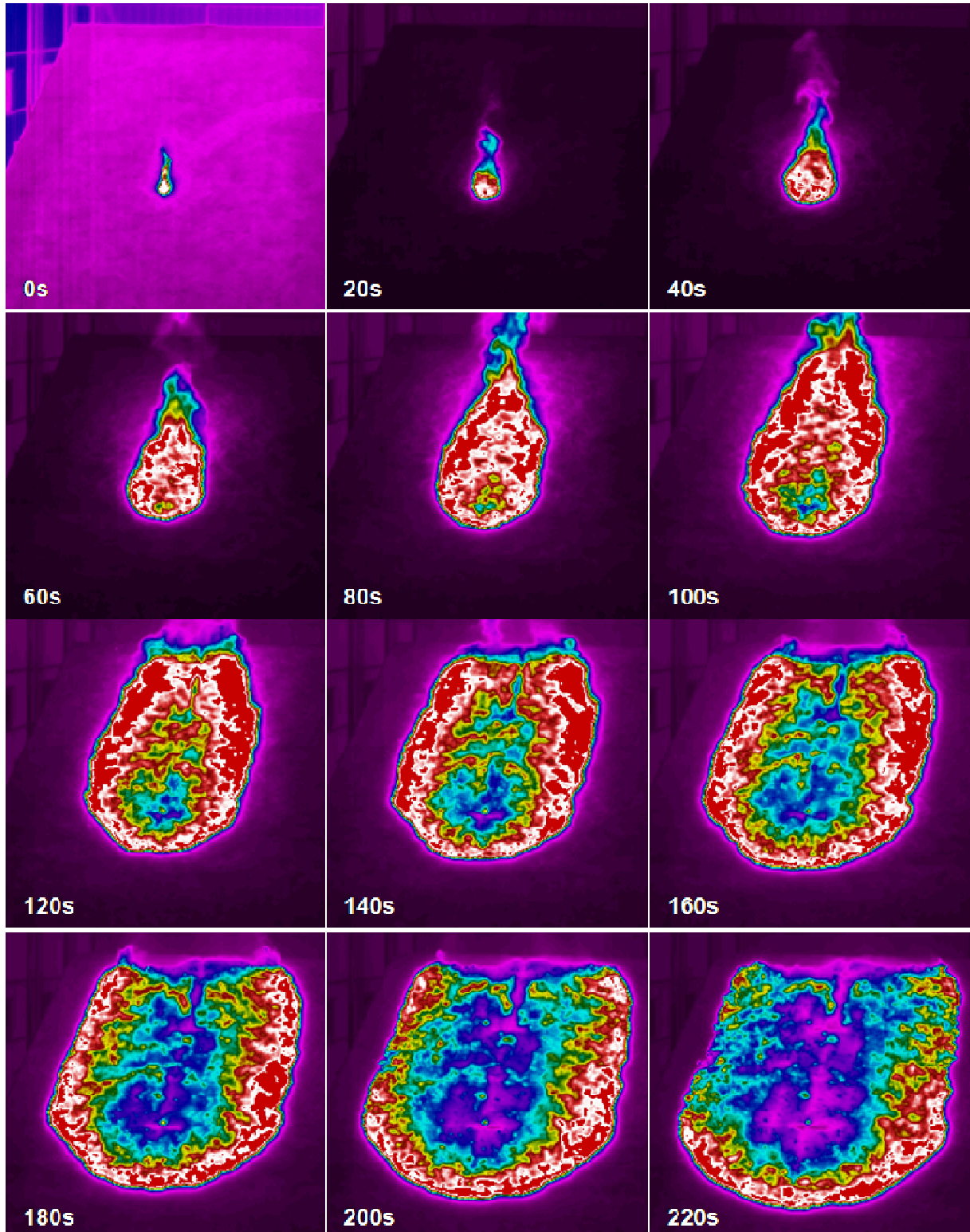
Figure 4.32 – Sequence of infrared frames for the experiment FL-DE4-01 on the Canyon Table DE4, fuel bed: straw, fuel load: $0.6\,kg/m^2$, slope: 30°. The time since ignition is indicated in each frame.

ROS data and the fire line evolution were analyzed in these experiments. The ROS was measured in three directions: head fire spread, backfire spread and lateral fire spread. The first two were estimated using the known times that the fire took to burn each string. The lateral ROS was estimated by using the infrared images to determine the position of the fire line at given time instants. It was chosen to do so because in the initial instants of the experiment the lateral elements of the fire line, due to their proximity, suffer a back draft effect caused by the opposite lateral fire line elements. For this reason, the computed ROS based on the three strings placed for this purpose yielded a value lower than that after the lateral fire line is out of that back draft effect. For each experiment, the selected eight fire line contours, from each side of the fire perimeter, for estimating the lateral ROS were at least 0.25 cm away from the ignition point. The computed ROS was considered to be the average from the left and right results. Regarding the head fire and back fire ROS this effect was negligible, given that those fire line elements spread apart very fast.
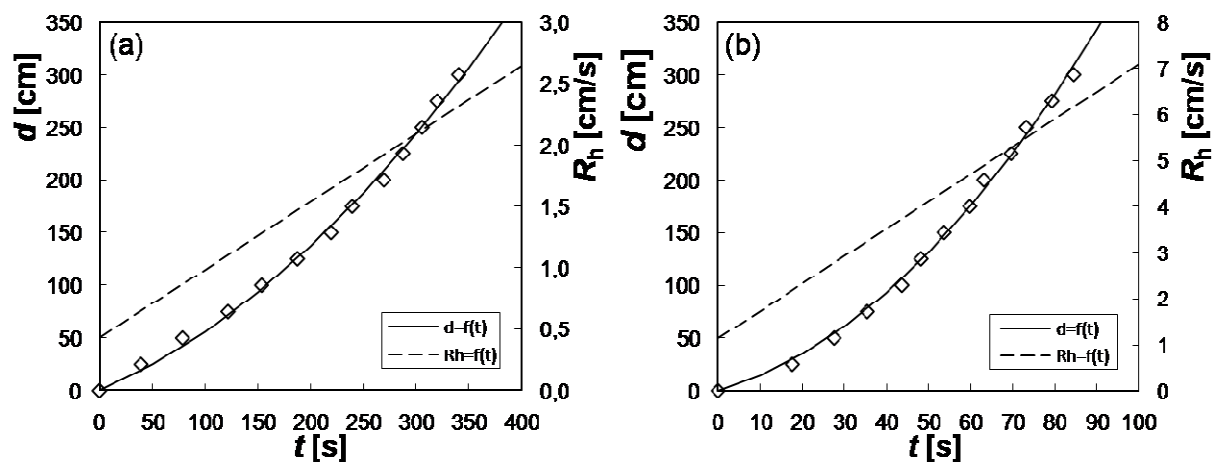

Figure 4.33 – Distance travelled by the head fire and ROS (Table 4.10) as a function of time, slope: 30°, fuel load: 0.6 kg/m²: (a) Ref.: FL-DE4-02, fuel bed: pine needles, fuel moisture: 10.5 %, $d=1.267\times10^{-3}t^2+0.4335t$, $r^2=0.997$. (b) Ref.: FL-DE4-01, fuel bed: straw, fuel moisture: 13.2 %, $d=2.975\times10^{-2}t^2+1.138t$, $r^2=0.997$.

Plotting the distance travelled by fire as a function of time and fitting a curve to each set of data, for each direction we can estimate the fire ROS. For the backwards and lateral spread, a linear fit, like shown in Figure 3.9a, yields correlation values r^2 always greater than 0.995 which indicates the ROS is well estimated by a constant value. On the other hand, for the head fire propagation a linear fit would yield poor correlation values when compared with a 2nd degree

polynomial fit, shown in Figure 4.33. For the first case we have r^2 values always above 0.963 and in the second case always above 0.997. This clearly shows that the head fire ROS cannot be accurately estimated by a constant value. This can easily be explained if we consider that in a slope driven fire caused by a point ignition we do not have the head fire narrowing, observed in the line ignition fires like previously referred, that diminishes the heat received by radiation from the fuel ahead of the most advanced part of the fire line. Without this opposing effect to the fire spread the fire acceleration is easily observed, even for shorter fuels beds.

Deriving the 2nd degree polynomials of the distance travelled by fire as a function of time we obtain the 1st degree polynomials that give the ROS as a function of time (Table 4.10).

Table 4.9 – Main parameters of the FL-DE4 experiments on the Canyon Table DE4 test rig.

Test parameters		Fuel bed data				Air conditions	
Ref.	α [º]	Type	W [kg/m²]	m_f [%]	Bulk den. [kg/m³]	Temp. [ºC]	RH [%]
FL-DE4-01	30	Straw	0.6	13.2	7.2	25.7	53
FL-DE4-02	30	Pine needles	0.6	10.5	9.7	29.5	41

Table 4.10 – ROS data of the FL-DE4 experiments on the Canyon Table DE4 test rig.

Ref.	R0S data						
	R_0 [cm/s]	R_h [cm/s]	R_b [cm/s]	R_f [cm/s]	R'_h	R'_b	R'_f
FL-DE4-01	0.9838	$5.950\times10^{-2}t+1.138$	0.7096	0.7533	$6.048\times10^{-2}t+1.156$	0.7213	0.7656
FL-DE4-02	0.2796	$2.534\times10^{-3}t+0.4335$	0.2226	0.2072	$9.063\times10^{-3}t+1.550$	0.7963	0.7412

Like already described in Chapter 3, the fire line evolution contours are obtained by infrared image analysis. Again, an adequate time interval dt was chosen in order to have a reasonable number of frames to process and to have an adequate description of the evolution of the fire perimeter. The time interval between frames was chosen to be 60 s for the pine needles experiment and 20 s for the straw experiment. In these tests, the data processing is finished with the drawing and correction to represent orthogonal projections of the fire contours to a plane parallel to the camera lens of the fire line contours for each frame (Figures 4.38 and 4.39).

4.2.2. Model results and analysis

Fire line partition

The simulation of the fire line evolution was made by combining the models developed for the flank rotation and backwards rotation. As referred, in the initial instants of the experiments, the

lateral fire line elements suffer a back draft effect caused by the opposite fire line and for that reason it was chosen to initiate the simulation when they were at least 1.5 m apart.
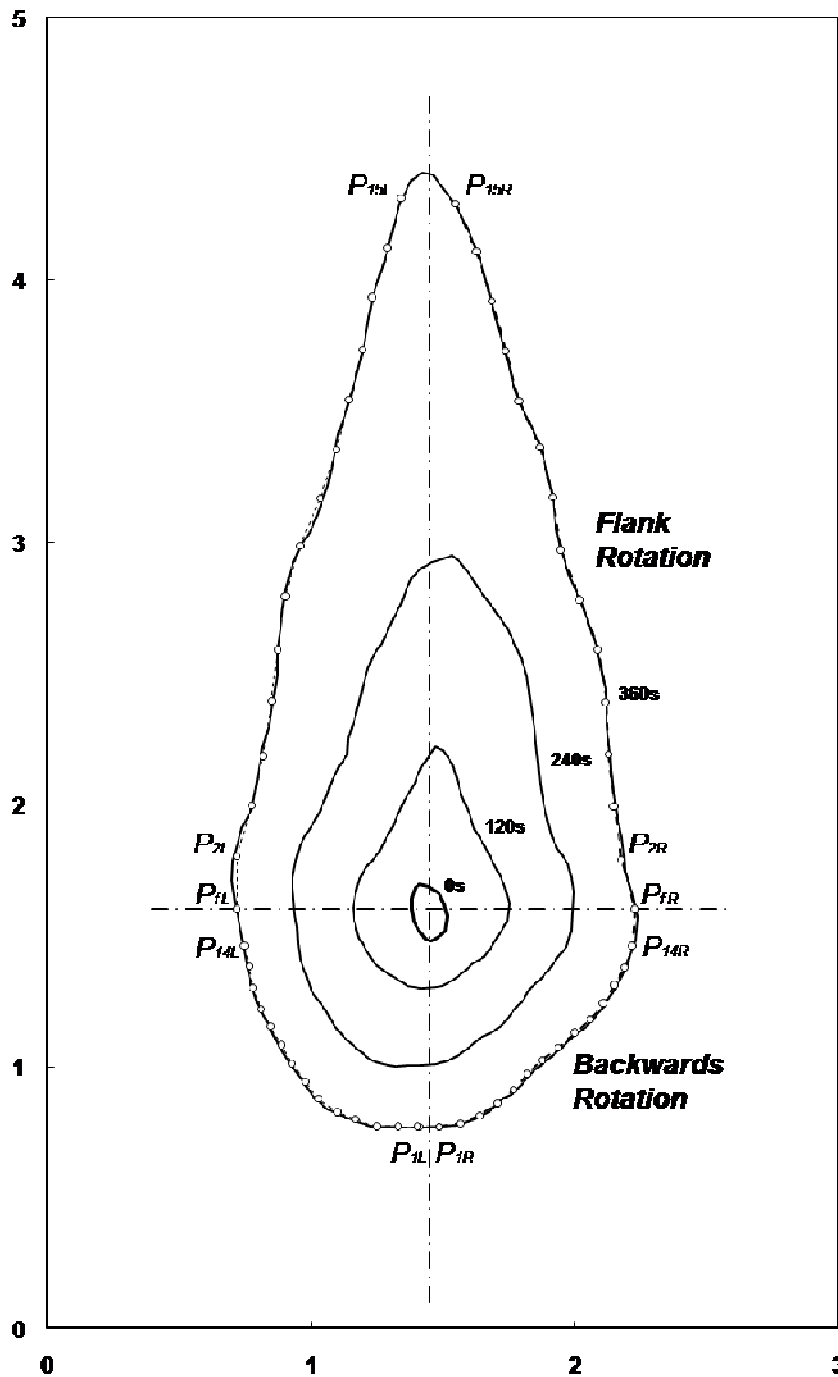

Figure 4.34 – Example of fire line partition for application of the fire line evolution prediction model for an experiment on the Canyon Table DE4, ref.: FL-DE4-02, fuel bed: pine needles, slope: 30°, fuel load: $0.6\,kg/m^2$. Burn area dimensions in [m].

The first step in the model application is, for the fire line perimeter corresponding to the considered initial time instant, choosing *n* points that define *n-1* fire line segments, as shown in Figure 4.34. Around fifteen points were considered in each quadrant which corresponds to an initial length of 8 cm for the backwards fire line elements and 20 cm for the forward fire line elements. The points above and below the horizontal line are placed like shown in Figures 3.10 and 3.11, respectively. In the right and left sides, the first point, P_{fR} or P_{fL}, is placed over the horizontal line and the position of the remaining ones is determined by defining 20 cm segments. It is considered that those points will spread parallel to the OX axis at a ROS R_f (Table 4.10). Below that line, first the central segment S_{CL} is placed and from their right and left ends, P_{1R} and P_{1L}, respectively, the position of the remaining points is determined by defining 8 cm segments. Between the last point and the point in the horizontal line, P_{fR} or P_{fL}, a segment with variable length is defined. It is considered that points P_{1R} and P_{1L} will have a vertical translation, parallel to the OY axis at a ROS R_b (Table 4.10).

Flank rotation

In Figure 4.35, it is shown the scheme of the flank rotation model calculus process as well as the equations used and the tables where the input parameters are given. As we do not have, at this point, enough data for developing a model for predicting the lateral ROS R_f, that determined by the experiments (Table 4.10) will be considered as an input.

The first step consists of the calculus of the equivalent wind to a 30º slope. Afterwards, we determine the translation of the points over the horizontal symmetry axis P_{fR} and P_{fL} (Figures 4.34 and 3.10) on the right and left sides of the vertical symmetry axis, respectively. That translation is considered to have only a horizontal component. Finally, for all segments in each time step *dt*, we compute the final length, rotational velocity and final angle.

When the fire line segments become vertical we have a transition from flank rotation to backwards rotation. As we do not have enough data to fully understand how does this transition process, it was considered that when the segments attained an angle $\beta = 90º$ the rotational velocity was null from there forth. Knowing the position of P'_{fR} and P'_{fL} at time instant $t' = t+d$t, the fireline perimeter is then determined by computing successively the coordinates of the end of each segment, using the previously determined angle and length.
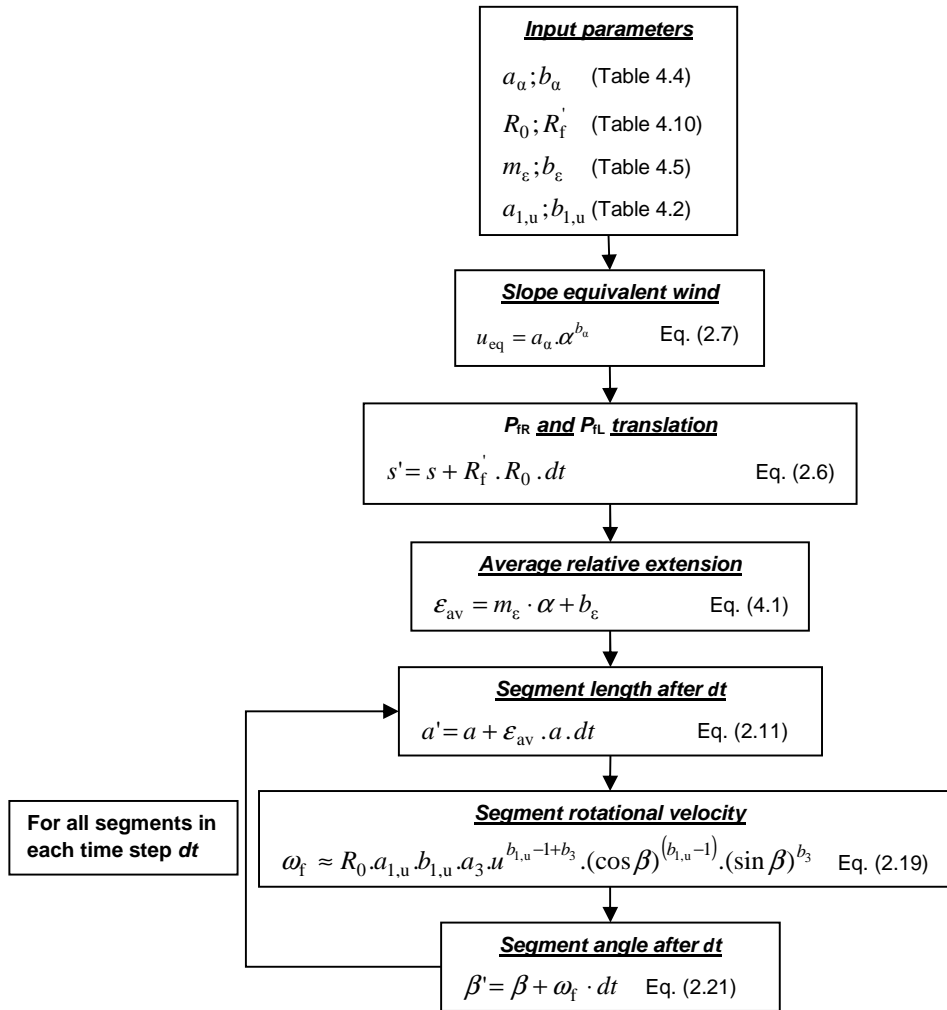
Figure 4.35 – Scheme of the flank rotation model calculus process.

The flowchart contains the following boxes:

Input parameters
$a_\alpha ; b_\alpha$ (Table 4.4)
$R_0 ; R_f'$ (Table 4.10)
$m_\varepsilon ; b_\varepsilon$ (Table 4.5)
$a_{1,u} ; b_{1,u}$ (Table 4.2)

Slope equivalent wind
$u_{eq} = a_\alpha . \alpha^{b_\alpha}$ Eq. (2.7)

P_{1R} and P_{1L} translation
$s' = s + R_f' . R_0 . dt$ Eq. (2.6)

Average relative extension
$\varepsilon_{av} = m_\varepsilon \cdot \alpha + b_\varepsilon$ Eq. (4.1)

Segment length after dt
$a' = a + \varepsilon_{av} . a . dt$ Eq. (2.11)

Segment rotational velocity
$\omega_f \approx R_0 . a_{1,u} . b_{1,u} . a_3 . u^{b_{1,u}-1+b_3} . (\cos \beta)^{(b_{1,u}-1)} . (\sin \beta)^{b_3}$ Eq. (2.19)

Segment angle after dt
$\beta' = \beta + \omega_f \cdot dt$ Eq. (2.21)

For all segments in each time step dt

Backwards rotation

The scheme of the backwards rotation model calculus process shown in Figure 4.36 is similar to the one presented for the flank rotation, differing essentially in the rotational velocity computation. Although data was presented on the backwards ROS R_b in Chapter 4, we do not have, at this point, a model for predicting it. For that reason, that determined by the experiments (Table 4.10) will be also considered as an input.

The first step consists of the calculus of the vertical translation of points P_{1R} and P_{1L} that define the central segment S_{CL}. For all segments in each time step dt, the final length, rotational velocity and final angle are then computed. The position of P'_{1R} and P'_{1L} at time instant $t' = t + dt$

is determined after computing the modulus of their horizontal translation considered to be the same and equal to half the length variation of S_{CL}.

Then, for the right side of the vertical line, knowing the coordinates of P'_{1R}, the fireline perimeter is determined by computing successively the coordinates of the end of each segment using the previously determined angle and length. The same process is applied on the left side, this time starting with the coordinates of P'_{1L}.
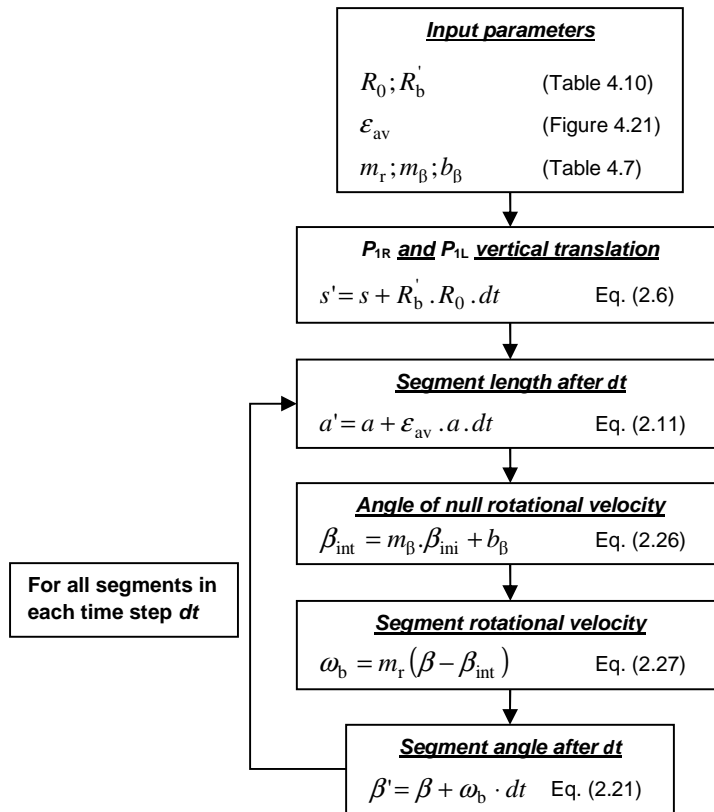
Input parameters

$R_0 ; R'_b$	(Table 4.10)
ε_{av}	(Figure 4.21)
$m_r ; m_\beta ; b_\beta$	(Table 4.7)

P_{1R} _and_ P_{1L} _vertical translation_

$s' = s + R'_b . R_0 . dt$ 　　　　Eq. (2.6)

Segment length after dt

$a' = a + \varepsilon_{av} . a . dt$ 　　　　Eq. (2.11)

Angle of null rotational velocity

$\beta_{int} = m_\beta . \beta_{ini} + b_\beta$ 　　　　Eq. (2.26)

For all segments in each time step _dt_

Segment rotational velocity

$\omega_b = m_r \left(\beta - \beta_{int} \right)$ 　　　　Eq. (2.27)

Segment angle after dt

$\beta' = \beta + \omega_b \cdot dt$ 　　Eq. (2.21)

Figure 4.36 – Scheme of the backwards rotation model calculus process.

Results and analysis

In Figures 4.38 and 4.39, we have the comparison between the experimental and model results for pine needles and straw fuel beds, respectively. The full coloured lines represent the experimental results and the dashed black lines represent the model results.

Considering the pine needles fuel bed experiment, we can see that the predicted backwards fire line evolution is very similar to the real one, especially for the left side. However, in the right side of the backwards fire line, despite the first simulated perimeter has a considerable deviation from the real one, in the remaining time steps the simulated and real fire lines become closer.

Regarding the flank fire evolution, although on both sides the simulations corresponding to the 360 and 420 s time instants, especially for the right side, are reasonably similar to the real fire line the same does not happen in the remaining time steps where the fire line rotation is under predicted. The results for the straw fuel bed experiment are not as good as for the pine needles, especially when comparing the back fire evolution. However the flank rotation results are reasonable, in particular for the left side.

Field fires

Although, in this work, no comparison is made between the model results and real cases, it is considered that it is valid at a field scale based on the fact that the test rigs used were very large. The model should also be valid for other fuel beds, provided that the necessary input parameters, presented in Figures 4.35 and 4.36, are determined, considering that the fire perimeter evolution is very similar between the two tested fuel beds, despite the obvious differences in terms of absolute ROS.

Figure 4.37 – (a) Field experiment under slope and wind effects, Lousã, Central Portugal (02-06-2004). (b) Forest fire spreading upslope in Oleiros, Central Portugal (31-07-2003).

The similarity between the fire line perimeter evolution in the experiments, when compared with that in the forest fire and the field experiment shown in Figure 4.37, both spreading in low shrubs, indicates that the hypothesis of the model validity in real cases and for other fuel beds is reasonable. The input parameters (Figures 4.35 and 4.36) determined for the pine needles and straw fuel beds would probably yield reasonable results for pine needles litter and herbaceous fuels, respectively. However for other fuels, like shrubs, those parameters,

96

considered to be dependent on the fuel bed, should be determined by field or laboratory experiments. Practical application of the model to real cases and other fuel beds is being considered as future work.
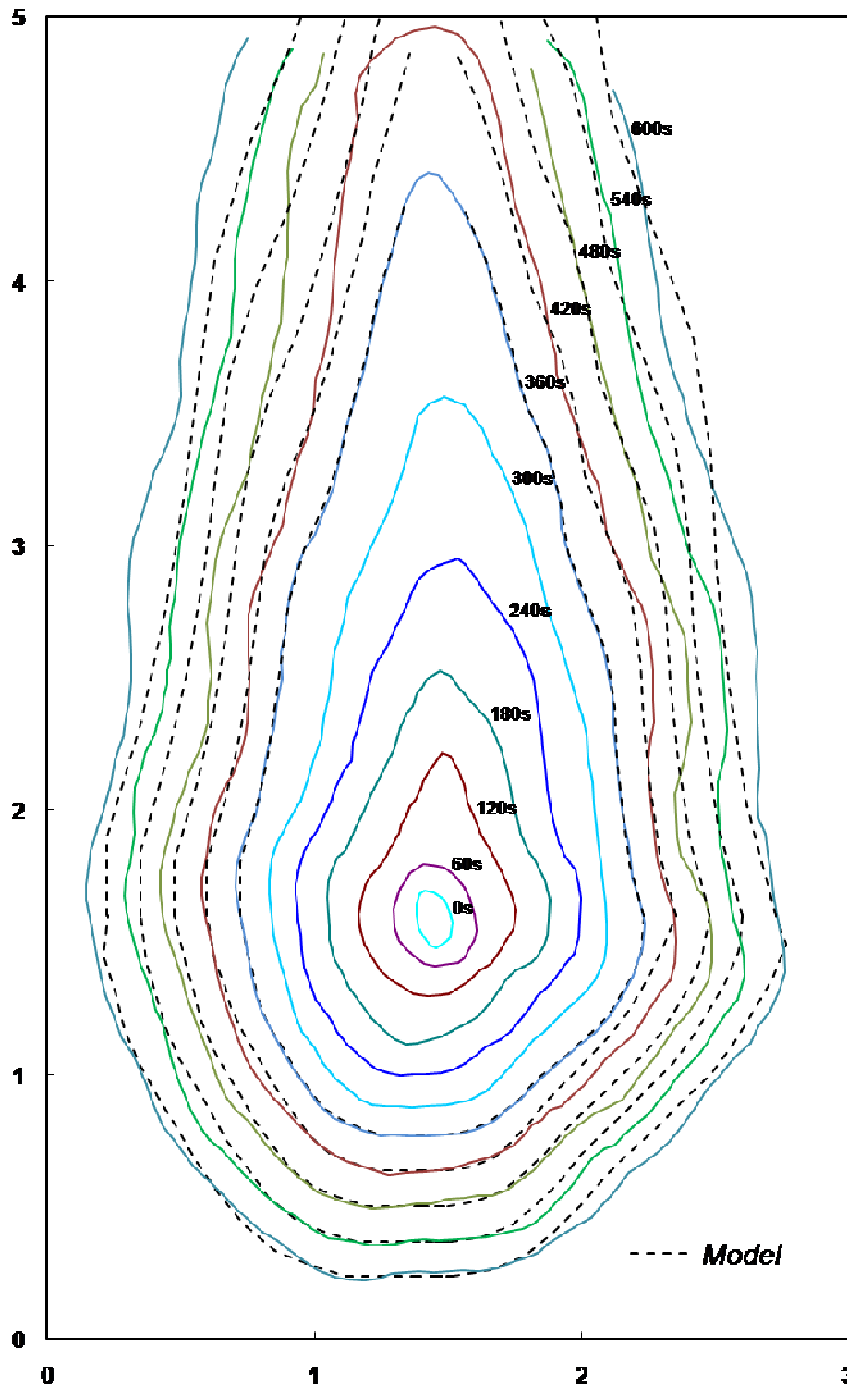

Figure 4.38 – Experimental *Vs* model results for the experiment FL-DE4-02 on the Canyon Table DE4, fuel bed: pine needles, fuel load: $0.6\,kg/m^2$, slope: 30°. Burn area dimensions in [m]. Simulation starts at time instant 360 s with the fire line perimeter as an input.
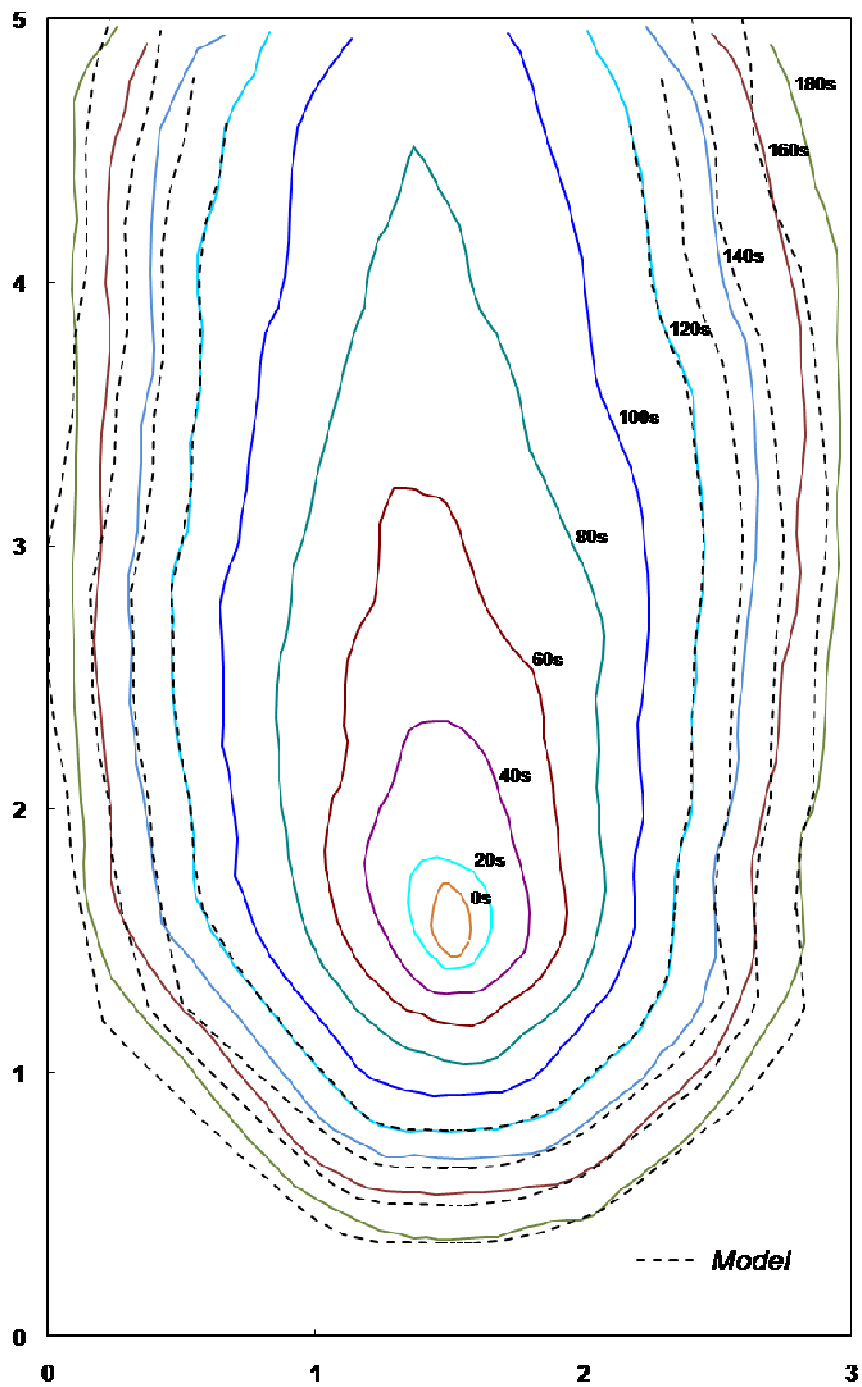
Figure 4.39 – Experimental *Vs* model results for the experiment FL-DE4-01 on the Canyon Table DE4, fuel bed: straw, fuel load: 0.6 kg/m^2, slope: 30°. Burn area dimensions in [m]. Simulation starts at time instant 120 s with the fire line perimeter as an input.

5. *Conclusion*

Surface forest fires behaviour on dead fine fuels was analysed based on a total of 155 laboratory experiments. Tests of fire spread on level ground in the absence of wind ($4 < m_f < 19\,\%$), under the effects of favourable and contrary wind ($-4.5 < u < 4.5$ m/s), and favourable and contrary slope ($-55 < \alpha < 40°$) were made, using four experimental rigs. Fuel beds of *Pinus pinaster* dead needles, dry straw and in some cases also *Eucalyptus globulus* slash fuel beds were tested with a fuel load of 0.6 kg/m², as this is a typical value found in nature for fine fuel beds, and in some cases also 0.8 and 1.0 kg/m².

Parameters were determined, based on the laboratory experiments, for an empirical model for the dependence of the ROS on the fuel moisture content for fire spreading with no wind or slope for the three tested fuel beds. The fuel load was found not to have a significant influence on the basic ROS R_0, at least for the tested range of fuel moisture and load.

Based on the results from the wind-driven or slope-driven experimental fires, parameters for two empirical models, one for the dependence of the ROS on wind and another for the dependence on slope, were determined. Based on them, an equation for computing an equivalent wind velocity u_{eq} that produces the same ROS value on a horizontal ground as a given slope angle α was derived. These tests, performed in two large test rigs for minimizing the scaling effect, suggest that the ROS does not have a relevant dependence on the fuel load. It was also concluded that small differences in the fuel moisture content in the order of $1-2\,\%$ also do not seem to have a relevant influence on the ROS. Within a given set of test fires, coherence was found between each experiment and differences between sets are attributed to parameters external to the fuel beds.

The ROS of fires spreading with contrary wind or slope was also studied, a subject that has not deserved much attention in previous research. It was shown that, when compared with spread on level ground in still air, wind or slope back fires have slightly lower ROS values and that the spread velocity successively decreases and increases as we increase the absolute value of the wind velocity or slope angle. This behaviour is attributed to variations in the flame geometry that can produce changes in the amount of heat transfer by flame radiation over the fuel bed and convective heat transfer, inside and over the fuel bed, caused by the balance between the buoyancy forces and the air flow parallel to the test rig. For wind velocities high enough, fire spread is not sustained and for slopes over a given angle spotting started to occur due to falling

embers, originating spot fires ahead of the original fire line that would spread upwards and change the mechanism of spread.

Also, as a complement to the usual ROS to describe the fire line movement, the concepts of fire line extension and rotation were introduced as tools to analytically describe the movement of a forward or backwards propagation fire line. It was considered that for a fire under the effect of slope or wind, when the ROS vector of a fire line element is not aligned with the slope gradient or wind direction, there is a convective flow along the fire line inducing differences on the combustion reaction intensity, causing a variation of the ROS. Different ROS along a fire line element length will imply a rotation. It was shown that with time the fire line elements increase their length and the curvature of the fire line is reduced.

Rotation and extension of the fire line elements depend on the fuel bed. It was found that flank fire line elements rotate with variable positive rotational velocity with time, tending to become parallel to the direction of the ambient flow or slope, and increase their length with an average relative extension that varies linearly with wind velocity or slope angle. On the other hand, back fire line elements rotate with variable rotational velocity that alternates between positive and negative values with time and increase their length with an average relative extension that does not vary significantly with wind velocity or slope angle. Due to the joint effect of extension and rotation, the back fire line elements tend to become perpendicular to the direction of the ambient flow or slope.

Using semi-physical and empirical formulations, a model for the fire line perimeter evolution of a point ignition fire under constant wind or slope, considering the fire line elements extension and rotation, was proposed. Empirical parameters required by the model were determined experimentally. The model was compared with experimental results of fire spreading on a slope for pine needles and straw fuel beds. There was a reasonable agreement between the predicted and measured fire line evolution.

In terms of future research, two phases of work are being planned. The first is to be made at laboratory scale with the objectives of modelling the parameters that currently are considered as inputs, such as the head fire and the lateral ROS, and during the experiments assess parameters that are thought to be responsible by systematic differences between sets of experiments, apparently under very similar conditions. This phase should include tests of point ignition fires on a large slope test rig (8×4 m^2) that would enable the modelling of the fire

perimeter lateral ROS and the determination of the parameters for modelling the head fire ROS using the model proposed by Viegas (2005). In these experiments, the temperature of the surrounding surfaces and of the vertical air field at the beginning and during the experiments should be assessed, using thermocouples and portable weather stations. The second phase consists of field fires with the objective of extending the model to the prediction of real fires. Experiments should assess the fire spread of a point ignition on a slope with the minimum influence of wind and on level ground under the influence of wind. The tests should be monitored using video and infrared cameras for evaluating the fire perimeter evolution and measurements of the head, back, and lateral fires should be taken. Based on the wind or slope head and contrary fires data, and following the same procedures of the laboratory experiments analysis, the model's parameters would be determined.

References

Albini FA (1967) A physical model for firespread in brush. *1lth International Symposium on Combustion*. The Combustion Institute. 553-560.

Albini FA (1976) Combining wind and slope effects on spread rate. *Unpublished memo to R.C. Rothermel dated 19-01-1976*. Intermountain Fire Sciences Laboratory. Missoula, Montana, USA. 16 pp.

Albini FA and Baughman RG (1979) Estimating wind speeds for predicting wildland fire behavior. *Research Paper INT-221*. USDA Forest Service. Intermountain Forest and Range Experiment Station. Ogden, Utah, USA. 12 pp.

Albini FA (1981) A model for the wind-blown flame from a line fire. *Combustion and Flame*, **43**, 155-174.

Albini FA (1982) Response of free-burning fires to nonsteady wind. *Combustion Science and Technology*, **29**, 225-241.

Albini FA (1985) A model for fire spread in wildland fuels by radiation. *Combustion Science and Technology*, **42**, 229-258.

Albini FA (1986) Wildland spread by radiation – a model including fuel cooling by natural convection. *Combustion Science and Technology*, **45**, 101-113.

Albini FA (1993) Dynamics and modeling of vegetation fires: observations. *Crutzen PJ and Goldammer JG (eds) Fire in the environment: The ecological, atmospheric, and climatic importance of vegetation fires*. Report on the Dahlem Workshop, Berlin 15-20 March 1992. John Wiley & Sons. Chichester, UK. 39-52.

Albini FA and Reinhardt ED (1995) Modeling ignition and burning rate of large woody natural fuels. *International Journal of Wildland Fire*, **5 (2)**, 81-91.

Albini FA, Brown JK, Reinhardt ED and Ottmar RD (1995) Calibration of a large fuel burnout model. *International Journal of Wildland Fire*, **5 (3)**, 173-192.

Albini FA and Reinhardt ED (1997) Improved calibration of a large fuel burnout model. *International Journal of Wildland Fire*, **7 (1)**, 21-28.

Alexander ME (1982) Calculating and interpreting forest fire intensities. *Canadian Journal of Botany*, **60**, 349-357

Anderson DH, Catchpole EA, de Mestre NJ and Parkes T (1982) Modelling the spread of grass fires. *Journal of Australian Mathematics Society (Series B)*, **23**, 451-466.

Anderson HE (1964) Mechanisms of fire spread – Research progress report Nº 1. *Research Paper INT-8*. USDA Forest Service. Intermountain Forest and Range Experiment Station. Ogden, Utah, USA. 20 pp.

Anderson HE and Rothermel RC (1965). Influence of moisture and wind upon the characteristics of free-burning fires. *10th International Symposium on Combustion*. The Combustion Institute. Pittsburgh, USA. 1009-1019.

Anderson HE (1968) Fire spread and flame shape. *Fire Technology*, **4**. 51-58.

Anderson HE (1969) Heat transfer and fire spread. *Research Paper INT-69*. USDA Forest Service. Intermountain Forest and Range Experiment Station. Ogden, Utah, USA. 20 pp.

André JC and Viegas DX (2001) Modelos de propagação de fogos florestais: Estado da arte para utilizadores. Parte I: Introdução e modelos locais. *Silva Lusitana (in Portuguese)*, **9 (2)**, 237-265.

André JC and Viegas DX (2002) Modelos de propagação de fogos florestais: Estado da arte para utilizadores. Parte II: Modelos globais e sistemas informáticos. *Silva Lusitana (in Portuguese)*, **10 (2)**, 217-233.

Andrews PL (1986) BEHAVE: fire behaviour prediction and fuel modelling system – BURN Subsystem, Part 1. *General Technical Report INT-194*. USDA Forest Service, Ogden, USA. 130 pp.

Andrews PL and Chase CH (1989) BEHAVE: fire behaviour prediction and fuel modelling system – BURN Subsystem, Part 2. *General Technical Report INT-260*. USDA Forest Service, Ogden, USA. 93 pp.

Andrews PL, Bevins CD and Seli RC (2003) BehavePlus fire modeling system, version2.0: User's Guide. *General Technical Report RMRS-GTR-106WWW*. USDA Forest Service, Ogden, USA. 132 pp.

Baines PG (1990) Physical mechanisms for the propagation of surface fires. Mathematical and Computer Modelling, **13 (12)**, 83-94.

Balbi JH, Santoni PA and Dupuy JL (1999) Dynamic modelling of fire spread across a fuel bed. *International Journal of Wildland Fire*. **9**, 275-284.

Ball GL and Guertin DP (1992) Improved fire growth modeling. *International Journal of Wildland Fire*, **2 (2)**, 47-54.

Baughman RG and Albini FA (1980) Estimating midflame wind speeds. *6th Conference on Fire and Forest Meteorology*. Society of American Foresters. Seattle, Washington, USA. 88-92.

Beck J, Parminter J, Alexander M, MacDermid E, Van Nest T and Beaver A (2005) Fire ecology and management. *Forestry handbook for British Columbia, 5th edition*. Forestry Undergraduate Society. Faculty of Forestry, University of British Columbia, Vancouver, B.C., Canada. 485-521.

Beer T (1993) The speed of a fire front and its dependence on wind speed. *International Journal of Wildland Fire*. **3 (4)**, 193-202.

Beer T (1995) Fire propagation in vertical stick arrays: the effects of wind. *International Journal of Wildland Fire*. **5 (1)**, 43-49.

Beyreis JR, Monsen HW and Abbasi AF (1971) Properties of wood crib flames. *Fire Technology*, **7 (2)**. 145-155.

Brain CK and Sillen A (1988) Evidence from the Swartkans Cave for the earliest use of fire. *Nature*, **336**, 464-466.

Burgan RE and Rothermel RC (1984) BEHAVE: fire behaviour prediction and fuel modelling system – FUEL Subsystem. *General Technical Report INT-167*. USDA Forest Service, Ogden, USA. 126 pp.

Butler BW (2006) The effect of solar radiation on the spread rate of fires burning over a horizontal fuel array. *Proceedings of the V International Conference on Forest Fire Research*. 27-30 November 2006, Figueira da Foz, Portugal.

Byram GM (1959) Combustion of forest fuels. *Davis KP (ed) Forest fire: control and use*. McGraw-Hill. New York. 61-89.

Carrier GF, Fendell FE and Wolff MF (1991) Wind-aided fire spread across arrays of discrete fuel elements I: Theory. *Combustion Science and Technology*, **75**, 31-51.

Catchpole EA, de Mestre NJ and Gill AM (1982) Intensity of fire at its perimeter. *Australian Forestry Research*, **12**, 47-54.

Catchpole EA and de Mestre NJ (1986) Physical models for a spreading line fire. *Australian Forestry*, **49 (2)**, 102-111.

Catchpole EA and Catchpole WR (1991) Modelling moisture damping for fire spread in a mixture of live and dead fuels. *International Journal of Wildland Fire*, **1 (2)**, 101-106.

Catchpole EA, Alexander ME and Gill AM (1992) Elliptical-fire perimeter- and area-intensity distributions. *Canadian Journal of Forest Research*, **22**, 968-972.

Catchpole EA, Catchpole WR and Rothermel RC (1993) Fire behavior experiments in mixed fuel complexes. *International Journal of Wildland Fire*, **3 (1)**, 45-57.

Catchpole WR, Catchpole EA, Butler BW, Rothermel RC, Morris GA and Latham DJ (1998a) Rate of spread of free-burning fires in woody fuels in a wind tunnel. *Combustion Science and Technology*, **131**, 1-37.

Catchpole W, Bradstock R, Choate J, Fogarty L, Gellie N, McCarthy C, McCaw L, Marsden-Smedley J and Pierce G (1998b) Cooperative development of equations for heathland fire behaviour. *Proceedings of the III International Conference on Forest Fire Research*. 16-20 November 1998, Luso, Portugal. 631-645.

Cekirge HM (1978) Propagation of fire fronts in forests. *Computers & Mathematics with Applications*, **4**, 325-332.

Chandler CC, Cheney NP, Thomas P, Trabaud L and Williams D (1983). Fire in forestry. Volume 1: forest fire behaviour and effects. Wiley. New York.

Cheney NP (1981) Fire behaviour. *Gill AM, Groves RH and Noble IR (eds) Fire and the Australian Biota*. Australian Academy of Science, Canberra. Australia. 151-175.

Cheney NP (1990) Quantifying bushfires. *Mathematical and Computer Modelling*, **13 (12)**, 9-15.

Cheney NP, Gould JS and Catchpole WR (1993) The influence of fuel, weather and fire shape variables on fire-spread in grasslands. *International Journal of Wildland Fire*, **3 (1)**, 31-44.

Cheney NP and Gould JS (1995) Fire growth in grassland fuels. *International Journal of Wildland Fire*, **5**, 237-247.

Clark TL, Coen JL and Latham D (2004) Description of a coupled atmosphere-fire model. *International Journal of Wildland Fire*, **13**, 49-63.

Coen JL (2005) Simulation of the Big Elk Fire using coupled atmosphere-fire modeling. *International Journal of Wildland Fire*, **14**, 49-59.

Cramer W (2001) Fire ecology, Mediterranean forests and global change. *Forest Ecology and Management*, **147**, 1-2.

Curry JR and Fons WL (1938) Rate of spread of surface fires of surface fires in the Ponderosa pine type of California. *Journal of Agricultural Research*, **57 (4)**, 239-267.

Damasceno P and Silva JS (2007). As causas dos incêndios em Portugal (*in Portuguese*). *Silva JS (ed) Proteger a floresta: incêndios, pragas e doenças*. Lisboa, Portugal. 41-67.

De Mestre NJ, Catchpole EA, Anderson DH and Rothermel RC (1989) Uniform propagation of a planar fire front without wind. *Combustion Science and Technology*, **65**, 231-244.

Dijkstra EW (1959) A note on two problems in connection with graphs. *Numerische Mathematik*, **1**, 269-271.

Durão RM and Real JC (2006). Alterações climáticas: futuro dos acontecimentos extremos e do risco de incêndio (*in Portuguese*). *Pereira JS, Pereira JM, Rego FC, Silva JS and Silva TP (eds) Incêndios florestais em Portugal: caracterização, impactes e prevenção*. Instituto Superior de Agronomia, Lisboa, Portugal. 231-255.

Emmons HW and Shen T (1971) Fire spread in paper arrays. *13th International Symposium on Combustion*. The Combustion Institute. 917-927.

FAO (2007) Fire management – global assessment 2006. *FAO Forestry Paper nº151*, Rome, Italy. 121 pp.

FAO (2008) Status of wildfires in the African region. *FAO Meeting on Forests and Wildfires*, 18-21 February 2008, Khartoum, Republic of the Sudan. 4 pp.

Fernandes PM (2001) Fire spread prediction in shrub fuels in Portugal. *Forest Ecology and Management*, **144**, 67-74.

Finney MA (1998) FARSITE: Fire area simulator – model development and evaluation. *Research Paper RMRS-RP-4*. USDA Forest Service, Rocky Mountain Research Station, Ogden, Utah, 47 pp.

Fleeter RD, Fendel FE, Cohen LM, Gat N and Witte AB (1984) Laboratory facility for wind-aided firespread along a fuel matrix. *Combustion and Flame*, **57**, 289-311.

Fons WL (1946) Analysis of fire spread in light forest fuels. *Journal of Agricultural Research*, **72 (3)**, 93-121.

Fons WL, Clements HB and George PM (1963) Scale effects on propagation rate of laboratory crib fires. *9th International Symposium on Combustion*. The Combustion Institute. Pittsburgh, Pennsylvania, USA. 860-866.

Forestry Canada Fire Danger Group (1992) Development and structure of the Canadian Forest Fire Behaviour Prediction System. *Information Report ST-X-3*. Canadian Forest Service, Ottawa, Canada. 63 pp.

Frandsen WH (1971) Fire spread through porous fuels from the conservation of energy. *Combustion and Flame*, **16 (1)**, 9-16.

Frandsen WH (1973a) Effective heating of fuel ahead of spreading fire. *Research Paper INT-140*. USDA Forest Service. Intermountain Forest and Range Experiment Station. Ogden, Utah, USA. 16 pp.

Frandsen WH (1973b) Using the effective heating number as a weighting factor in Rothermel's fire spread model. *General Technical Report INT-10*. USDA Forest Service. Intermountain Forest and Range Experiment Station. Ogden, Utah, USA. 7 pp.

Frandsen WH and Schuette RD (1978) Fuel burning rates of downward versus horizontally spreading fires. *Research Paper INT-214*. USDA Forest Service. Intermountain Forest and Range Experiment Station. Ogden, Utah, USA.

Frandsen WH and Andrews PL (1979) Fire behaviour in non-uniform fuels. *Research Paper INT-232*. USDA Forest Service. Intermountain Forest and Range Experiment Station. Ogden, Utah, USA. 34 pp.

French IA, Anderson DH and Catchpole EA (1990) Graphical simulation of bushfires spread. *Mathematical and Computer Modelling*, **13 (12)**, 67-71.

Fujii N, Hasegawa J, Pallop L and Sakawa Y (1980) A nonstationary model of firespreading. *Applied Mathematical Modelling*, **4**, 176-180.

Gill AM (1981). Post-settlement fire history in the Victorian landscape. *Gill AM, Groves RH and Noble IR (eds) Fire and the Australian biota*. Australian Academy of Science, Canberra, Australia. 77-98.

Gill AM and Knight IK (1991) Fire measurement. *Cheney NP and Gill AM (eds) Proceedings of Conference on Bushfire Modelling and Fire Danger Rating Systems*. 137-146.

Green DG (1983) Shapes of simulated fires. *Ecological Modelling*, **20**, 21-32.

Gonçalves JC (2000) Experiências de propagação de frentes de fogo em leitos porosos homogéneos e inclinados. *MsC Thesis in Mechanical Engineering (in Portuguese)*. University of Coimbra, Portugal.

Grishin AM (1997). Mathematical modeling of forest fires and new methods of fighting them. *Albini F (ed)*. Publishing House. Tomsk State University, Tomsk, Russia. 390 pp.

Higgins SI, Bond WJ, Trollope WS and Williams RJ (2008) Physically motivated empirical models for the spread and intensity of grass fires. *International Journal of Wildland Fire*, **17**, 595-601.

Hirsch KH (1996) Canadian Forest Fire Behaviour Prediction (FBP) System: user's guide. *For. Special Report 7*. Canadian Forest Service, Northwest Region, Northern Forestry Center. Edmonton, Canada. 122 pp.

Hottel HC (1961) Fire Modelling. *Berl WG (ed) The Use of Models in Fire Research*. Washington D.C., National Academy of Sciences – National Research Council, Publication 786, 32-47.

Hottel HC, Williams GC and Steward FR (1965) The modeling of firespread through a fuel bed. *10th International Symposium on Combustion*. The Combustion Institute. Pittsburgh, USA. 997–1007.

Hwang CC and Yusheng X (1984) Flame propagation along matchstick arrays on inclined base boards. *Combustion Science and Technology*, **42**, 1-12.

Julio G (2008) Managing efforts to prevent forest fires in South America. *Proceedings of the 2nd International Symposium on Fire Economics, Planning, and Policy: A Global View*. *General Technical Report PSW-GTR-208*. USDA Forest Service, USA. 661-671.

Kimmerer RW and Lake FK (2001) Role of Indigenous burning in land management. *Journal of Forestry*, **99 (11)**, 36-41.

Kourtz PH and O'Regan WG (1971) A model for a small forest fire, to simulate burned and burning areas for use in a detection model. *Forest Science*, **17**, 163-169.

Larini M, Giroud F, Porterie B and Loraud JC (1998) A multiphase formulation for fire propagation in heterogeneous combustible media. *International Journal of Heat and Mass Transfer*, **41**, 881-897.

Linn R (1997) Transport model for prediction of wildfire behavior. *Scientific Report LA13334-T*. Los Alamos National Laboratory, New Mexico, USA.

Linn R, Winterkamp J, Colman JJ, Edminster C and Bailey JD (2005) Modeling interactions between fire and atmosphere in discrete element fuel beds. *International Journal of Wildland Fire*, **14**, 37-48.

Linn R, Winterkamp J, Edminster C, Colman JJ and Smith WS (2007) Coupled influences of topography and wind on wildland fire behaviour. *International Journal of Wildland Fire*, **16**, 183-195.

Lopes AM, Sousa AC and Viegas DX (1995) Numerical simulation of turbulent flow and fire propagation in complex topography. *Numerical Heat Transfer, Part A*, **27**, 229-253.

Lopes AM, Cruz MG and Viegas DX (1998) FireStation – an integrated system for the simulation of wind flow and fire spread over complex topography. *Proceedings of the III International Conference on Forest Fire Research*. 16-20 November 1998, Luso, Portugal. 741-754.

Luke RH and McArthur AG (1978) Bushfires in Australia. *Australia Government Publishing Service*. Canberra, Australia. 359 pp.

Lyons PR and Weber RO (1993) Geometrical effects on flame spread rate for wildland fine fuels. *Combustion Science and Technology*, **89**, 153-165.

Margerit J and Séro-Guillaume O (2002) Modelling forest fires – Part II: reduction to two-dimensional models and simulation of propagation. *International Journal of Heat and Mass Transfer*, **45**, 1723-1737.

Marsden-Smedley JB, Catchpole WR and Pyrke A (2001) Fire modelling in Tasmanian buttongrass moorlands, IV: Sustaining versus non-sustaining fires. *Int. J. Wildland Fire*, **10**, 255-262.

McAlpine RS, Lawson BD and Taylor E (1991) Fire spread across a slope. *Andrews PL and Potts DF (eds) Proceedings of the 11th Conference on Fires and Forest Meteorology*. Society of American Foresters. 16-19 April 1991, Bethesda, Maryland, USA. 218-225.

McArthur AG (1966) Weather and grassland fire behaviour. *Australian Forestry and Timber Bureau Leaflet No. 100.* Forestry and Timber Bureau Department of National Development. Canberra, Australia. 23 pp.

McArthur AG (1967) Fire behaviour in eucalypt forests. *Australian Forestry and Timber Bureau Leaflet No. 107*. Forestry and Timber Bureau Department of National Development. Canberra, Australia. 36 pp.

McArthur AG (1973) Forest fire danger meter Mark V. *Australian Forestry and Timber Bureau.* Canberra, Australia.

Mell W, Jenkins MA, Gould J and Cheney P (2007) A physics-based approach to modelling grassland fires. *International Journal of Wildland Fire*, **16**, 1-22.

Mendes-Lopes JM, Ventura JM and Amaral JM (2003) Flame characteristics, temperature-time curves, and rate of spread in fires propagating in a bed of *Pinus pinaster* needles. *International Journal of Wildland Fire*, **12**, 67-84.

Morandini F, Santoni PA, Balbi JH (2000) Analogy between wind and slope effects on fire spread across a fuel bed – Modelling and validations. *3rd International Seminar on Fire and Explosion Hazards*. 10-14 April 2000, Lake Windermere, UK.

Morandini F, Santoni PA, Balbi JH (2001) Validation study of a two-dimensional model of fire spread across a fuel bed. *Combustion Science and Technology*, **166**, 67-90.

Morandini F, Santoni PA, Balbi JH, Ventura JM and Mendes-Lopes JM (2002) A two-dimensional model of fire spread across a fuel bed including wind combined with slope conditions. *International Journal of Wildland Fire*, **11**, 53-64.

Morandini F, Simeoni A, Santoni PA, Balbi JH (2005) A model for the spread of fire across a fuel bed incorporating the effects of wind and slope. *Combustion Science and Technology*, **177**, 1381-1418.

Morandini F, Silvani X, Rossi L, Santoni PA, Simeoni A, Balbi JH, Rossi JL and Marcelli T (2006) Fire spread experiment across Mediterranean shrub: Influence of wind on flame front properties. *Fire Safety Journal*, **41**, 229-235.

Nelson RM and Adkins CW (1986) Flame characteristics of wind-driven surface fires. *Canadian Journal of Forest Research*, **16**, 1293-1300.

Nelson RM and Adkins CW (1988) A dimensionless correlation for the spread of wind-driven surface fires. *Canadian Journal of Forest Research*, **18**, 391-397.

Nelson RM (2002) An effective wind speed for models of fire spread. *International Journal of Wildland Fire*, **11**, 153-161.

Noble IR, Barry GA and Gill AM (1980) McArthur's fire danger meters expressed as equations. *Australian Journal of Ecology*, **5**, 201-203.

Oliveras I, Piñol J and Viegas DX (2006) Generalization of the fire line rotation model to curved fire lines. *International Journal of Wildland Fire*, **15**, 447-456.

Packham D and Pompe A (1971) Radiation temperatures of forest fires. *Australian Forest Research*, **5 (3)**, 1-8.

Pastor E, Zárate L, Planas E and Arnaldos J (2003) Mathematical models and calculation systems for the study of Wildland fire behaviour. *Progress in Energy and Combustion Science*, **29**, 139-153.

Pagni PJ and Peterson TG (1973) Flame spread through porous fuel. *14th International Symposium on Combustion*. The Combustion Institute. Pittsburgh, USA. 1099-1107.

Perry GL (1998) Current approaches to modelling the spread of wildland fire: a review. *Progress in Physical Geography*, **22 (2)**, 222-245.

Porterie B, Morvan D, Larini M and Loraud JC (1998) Wildfire propagation: a two-dimensional multiphase approach. *Combustion, Explosion and Shock Waves*, **34**, 139-150.

Pyne SJ (2001) The fires this time, and next. *Science*, **294 (5544)**, 1005-1006.

Reisner J, Swynne S, Margolin L and Linn R (2000) Coupled atmospheric-fire modeling employing the method of averages. *Monthly Weather Review*, **128**, 3683-3691.

Ribeiro LM (2008) Caracterização do problema dos incêndios na Interface Urbano-Florestal em Portugal (*in Portuguese*). *Technical report of task 2.3 of the research project "Caracterização da Interface Urbano-Florestal em Portugal"*, financed by AFN. Center of Studies on Forest Fires (CEIF), ADAI. Coimbra, Portugal. 144 pp.

Rossa CG (2009) Protocol for the experiments made in LEIF in the scope of the ENB training given by CEIF. *Internal technical report*. Centre of Studies on Forest Fires (CEIF), ADAI. Coimbra, Portugal. 17 pp.

Rossa CG and Viegas DX (2009). Propagation of wind and slope backfires. *Anderssen RS, Braddock RD and Newham LT (eds) 18th World IMACS Congress and MODSIM09 International Congress on Modelling and Simulation*. Modelling and Simulation Society of Australia and New Zealand and International Association for Mathematics and Computers in Simulation. 13-17 July 2009, Cairns, Australia. 261-267.

Rothermel RC and Anderson HE (1966) Fire spread characteristics determined in the laboratory. *Research Paper INT-30*. USDA Forest Service. Intermountain Forest and Range Experiment Station. Ogden, Utah, USA. 34 pp.

Rothermel RC (1972) A mathematical model for predicting fire spread in wildland fuels. *Research Paper INT-115*. USDA Forest Service. Intermountain Forest and Range Experiment Station. Ogden, Utah, USA. 40 pp.

Rothermel RC and Deeming JE (1980) Measuring and interpreting fire behavior for correlation with fire effects. *General Technical Report INT-93*. USDA Forest Service. Intermountain Forest and Range Experiment Station. Ogden, Utah, USA. 3 pp.

Rothermel RC (1983) How to predict the spread and intensity of forest and range fires. *General Technical Report INT-143*. USDA Forest Service. Intermountain Forest and Range Experiment Station. Ogden, Utah, USA. 161 pp.

Schuette RD (1965) Preparing reproducible pine needle fuel beds. *Research Note INT-36*. USDA Forest Service. Intermountain Forest and Range Experiment Station. Ogden, Utah, USA. 7 pp.

Séro-Guillaume O and Margerit J (2002) Modelling forest fires. Part I: a complete set of equations derived by extended irreversible thermodynamics. *International Journal of Heat and Mass Transfer*, **45**, 1705-1722.

Shea RW, Shea BW, Kauffman JB, Ward DE, Haskins CI and Scholes MC (1996) Fuel biomass and combustion factors associated with fires in savanna ecosystems of South Africa and Zambia. *Journal of Geophysical Research*, **101**, 23551-23568.

Show SB (1919) Climate and Forest Fires in Northern California. *Journal of Forestry*, **17 (8)**, 965-979.

Simeoni A, Santoni PA, Larini M and Balbi JH (2001) Proposal for theoretical improvement of semi-physical forest fire spread models thanks to a multiphase approach: application to a fire spread model across a fuel bed. *Combustion Science and Technology*, **162**, 59-83.

Simeoni A, Santoni PA, Larini M and Balbi JH (2003) Reduction of a multiphase formulation to include a simplified flow in a semi-physical model of fire spread across a fuel bed. *International Journal of Thermal Sciences*, **42**, 95-105.

Streeks TJ, Owens MK and Whisenant SG (2005) Examining fire behavior in mesquite-acacia shrublands. *International Journal of Wildland Fire*, **14**, 131-140.

Sullivan AL and Knight IK (2001) Estimating error in wind speed measurements for experimental fires. *Canadian Journal of Forest Research*, **31**, 401-409.

Sullivan AL, Knight IK and Cheney NP (2002) Predicting the radiant heat flux from burning logs in a forest following a fire. *Australian Forestry*, **65 (1)**, 59-67.

Sullivan AL (2009a) Wildland surface fire spread modelling; 1990-2007. 1: Physical and quasi-physical models. *International Journal of Wildland Fire*, **18 (4)**, 349-368.

Sullivan AL (2009b) Wildland surface fire spread modelling; 1990-2007. 2: Empirical and quasi-empirical models. *International Journal of Wildland Fire*, **18 (4)**, 369-386.

Sullivan AL (2009c) Wildland surface fire spread modelling; 1990-2007. 3: Mathematical analogues and simulation models. *International Journal of Wildland Fire*, **18 (4)**, 387-403.

Sun L, Zhou X, Mahalingam S and Weise DR (2006) Comparison of burning characteristics of live and dead chaparral fuels. *Combustion and Flame*, **144**. 349-359.

Sun R, Krueger SK, Jenkins MA, Zulauf MA and Charney JJ (2009) The importance of fire-atmosphere coupling and boundary-layer turbulence to wildfire spread. *International Journal of Wildland Fire*, **18**, 50-60.

Taylor GI (1961) Fire under influence of natural convection. *Berl, W. G. (ed) The Use of Models in Fire Research*. National Academy of Sciences – National Research Council, Publication 786. Washington D.C., USA. 10-31.

Telisin HP (1974) Flame radiation as a mechanism of fire spread in forests. *Afgan NH and Beer J (eds) Heat Transfer in Flames, Chapter 29*. John Wiley and Sons, New York, USA. 441-449.

Thomas PH (1960) On the rate of burning of wood. *Fire Research Note 446*. Joint Fire Research Organization, Fire Research Station. Boreham Wood, UK. 11 pp.

Thomas PH (1963) The size of flames of natural fires. *9 th International Symposium on Combustion*. 27 August - 1 September 1962. Ithaca, NY. New York: Academic Press. 844-859.

Thomas PH (1964) The effect of wind on plumes from a line heat source. *Fire Research Note 572*. Joint Fire Research Organization, Fire Research Station. Boreham Wood, UK. 36 pp.

Thomas PH and Simms DL (1964) A study of fire spread in forest fires. *Report on Forest Research for the year ended March 1963*. Forestry Commission. H.M. Stationary Office. London, England. 108-112.

Thomas PH and Law M (1965) Experiments on the spread of fire. *Report on Forest Research 1965*. Forestry Commission. H.M. Stationary Office. London, England. 124-130.

Thomas PH (1967) Some aspects of the growth and spread of fire in the open. *Forestry*, **40 (2)**, 139-164.

Thomas PH (1970) The rates of spread of head fires in gorse and heather. *Fire Research Note No. 796*. Joint Fire Research Organization. Fire Research Station, Boreham Wood, Herts, UK. 37 pp.

Thomas PH (1971) Rates of spread of some wind-driven fires. *Forestry*, **44 (2)**, 155-175.

Trollope WS (1998) Effect and use of fire in the savanna areas of southern Africa. *Occasional Report*. Department of Livestock and Pasture Science, Faculty of Agriculture, University of Fort Hare. Fort Hare, Alice, South Africa.

Van Wilgen BW, Le Maitre DC and Kruger FK (1985) Fire behaviour in South African fynbos macchia vegetation and predictions from Rothermel's fire model. *Journal of Applied Ecology*, **22**, 207-216.

Van Wagner CE (1968) Fire behaviour mechanisms in a red pine plantation: field and laboratory evidence. *Forestry Branch Departmental Publication No. 1229*. Ottawa, Canada. 30 pp.

Van Wagner CE (1977) Effect of slope on fire spread rate. *Canadian Forestry Service By-monthly Research Notes*, **33 (1)**, 7-8.

Van Wagner CE (1988) Effect of slope on fires spreading downhill. *Canadian Journal of Forest Research*, **18**, 818-820.

Vaz GC, André JC and Viegas DX (2004a) Fire spread model for a linear front in a horizontal solid porous fuel bed in still air. *Combustion Science and Technology*, **176**, 135-182.

Vaz GC, André JC and Viegas DX (2004b) Estimation of the radiation extinction coefficient of natural fuel beds. *International Journal of Wildland Fire*, **13**, 65-71.

Vega JA, Cuinas P, Fonturbel T, Perez-Gorostiaga P and Fernandez C (1998) Predicting fire behaviour in Galician shrubland fuel complexes. *Proceedings of the III International Conference on Forest Fire Research.* 16-20 November 1998, Luso, Portugal. 713-728.

Ventura JM and Rego FM (1998) Modeling the shape of temperature-time curves. *Proceedings of the 13th Fire and Forest Meteorology Conference, Vol. 1.* 24 October-2 November 1996, Lorne, Australia. 197-201.

Ventura JM, Mendes-Lopes JM and Ripado LM (1998) Temperature-time curves in fire propagation in beds of pine needles. *Proceedings of the III International Conference on Forest Fire Research.* 16-20 November 1998, Luso, Portugal. 699-711.

Viegas DX and Neto LP (1991) Wall shear-stress as a parameter to correlate the rate of spread of a wind induced forest fire. *International Journal of Wildland Fire*, **1 (3)**, 177-188.

Viegas DX, Varela V and Borges CP (1994) On the evolution of a linear fire front in a slope. *Proceedings of the II International Conference on Forest Fire Research.* November 1994, Coimbra, Portugal. 301-318.

Viegas DX, Ribeiro PR and Maricato L (1998) An Empirical Model for the Spread of a Fireline Inclined in Relation to the Slope Gradient or to Wind Direction. *Proceedings of the III International Conference on Forest Fire Research.* 16-20 November 1998, Luso, Portugal. 325-342.

Viegas DX (2002) Fire line rotation as a mechanism for fire spread on a uniform slope. *International Journal of Wildland Fire*, **11**, 11-23.

Viegas DX (2004a) On the existence of a steady-state regime for slope and wind driven fire. *International Journal of Wildland Fire*, **13 (1)**, 101-117.

Viegas DX (2004b) Slope and Wind Effects on Fire Propagation. *International Journal of Wildland Fire,* **13 (2)**, 143-156.

Viegas DX (2004c) Cercados pelo fogo. *Minerva Editora* (*in Portuguese*). Coimbra, Portugal. 274 pp.

Viegas DX and Pita LP (2004) Fire spread in canyons. *International Journal of Wildland Fire*, **13**, 253-274.

Viegas DX (2005) A Mathematical Model for Forest Fires Blow-up. *Combustion Science and Technology*. **177**, 1-25.

Viegas DX (2006) Parametric study of an eruptive fire behaviour model. *International Journal of Wildland Fire*, **15**, 169-177.

Viegas DX, Rossa CG, Caballero D, Pita LP and Palheiro P (2006a) Analysis of Accidents in 2005 Fires in Portugal and Spain. *Proceedings of the V International Conference on Forest Fire Research*. 27-30 November 2006, Figueira da Foz, Portugal.

Viegas DX, Rossa CG, Oliveras I and Piñol J (2006b) Fireline Rotation Model. *Proceedings of the V International Conference on Forest Fire Research*. 27-30 November 2006, Figueira da Foz, Portugal.

Viegas DX (2007a) Climate, Man and forest fires. *Elements for Life*. World Meteorological Organization, 148-149.

Viegas DX (2007b) Zigzag shape of the fire front. *International Journal of Wildland Fire*, **16**, 763-764.

Viegas DX and Rossa CG (2009) Fireline Rotation Analysis. *Combustion Science and Technology*, **181 (12)**, 1495-1525.

Vogel M and Williams FA (1970) Flame propagation along matchstick arrays. *Combustion Science and Technology*. **1**, 429-436.

Weber RO (1989) Analytical models for fire spread due to radiation. *Combustion and Flame*, **78**, 398-408.

Weber RO (1990) A model for fire propagation in arrays. *Mathematical and Computer Modelling*, **13(12)**, 95-102.

Weber RO (1991) Modelling fire spread through fuel beds. *Progress in Energy and Combustion Science*, **17**, 67-82.

Weise DR (1993) Modelling wind and slope induced wildland fire behaviour. *PhD Thesis*. University of California, Berkeley, USA. 130 pp.

Weise DR and Biging GS (1997) A qualitative comparison of fire spread models incorporating wind and slope effects. *Forest Sci.*, **43 (2)**, 170-180.

Weise DR, Zhou X, Lulu S and Mahalingam S (2005) Fire spread in chaparral – 'go or no go?'. *International Journal of Wildland Fire*, **14**, 99-106.

Williams RJ, Gill AM and Moore PH (1998) Seasonal changes in fire behaviour in a tropical savanna in northern Australia. *International Journal of Wildland Fire*, **8**, 227-239.

Wolff MF, Carrier GF and Fendell FE (1991) Wind-aided fire spread across arrays of discrete fuel elements II: Experiment. *Combustion Science and Technology*, **77**, 261-289.

Woolliscroft MJ (1968) A report on forest fire fieldwork (New Forest, March 1966). *Fire Research Note No. 693*. Joint Fire Research Organization. Fire Research Station, Boreham Wood, UK. 14 pp.

Woolliscroft MJ (1969a) Notes on forest fire fieldwork (New Forest, 1967). *Fire Research Note No. 740*. Joint Fire Research Organization. Fire Research Station, Boreham Wood, UK 14pp.

Woolliscroft MJ (1969b). A report on forest fire fieldwork (New Forest, March 1968). Joint Fire Research Organization. *Fire Research Note No. 744*. Fire Research Station, Boreham Wood. UK 12 pp.

Zhou X, Weise DR and Mahalingam S (2005) Experimental measurements and numerical modeling of marginal burning in live chaparral fuel beds. *Proceedings of the Combustion Institute*, **30**, 2287-2294.

Zulauf MA (2001) Modelling the effects of boundary layer circulations generated by cumulus convection and leads on large-scale surface fluxes. *PhD Thesis*. Department of Meteorology, University of Utah, USA. 177 pp.